

182 10011

CTR-144818

"Made available under NASA sponsorship
in the interest of early and wide dis-
semination of Earth Resources Survey
Program information and without liability
for any use made thereof."

**GEOLOGIC APPLICATIONS OF THERMAL-INERTIA
MAPPING FROM SATELLITE**

Original photography may be purchased from
EROS Data Center

Sioux Falls, SD 57198

July 1981
Final Report - HCMM Investigation S-40256-B

Submitted by: Kenneth Watson
Susanne Hummer-Miller
Terry W. Offield - Principal Investigator

U.S. Geological Survey
MS 964, Box 25046, DFC
Denver, CO 80225

(F82-10011) GEOLOGIC APPLICATIONS OF
THERMAL-INERTIA MAPPING FROM SATELLITE
Final report (Geological Survey) 109 p
HC AGG/ME PJ1 CSCL 088

N82-15489

Unclass
G3/43 JC011

Prepared for: GODDARD SPACE FLIGHT CENTER
HCMM Investigations
Greenbelt, MD 20771

RECEIVED

AUG 17 1981

5179026

HCMM-027

Type III Final

TECHNICAL REPORT STANDARD TITLE PAGE

1. Report No.	2. Government Accession No.	3. Recipient's Catalog No.
4. Title and Subtitle Geologic applications of thermal-inertia mapping from satellite		5. Report Date July 1981
7. Author(s) Kenneth Watson, Susanne Hummer-Miller, Terry W. Offield		6. Performing Organization Code
9. Performing Organization Name and Address U.S. Geological Survey Box 25046 Federal Center Stop 964 Denver, Colorado 80225		8. Performing Organization Report No.
12. Sponsoring Agency Name and Address James C. Broderick HCMM Investigative Support Goddard Space Flight Center, Code 902-6 Greenbelt, Maryland 20771		10. Work Unit No.
		11. Contract or Grant No. S-40256-B
		13. Type of Report and Period Covered Type III, Final Report 12/77 to 1/81
		14. Sponsoring Agency Code
15. Supplementary Notes		
16. Abstract <p>This study is an evaluation of HCMM (Heat Capacity Mapping Mission) satellite data to detect and map geologic features for energy-resource and mineral-deposit investigations. In the Powder River Basin, Wyo., narrow geologic units having thermal inertias which contrast with their surroundings can be discriminated in optimal images. A few subtle but mappable thermal-inertia anomalies coincide with areas of helium leakage believed to be associated with deep oil and gas concentrations. Similar changes were not found in areas of uranium deposits possibly due to their minor and discontinuous nature at satellite resolution.</p> <p>The most important results involved delineation of tectonic framework elements some of which were not previously recognized. Thermal and thermal-inertia images also permit mapping of geomorphic textural domains. A thermal lineament not on existing geologic maps or detected on Landsat images appears to reveal a basement discontinuity which involves the famous Homestake Mine in the Black Hill, a zone of Tertiary igneous activity and facies control in oil-producing horizons.</p> <p>Applications of these data to the Cabeza Prieta, Ariz., area illustrate their potential for igneous rock-type discrimination. Extension to Yellowstone National Park resulted in the detection of additional structural information but surface hydrothermal features could not be distinguished with any confidence.</p> <p>Advances in modeling and image analysis included the development of a new thermal-inertia mapping algorithm, a fast and accurate image-registration technique, and an efficient topographic-slope and elevation-correction method.</p>		
17. Key Words (Selected by Author(s)) thermal infrared, Powder River Basin, modeling, thermal lineament, energy resources, mineral deposits, thermal-inertia mapping, image registration, Cabeza Prieta, Yellowstone, HCMM, remote sensing		18. Distribution Statement
19. Security Classif. (of this report)	20. Security Classif. (of this page)	21. No. of Pages 106
		22. Price*

*For sale by the Clearinghouse for Federal Scientific and Technical Information, Springfield, Virginia 22151.

ORIGINAL PAGE IS
OF POOR QUALITY

1.0 PREFACE

1.1 OBJECTIVES

The principal objective of this study was to investigate applications of HCMM (Heat Capacity Mapping Mission) satellite data in detecting and mapping geologic features for energy-resource and mineral-deposit studies. Other, related objectives involved the development of new techniques and approaches in thermal modeling and image processing.

1.2 SCOPE

The analysis was somewhat restricted by the limited number of sequential day/night image pairs free of major atmospheric/weather problems. For the Powder River Basin, Wyo. area, a single thermal-inertia image was formed using 20 August 1978 data. Four additional nighttime scenes were used to examine geologic formation boundaries and thermal lineaments. The analysis of the Cabeza Prieta, Ariz., area was done using a thermal-inertia image constructed from data acquired April 3 and 4, 1979. No successful U-2 aircraft data acquisition flights were conducted over these two sites so that comparison of different resolution thermal data was only conducted using USGS aircraft data. Despite all these limitations, significant geologic information was derived in this study, and the results suggest the importance of a follow-on thermal satellite experiment for improved mineral and energy resource exploration.

1.3 CONCLUSIONS

Despite limited data, investigations in the Powder River Basin area of eastern Wyoming and adjacent States clearly showed that geologic units as narrow as two or three resolution elements, but of moderate to high thermal-inertia contrast against surroundings, can be discriminated in optimal images. It appears likely that subtle facies differences in sedimentary basin-fill units can be delineated and mapped using satellite thermal-inertia images, especially if sequential images can be obtained during a drying cycle after rain or snow. A few subtle but mappable thermal-inertia anomalies coincide with areas of anomalous helium in soil gas believed to indicate leakage from deep oil and gas concentrations; the presence of thermal-inertia anomalies suggests that gas leakage has produced chemical changes and cementation at the surface. Such changes also are known to be associated with shallow uranium deposits and changes were looked for but not found in the thermal-inertia images; it is thought that the surface changes in this area are too minor and discontinuous to be detected from satellite.

The most consistently practical and important results involve delineation of tectonic framework elements such as lineaments bounding apparent structural blocks. These commonly can be seen even in less-than-optimal data. One pair of major thermal lineaments in the southern Powder River Basin seems to define structures not previously recognized but consistent with, and adding importantly to, an emerging story of basement-block movements and their direct influence on sedimentation, which in part controls the occurrence of large oil and gas resources. One of these lineaments matches up with aeromagnetic map data and appears to reveal a basement discontinuity which underlies the famous

Homestake Mine in the Black Hills and a zone of Tertiary igneous activity. Along with the newly identified lineaments, the thermal images also permit mapping of geomorphic textural domains. The geologic significance of these is not yet understood, but it seems likely that they connote structural and lithologic conditions which affect or control local ground-water regimes.

Similar applications of HCMM data to the Cabeza Prieta, Ariz., area illustrate the potential of using thermal-inertia data for discrimination between extrusive and intrusive rocks and for detecting differences in the mafic content of volcanics. Other results included detection of differences among surficial units - tentatively ascribed to changes in soil-moisture retention, discovery of discrepancies in existing geologic maps, and possible application of the thermal-inertia technique to mapping buried pediments.

Extension from beyond the originally proposed study areas to Yellowstone National Park was made to examine the usefulness of HCMM data in geothermal studies. Although we found that the night-thermal data could not be used with any confidence to distinguish surface hydrothermal features, we did detect additional structural information concerning the outline of the caldera which is the source of the volcanic heat. This reinforces our conclusion that a major utility of these data is in providing information about local-area or regional tectonic framework.

We have also made significant advances in modeling analysis and image-registration techniques. A thermal-inertia mapping algorithm has been developed based on a new method to derive the regional meteorologic parameters solely from the satellite data. An algorithm for determining the sensible-heat flux from ground-station data was also constructed. Simple forms for

four of the atmospheric flux terms were constructed from field measurements made during circumstances when satellite data are likely to be most useful. These forms eliminate the need for extensive continuous ground station data. Also, a method to correct thermal and thermal-inertia data for elevation variations in sky and solar flux was determined. In addition, we have devised a fast topographic adjustment algorithm which can be used in conjunction with digital terrain data to correct the thermal-inertia image for simple topographic slope effects. Finally, a fast image registration technique was developed that proved to be considerably more accurate than the NASA registered products.

Our analysis of the HCMM data has resulted in the recognition of features which suggest the existence of previously unmapped and unknown geologic structures. Their relationship to other geophysical and geochemical data provides important information for a basic resource-exploration strategy. Additionally, substantial progress has been made in modeling and image-processing techniques. This report covers new areas and represents significant advances in the processing and interpretation of thermal satellite data and in the integration of thermal-infrared data in regional geologic exploration.

1.4 RECOMMENDATIONS

From our experience to date, we would recommend that serious consideration be given to a follow-on thermal satellite mission with these general characteristics.

1. The current NEAT of HCMM seems adequate for most regional studies. Higher thermal resolution does not appear necessary.

2. Some increase in ground resolution (possibly 100-200 m) would be useful; however, there are trade-offs to consider here. The 500-m resolution from HCMM has proven very useful for regional structures - it does not appear promising for detecting alteration.

3. Some increase in the repeat times over a site is desirable. The HCMM data we have seen have often baffled us because of changing meteorologic effects. The increased repeat time would enhance the chances of "stable-clear" conditions and also provide coverage of regions under several meteorological and soil moisture conditions. The repeat time involves the orbit parameter selection; a 5-10 day repeat of coverage would be desirable.

4. The current overflight times of HCMM appear appropriate for geologic analysis. It should also be noted that the daytime maximum represents an optimum time to acquire multispectral thermal measurements as well.

5. Our analysis of HCMM data requires registration of day and night images and subsequent registration to a topographic base. The registered data provided by NASA often contained large registration errors. An essential requirement for analysis of these data is that the clear scene images be registered (day/night images) to a pixel, and to digital terrain data. If this registration accuracy cannot be achieved routinely, it is recommended that registered products not be provided to users.

CONTENTS

	Page
1.0 PREFACE	1
1.1 OBJECTIVES.	1
1.2 SCOPE	1
1.3 CONCLUSIONS	2
1.4 RECOMMENDATIONS	4
2.0 INTRODUCTION.	10
2.1 GEOLOGIC SETTING.	11
2.2 APPROACH.	12
2.3 RESULTS	14
2.3.1 <u>Thermal-inertia mapping for discrimination of</u> <u>geologic features</u>	14
2.3.1.1 Delineation and subdivision of geologic units.	14
2.3.1.2 Geomorphic domains and linear features	37
2.3.2 <u>Application to resource studies</u>	48
2.3.2.1 Oil and gas.	48
2.3.2.2 Uranium.	51
2.3.2.3 Geothermal flux.	53
2.3.2.4 Mapping geologic units in an arid desert environment	56
3.0 MODEL DEVELOPMENT	63
4.0 DIGITAL IMAGE PROCESSING.	66
5.0 REFERENCES.	70
5.1 APPENDIXES.	73
5.2 REFERENCE MATERIAL.	67

ILLUSTRATIONS

Figure	Page
1. Night thermal image, July 30, 1978, of the Powder River Basin, Wyoming, delineating the fold nose in the Mesaverde Formation and the Frontier Formation inlier. The standard convention of dark for low values and light for high values is employed on all images in this report.	15
2. Fold nose of the Mesaverde Formation as expressed on the July 30, 1978, nighttime HCMM image. Boundaries are from the state geologic map	16
3. Inlier of the Frontier Formation as expressed on the July 30, 1978, nighttime HCMM image	18
4. Night thermal image, September 5, 1978, of the Powder River Basin, Wyoming, showing the discrimination of the Pumpkin Buttes	19
5. Day thermal image, August 20, 1978, of the Powder River Basin, Wyoming, showing thermal boundaries.	21
6. Night thermal image, August 20, 1978, of the Powder River Basin, Wyoming, showing conspicuously warm areas. The unlabeled lines are profiles A-A' (north line) and B-B' (south line)	22
7. Thermal-inertia image, August 20, 1978, of the Powder River Basin, Wyoming	24
8a. Base map of the Powder River Basin, Wyoming, showing the location of the clinkers with respect to the warm areas which have high thermal inertias.	26

8b.	Comparison between profiles of total count gamma ray and the anomalously warm areas	28
9.	Thermal-inertia profile of line A-A'	29
10.	Elevation profile of line A-A'	31
11.	Topographic-gradient profile of line A-A'.	32
12.	Thermal-inertia profile of line B-B'	34
13.	Elevation profile of line B-B'	35
14.	Topographic-gradient profile of line B-B'.	36
15.	Night thermal image, September 27, 1978, of the Powder River Basin, Wyoming, showing the lineament.	39
16a.	Landsat image of the Powder River Basin area, Wyoming. The mosaic line is present roughly 100 km west of the Black Hills and run north-south.	41
16b.	Illuminated (0930 hrs, solar declination = -7.8°) topography image of the Powder River Basin, Wyoming, showing the divide which is coincident with the thermal lineament	42
17.	Total intensity magnetic field formline map, central Powder River Basin.	43
18.	Ground-water temperatures in the Madison Limestone and equivalent rocks	44
19.	Location of the HCMM thermal lineament with respect to the structural lineaments.	45
20.	Location of helium anomalies, uranium fields, and oil-gas fields in the Powder River Basin, Wyoming	49

21.	Major thermal and Landsat lineaments transecting the southern part of the Powder River Basin, and boundaries of topographic-temperature domains.	52
22.	Areas of underground coal fires near Sheridan, Wyo., as seen on HCMM and aircraft thermal data	54
23a.	Nighttime thermal image of Yellowstone Park with the caldera outlines	55
23b.	Location of hydrothermal features within Yellowstone Park with the caldera outlined	55
24a.	Nighttime temperatures of known hydrothermal features.	57
24b.	Ranking of thermal night anomalies	57
25a.	Landsat image of Yellowstone Park with the caldera outlined. . .	58
25b.	Gravity map of Yellowstone Park with the caldera outlined. . . .	58
26.	Thermal-inertia image, April 3-4, 1979, of Cabeza Prieta, Arizona.	60
27.	Flow chart of the image processing procedure	67
 Table		 Page
1.	Estimates of thermal inertia of various geologic materials . . .	61

2.0 INTRODUCTION

The HCMM data which we have examined have provided us with unique geologic information which is both complex to analyze and difficult to explain. In some cases we are astonished to see subtle distinctions of structure and geologic materials that are not found on detailed geologic maps. In other cases we are unable to differentiate widely dissimilar geologic materials or identify features which are clearly described on regional geologic maps or Landsat images. Commonly, geologic features are clearly displayed on a single image or part of an image and not on others. Further complicating the analysis of these data has been the experimental nature of the satellite mission, which has introduced both significant time lags between data acquisition and interpretation, and unique constraints in image registration and data calibration.

This report comprises pieces to a puzzle--a puzzle with tantalizing new information but sufficient gaps to preclude a complete overall assessment. We have examined the geologic implications of the HCMM data in the Powder River Basin of Wyoming and subsequently extended the analysis to the Cabeza Prieta area in Arizona. Enhanced nighttime images, thermal-inertia images based on our new algorithm, and several profiles of various data across the basin are presented in our analysis and subsequently compared with other map data (geologic, magnetic field, known areas of oil, gas, and uranium occurrence, helium anomalies, and ground water). Of equal importance with the geologic interpretation has been progress in modeling. We provide several new algorithms: thermal-inertia mapping, estimation of regional meteorological information from the fundamental remote sensing data, registration of satellite day-night

images, elevation correction of thermal and thermal-inertia data, and determination of sensible-heat flux. The concluding section of this report addresses our image processing techniques together with a listing of the computer programs used.

2.1 GEOLOGIC SETTING

The study areas are the Powder River Basin and environs in eastern Wyoming-Montana and the adjacent Dakotas and the Cabeza Prieta Range in southwest Arizona. The Powder River Basin (lat. 42°-45° N., long. 103°-107° W.) has large potential for coal, oil and gas, and uranium, and accordingly is now the target of several major geologic, water-resource, and land-use mapping projects. Covering an area of about 250 x 400 km, it is a semi-arid region of rolling low hills typically with thin to moderate grass and sage cover. Tertiary rock units (Fort Union and Wasatch Formations) in the central area of the basin, where the energy resources are known to occur, are exposed on scales sufficient for satellite measurements. The lower part of the Fort Union is sandstone exposed in belts 4 to 10 km wide; the upper Fort Union part is siltstone with major coal beds exposed in belts 10 to 30 km wide; and the Wasatch is siltstone and claystone covering areas 30 to 60 km wide.

The Cabeza Prieta Range in Arizona (lat. 32°-33° N., long. 112°-115° W.) is a proposed Wilderness area, and the USGS has begun a program to define the geology and mineral-resource potential of this virtually unmapped area. The State geologic map shows the area to contain granite, schist, mafic volcanic rocks, and alluvium. It lies very near the major mineral district at Ajo, Ariz., and contains old prospect developments in hydrothermally altered

ground. Because the area has been withdrawn from public access since World War II, the geology and mineral potential are barely known and thus the area is considered relatively important for modern study.

2.2. APPROACH

Initial data interpretation was performed by visual pattern recognition of areas significantly different than their surroundings. Several 1:1,000,000-scale photographic enlargements were made of the NASA thermal and reflectance images to match them to many of the other existing data map products (geologic, geophysical, topographic, Landsat lineaments, and so on). Because of the X-Y distortion and the large magnification, this method was not entirely satisfactory for detailed study. We then generated film products from the computer-compatible tapes (CCT's) and used a zoom transferscope with X-Y stretch capability to register the projected images onto a stream-network map. In most local areas, this permitted plotting of features to within one to three pixels of their true ground position. Few of the interpretations based on the temperature boundaries or on other features are significantly affected by this degree of mislocation.

During this stage of the investigation, we also discovered that the NASA-supplied ΔT and thermal-inertia images contained artifacts, such as double drainage, indicating misregistration in parts of these images of several to many pixels. Consequently we developed a registration algorithm (Watson and others, 1981b) which registers data to within two pixels. Also as part of the investigation, we developed a new thermal-inertia algorithm (Watson, 1981a) which was employed during the remainder of our analysis. Correlation of these

registered image products with the other geologic-geophysical data was performed primarily by using optically enlarged projections of the data on digitally enlarged image product at a scale of approximately 1:200,000. This enabled us to examine subtle features at the pixel level and also to employ our full profiling and histogram capability at the full dynamic range and resolution of the digital image data. We have thus been able to quantify many of the scene differences which had been observed on various image products.

We also examined the use of color-coded images for enhancing subtleties in the scene contrast. Generally this provided a more obvious demonstration of differences but did not appear to add any new information. Toward the end of our study, however, a color-coded thermal-inertia image was produced which provided a new - if unexplained - perspective of the scene. A north-northeast-trending rectangular pattern of ground, surrounding the Black Hills and roughly corresponding with major changes in the drainages of the Yellowstone and Missouri Rivers was observed. In retrospect, this feature can now also be seen on the black and white products. The color-coding of the image was also a very useful tool for quickly determining the numerical range of values. With an appropriate color-scale and using a high-powered magnification lens, it was possible to determine the thermal-inertia ranges of many geologic units quickly. In both these respects the color-coding can be regarded as a useful but not essential element in the analysis.

2.3 RESULTS

2.3.1 Thermal-inertia mapping for discrimination of geologic features

2.3.1.1 Delineation and subdivision of geologic units

Discrimination studies have been somewhat limited by the lack of sequential day-night image pairs free of major atmospheric/weather problems, but the 20 August 1978 set of day (AA0116-20010-1,2 and AA0116-20020-1,2) and night (AA0116-09040-3) scenes and our constructed temperature-difference (ΔT) and thermal-inertia images show several geologically significant features. Other good nighttime data from 30 July 1978 (AA0095-09170-3), 5 September 1978 (AA0132-09050-3), 27 September 1978 (AA0154-09190-3), and 10 June 1979 (AA0410-08450-3) passes have been used for delineation of several geologic boundaries, including some not within the area of, or not identified in, the 20 August 1978 data set.

A measure of discrimination capability, using optimal images and selection of geologic units which contrast well with their surroundings, is the clear delineation of the Mesaverde Formation. South of the Bighorn Mountains, in the vicinity of the towns of Midwest and Edgerton Wyo., the Mesaverde - a relatively massive sandstone - crops out between the Fox Hills Sandstone and the Cody Shale. On the night image (fig. 1) for 30 July 1978, all three units are relatively warm; however, the Mesaverde can be traced as a distinctly warmer unit ($1/4^{\circ}$ - $1/2^{\circ}$ C), along at least 40 km of strike length in which a fold nose is clearly defined (fig. 2). The Mesaverde outcrop here is 1-2 km wide or 2-4 resolution elements (pixels).

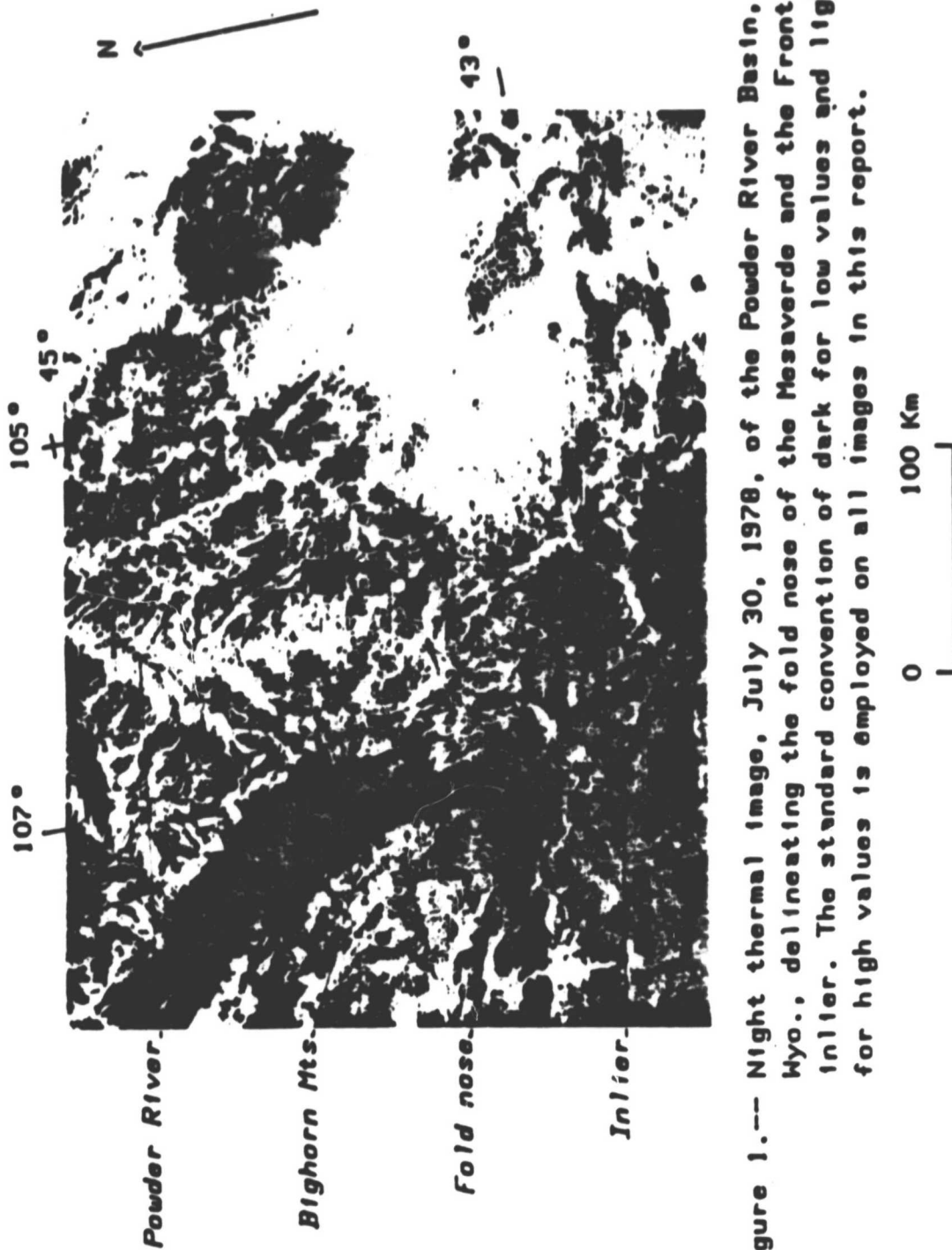
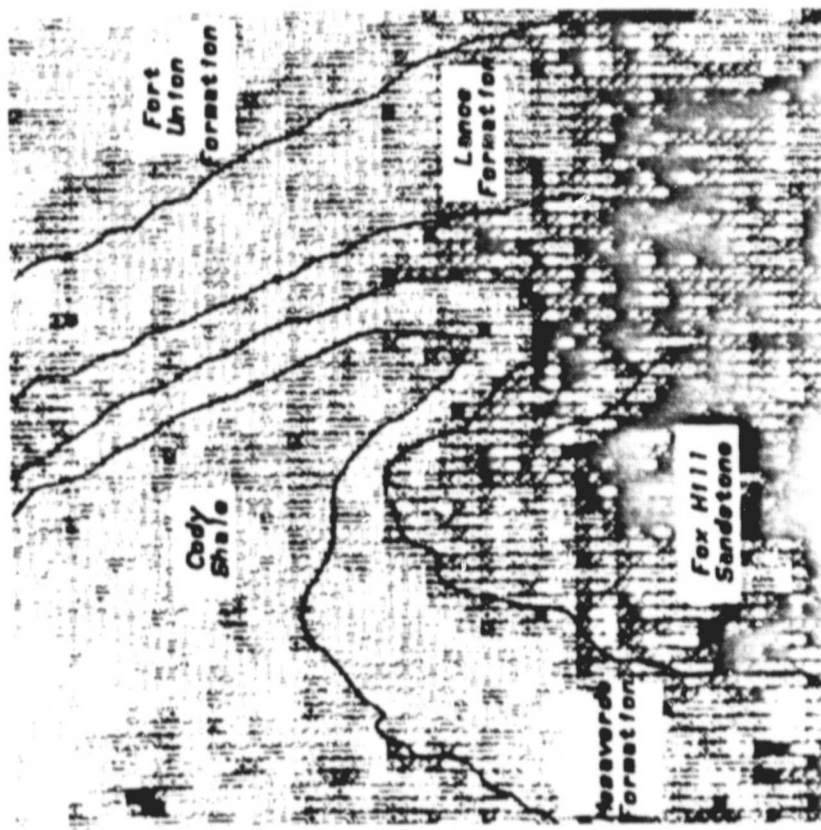


Figure 1.-- Night thermal image, July 30, 1978, of the Powder River Basin, Wyo., delineating the fold nose of the Mesaverde and the Frontier Inlier. The standard convention of dark for low values and light for high values is employed on all images in this report.



0 10 Km

Figure 2.— Fold nose of the Mesaverde Formation as expressed on the July 30, 1978, nighttime HCMH image. An unmarked image is provided for comparison.

Southwest of that area, south of the town of Powder River, within a large area of Cody Shale, is a sandstone inlier of Frontier Formation surrounding older shale and sandstone of the Cloverly and Morrison Formations. In the 30 July image, the Frontier is clearly a warm annulus around a cool center of the other units (fig. 1 and 3). The units in the cool central area are about 5 km wide and the warm Frontier annulus is 3.5 km wide. What is additionally interesting in this area is the apparently clear definition of a similar but smaller such feature to the northwest which does not match the shape of the contacts on the most recent geologic map (Love and others, compilers, 1955). This feature has not been field checked.

Another measure of discrimination is found in the area of the Pumpkin Buttes. These are very sharply defined in the 5 September 1978 night image (fig. 4). North Butte is about 3 km wide, and the combined topographic/geologic prominence of Middle and South Buttes measures about 4 by 8 km. These are warmer than their surroundings, as is expected of tuffaceous sandstones of the White River Formation, dense and resistant enough to form buttes where erosional remnants lie upon the softer sandstones and mudstones of the Wasatch Formation. Once again, when the geologic map was projected onto this HCMM scene, differences were observed. Unfortunately, on our only thermal-inertia image, clouds were present over the Buttes preventing the observation of the expected thermal-inertia contrast.

Definition of geologic features is highly variable from pass to pass and within single passes. The 30 July image (fig. 1) is excellent for the north half of the Powder River Basin and the areas west and southwest of the Basin. The image appears virtually washed out in the south half of the Basin,

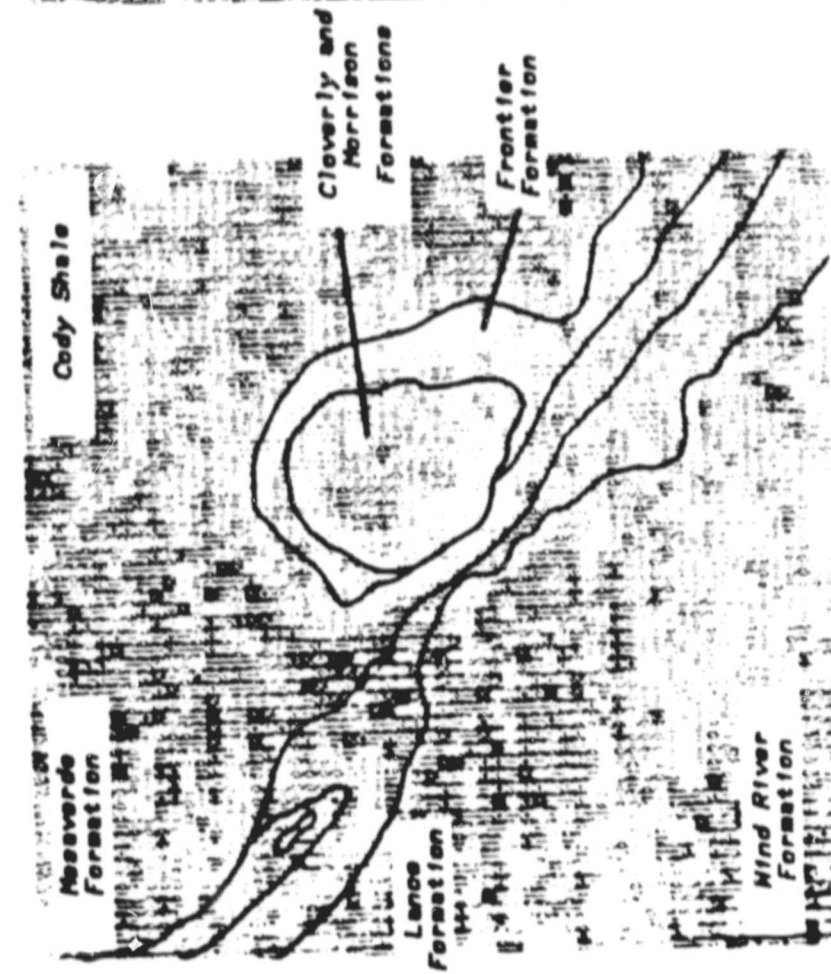
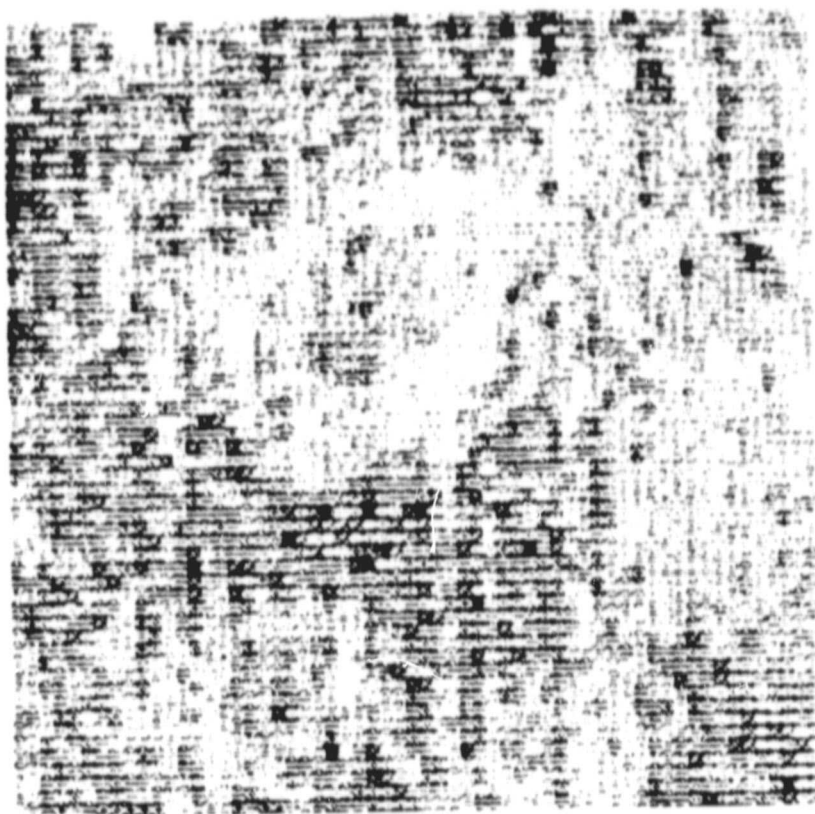


Figure 3.-- Inlier of the Frontier Formation as expressed on the July 30, 1978, nighttime HCMH image. An unmarked image is provided for comparison.

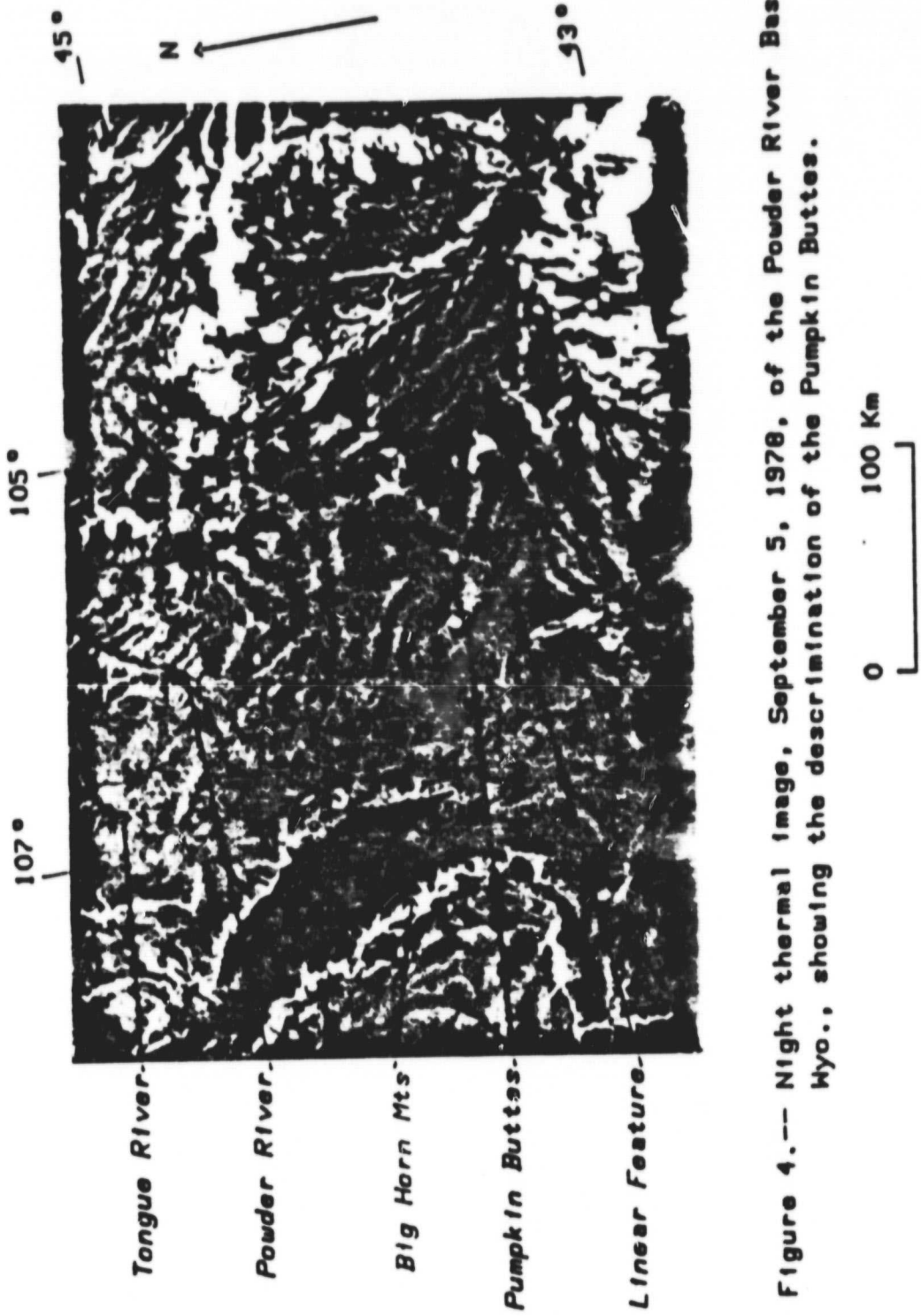


Figure 4.-- Night thermal image, September 5, 1978, of the Powder River Basin, Wyo., showing the descrimination of the Pumpkin Buttes.

showing high temperatures in an area conspicuously cool in all the other images. Because the image was examined long after it was acquired, it was not possible to obtain detailed field meteorological data. This is a generic problem in dealing with transient and local phenomena that commonly affect thermal surveys. Air temperature and precipitation data show fairly similar conditions at the 28 weather stations throughout the scene. From these data, the intrascene variations cannot readily be ascribed to local weather/moisture changes; however, the NOAA and DMSP (Defense Meteorological Satellite Program) Satellite data show that a major weather front had recently passed through the basin. Such intrascene differences are less pronounced or even absent in other passes, but none of the others expresses quite the same degree of geologic feature definition as the good portions of the 30 July image.

The multiple data sets of 20 August contain considerable geologic information, especially in comparing patterns seen variously in the day thermal, night thermal, ΔT , and thermal-inertia images. The day thermal image (fig. 5) shows large areas of warm ground north and east of the Black Hills. These do not correspond to lithologic subdivisions on any available geologic maps, nor to any patterns of weather across the scene during the previous few days. Small individual features of interest in the image are cool areas around the Tongue River and in a belt of small patches trending north-south up the center of the southern part of the basin. The very warm drainage area west of the Black Hills and the warm area south of the Black Hills are also noteworthy. The night image (fig. 6) offers busier patterns of finer scale definition, dominantly related to the topographic character of local areas. Much, but not all of the high ground between streams, is conspicuously warm. The long,

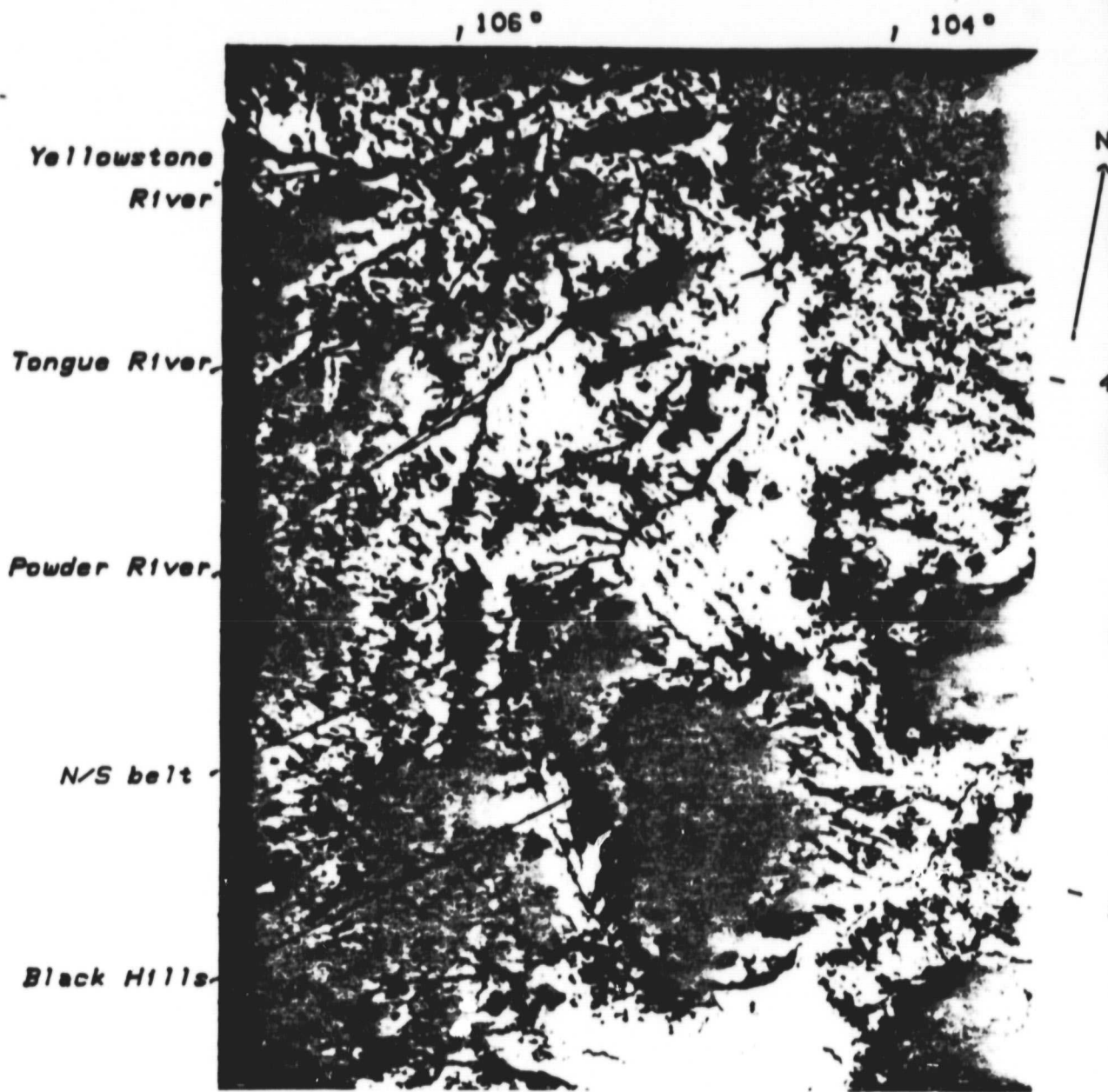


Figure 5.-- Day thermal image, August 20, 1978, of the Powder River Basin, Wyo., showing thermal boundaries.

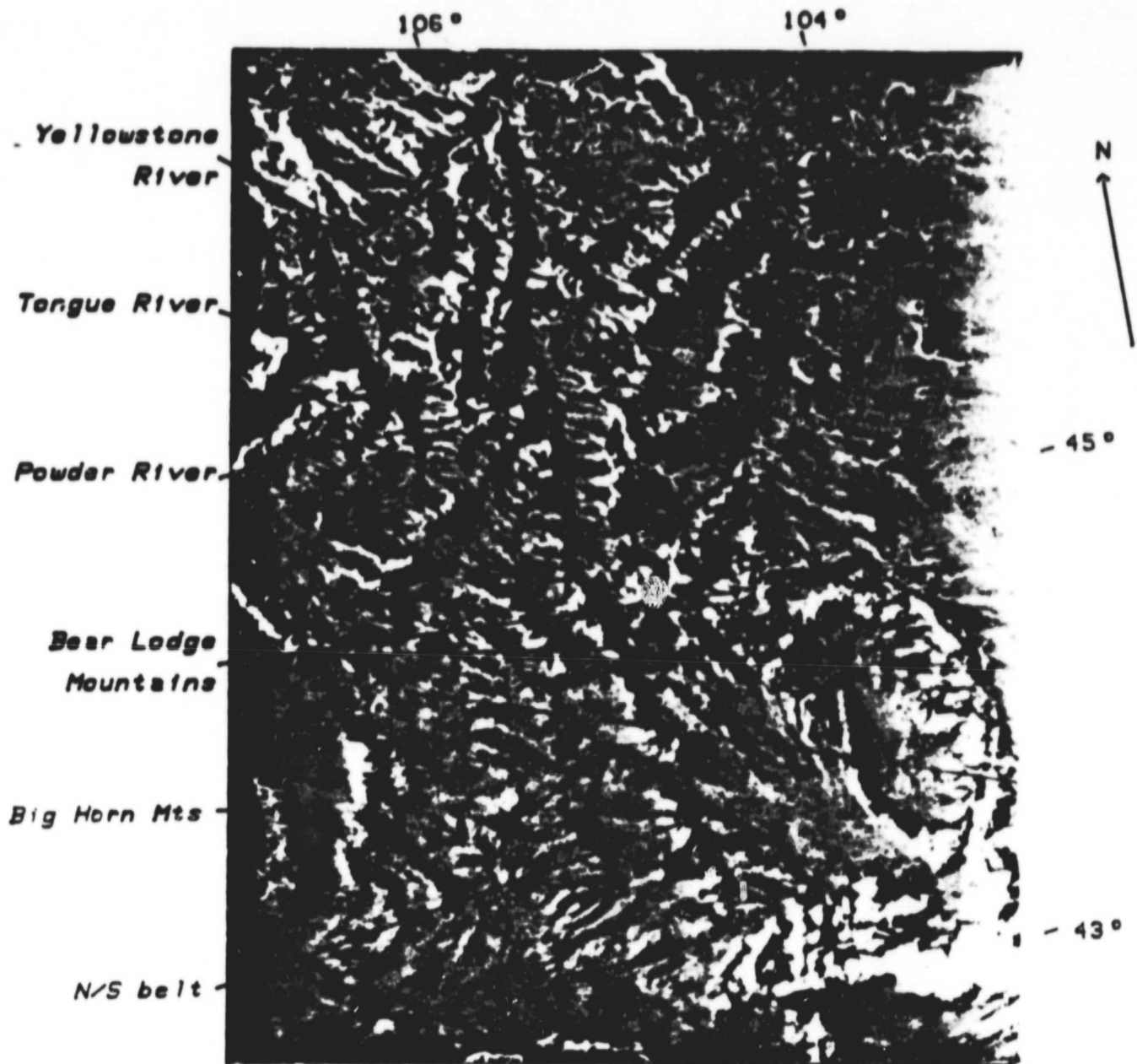


Figure 6.-- Night thermal image, August 20, 1978, of the Powder River Basin, Wyo., showing the conspicuously warm areas. The unlabeled lines are profiles A-A' (north line) and B-B' (south line).

0 100 Km

straight Powder River separates warm ground on its east flank from cooler ground on its west flank. This is not just an effect of east- vs. west-facing slopes, because most other stream areas do not show the same effect. The north-south belt in the southern part of the Basin shows as very warm patches of ground. Very warm areas ring the east flank of the Black Hills and occur just to the north throughout the Bear Lodge Mountains, but these do not correspond to the mapped geology. Other contrast stretches were tried including color slicing but the correlations of temperature areas with geology did not improve. What does appear to be true, however, is that within the Powder River Basin, conspicuously warm areas are much more abundant in the north half. For the most part, this is a result of greater dissection of the terrain and more exposure of bedrock, as compared with few outcrops and abundant windblown sand veneer in the south half.

Analysis of the thermal-inertia images, derived from our registration and modeling algorithms, showed that the Tongue River areas of cold ground in daytime are, in fact, areas of high thermal inertia (2000 Thermal inertia units (TIU); $1 \text{ TIU} = 1 \text{ W sec}^{1/2} \text{ m}^{-2}$). These areas (fig. 7) correspond quite well to areas mapped by Raines (Raines and others, 1978), using computer enhancements of Landsat images. They were mapped as the coarsest, sandiest lithofacies unit in the basin, which are relatively indurated and resistant and should crop out best and, depending on moisture conditions, should have the highest thermal inertia of the subunits in the Wasatch and Fort Union Formations. Other such correlations exist for several areas of this facies southeastward toward the Black Hills. Areas of the Wasatch and Fort Union, sampled from various parts of the Basin and which appear to be representative

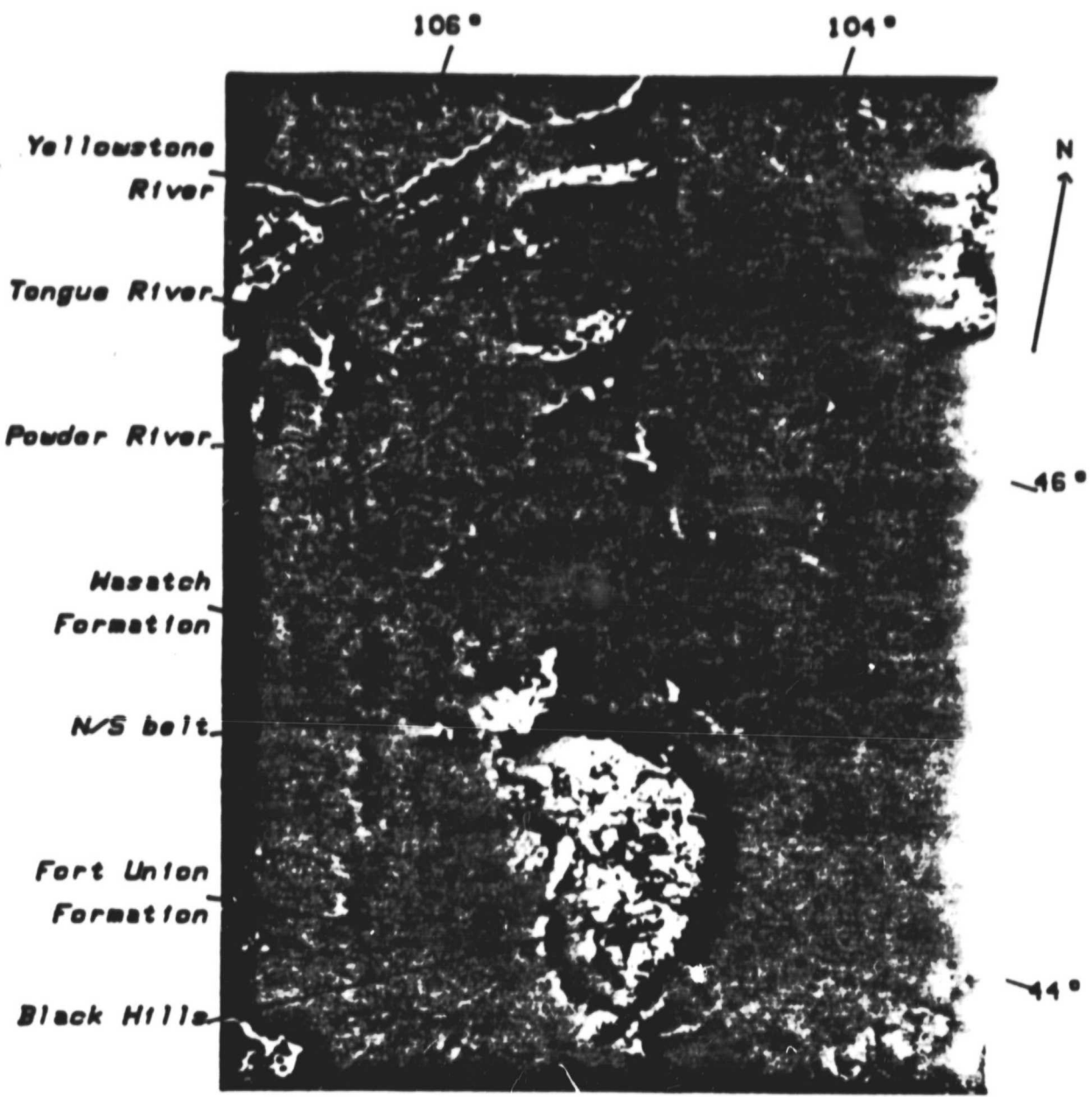


Figure 7.— Thermal-inertia image, August 20, 1978, of
the Powder River Basin, Wyo.

0 100 Km
└──────────────────┘

of larger surrounding areas have thermal-inertias of 1525 TIU and 1450 TIU, respectively. However, the thermal-inertia of these two units varies considerably throughout the basin and in some cases values for these two units are statistically inseparable. A possible explanation is that these units generally form low or flat topography where windblown sand obscures the underlying geology in extremely irregular (and unmapped) patterns. Another reason is that these units retain moisture differently and longer than sandier facies, and thus may have great irregularities in both thermal-inertia values and wind cooling patterns. If they are slightly wet, and not cooled by surface winds, their thermal inertia will be higher.

The north-south belt of high thermal inertia (fig. 7) was initially thought to correspond to burned ground over ancient natural coal fires. The night thermal image (fig. 4) was carefully registered to a base map and a composite map was made showing the areas of clinkers (as determined from a color ratio composite Landsat image) and the warm areas on the HCMM image (fig. 8a). We then examined the thermal-inertia image and determined that the clinker areas in fact have an intermediate thermal inertia (1300 TIU) and the N-S belt of warm ground in the night image just east of the clinker hills has a higher thermal inertia (1500 TIU). This north-south belt has been mapped in detail and the surface geology provides no clue as to why these areas have high thermal inertia. This does not conform with conditions produced where windblown sand accumulates in the lee of topographic highs. It is suspected that the highly fractured clinker hills are readily drained of their near-surface moisture and this ground water tends to pond just eastward in the direction of normal drainage, causing an increase in thermal inertia. This

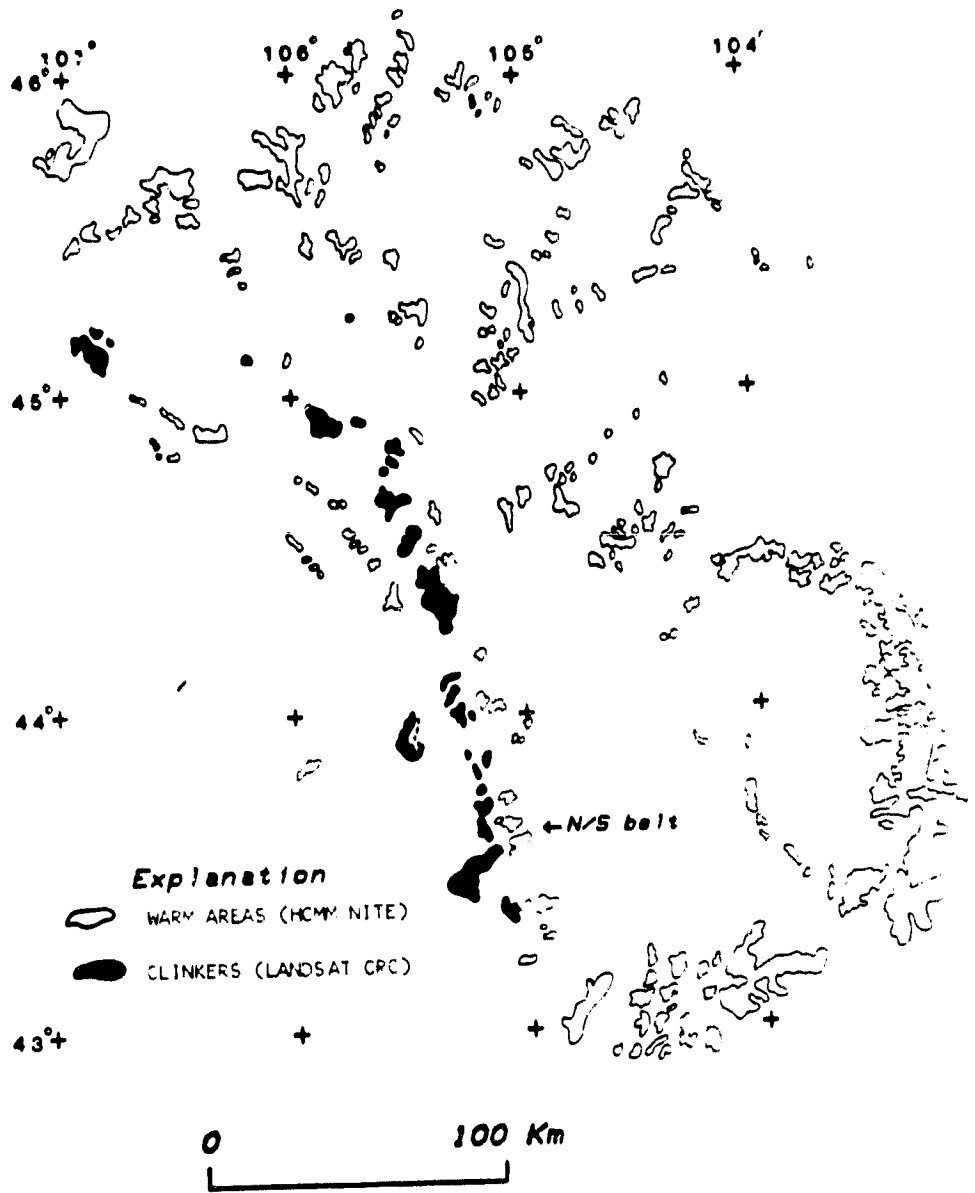


Figure 8a.-- Base map of the Powder River Basin, Wyo., showing the location of the clinkers with respect to the warm areas which have high thermal inertias.

hypothesis is given credence by an examination of the NURE gamma-ray profiles in this area. These areas coincide with lows in the total gamma-ray measurements (fig. 8b) as would be expected for areas of higher moisture content.

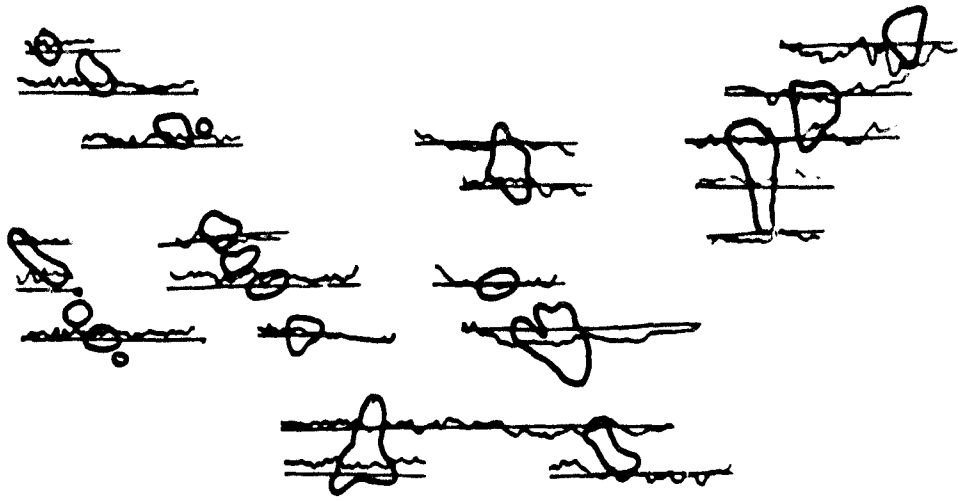
A rough order of magnitude estimate from these data is that the anomalous areas are associated with a 20 percent increase in thermal inertia and a 5 to 10 percent decrease in the total count values. The thermal inertia of soils increases rapidly with increasing soil moisture content and the effect can be estimated for low moisture contents by considering only that increase due to density and specific heat capacity. The ratio of the fractional change in thermal inertia to density is just one half the ratio of the specific heat capacity of water to soil or approximately 2.5. Thus a 20 percent increase in thermal inertia could be produced by a soil moisture change which increases the density by 8 percent (and decreases the total count by an equivalent percent).

To examine the basin further, two northwest-southeast profiles across the 20 August image (fig. 6, profiles A-A', B-B') were constructed. These profiles enabled us to look in detail (pixel level) at variations in thermal-inertia values and to examine relationships between temperature or thermal-inertia patterns and topography. Topographic data were taken from 1:250,000 USGS base maps with a contour interval of 200 feet. Figures 9 through 14 show profiles of thermal-inertia, elevation, and topographic gradient along lines A-A' and B-B'.

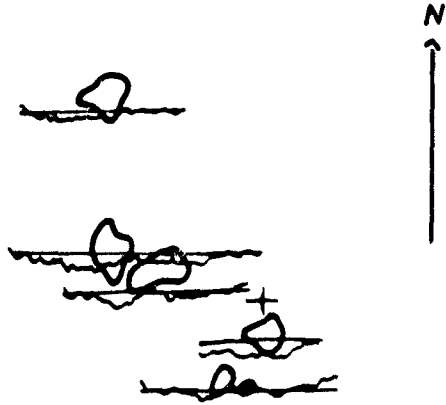
The profiles on A-A' have several interesting features. The line begins in the Wasatch Formation at the northwest end, and thermal-inertia values (fig. 9) decline into a broad low, about coincident with the Powder River

+

105
+ 45



106
44 +



0 25 Km

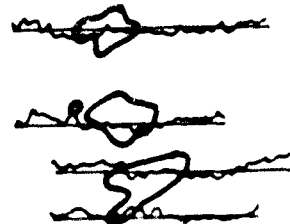


Figure 8b.-- Comparison between profiles of total count gamma ray and the anomalously warm areas. The straight lines indicate the geographic position of the profiles.

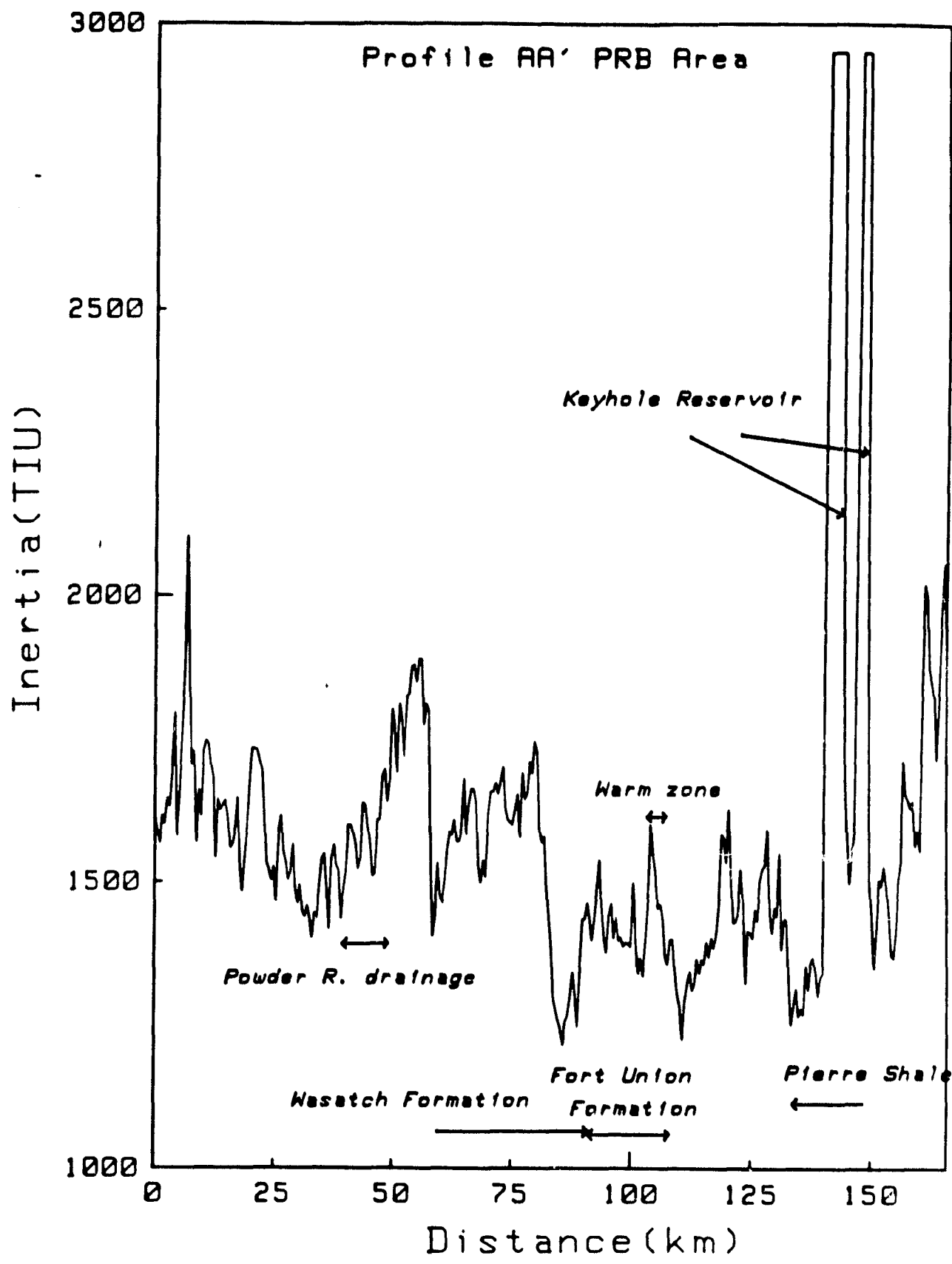


Figure 9.-- Thermal-inertia profile for line A-A'.

drainage seen so clearly in the topographic profile (fig. 10, 11), and then rise. This low approximately marks the basin axis, and the adjacent slopes of the thermal-inertia profile show the character of the upper part of the Wasatch on either side of that axis. The topography itself is somewhat different on opposite flanks of the Powder River drainage, and this probably explains the previous observation that the night-temperature image showed the two flanks differently, even though the thermal-inertia image indicated the two flanks to be underlain by similar material. The flanks have different slopes and bed dips, and the western flank generally is dissected more sharply and deeply than the eastern flank. At the next large drainage east of the Powder River, the thermal-inertia profile breaks sharply, suggesting either a previously unmapped lower unit of the Wasatch or a sharp change to the somewhat finer grained facies which has been noted in the lower part of the formation. Along this profile the Fort Union Formation has a roughly estimated average value of 1425 TIU, as compared with an equally rough, general average of the Wasatch of 1625 TIU. This difference is about what would be expected from the compositions of the two formations, although they are rather nonuniform on the scale of the whole basin. The "typical" areas of Fort Union and Wasatch that were sampled gave values of 1450 TIU and 1525 TIU, respectively. A sharp break in the thermal-inertia profile occurs between the two formations, but it falls 4 to 5 km west of the contact as shown on the geologic map. A break or dip also occurs in the profile at the contact of the upper (Lebo Shale) and lower (Tulloch) members of the Fort Union, but overall the members have about the same thermal inertia. The elevation profile shows a marked change in character of topography from Wasatch to Fort Union, as does

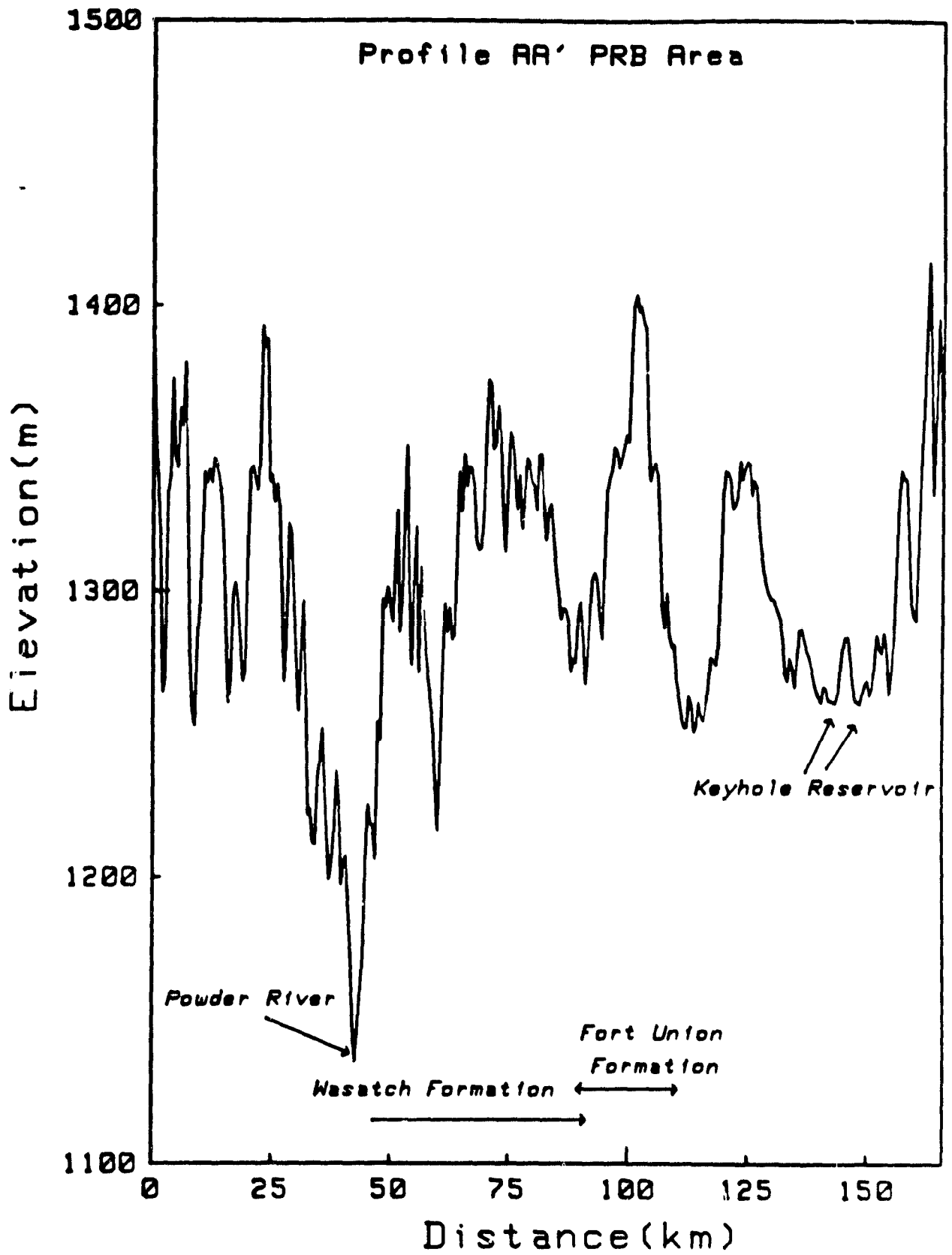


Figure 10.-- Elevation profile for line A-A'.

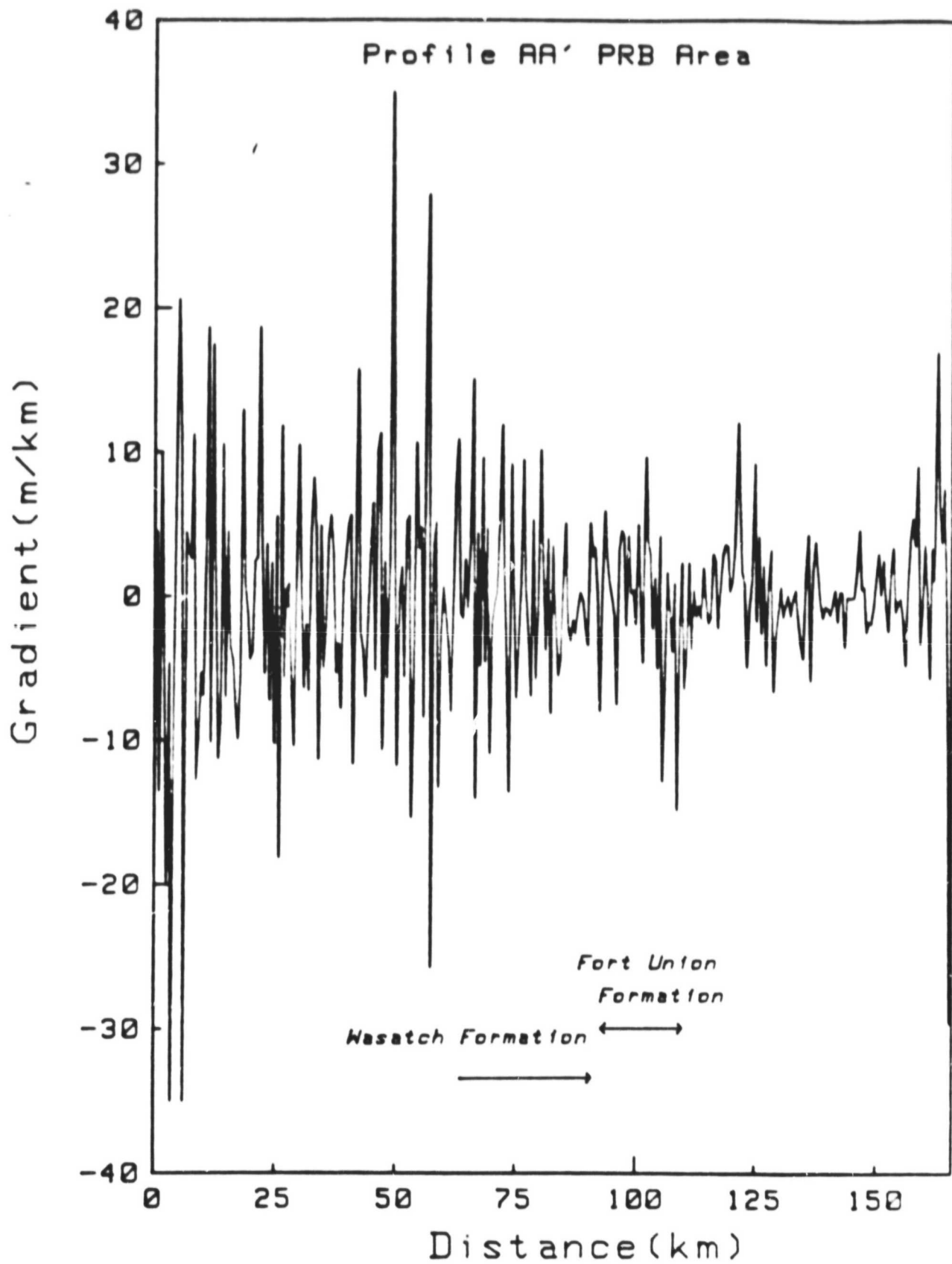


Figure 11.-- Topographic-gradient profile for line A-A'.

the topographic-gradient profile. The warm north-south zone is a narrow but prominent thermal-inertia spike in the lower part of the Lebo Shale Member of the Fort Union. The Pierre Shale has the lowest thermal-inertia of any units along the profile (about 1330 TIU), in huge contrast with the adjacent spikes which mark Keyhole Reservoir.

Line B-B' presents a rather different character in the profiles. The Wasatch thermal inertia (fig. 12) is not at all like that on line A-A'; most of its width on line B-B' is an area of unexplainedly low values which mark a very distinctive and nonrepresentative area within the widespread formation. Wasatch with relatively normal-appearing thermal-inertia image character appears next to the cloud area at the northwest end of the line; there its estimated average thermal inertia is 1550 TIU, only 5 percent different from that seen on line A-A'. The area of low values does not appear to be related to microclimatic factors, nor to any geologic feature of which we are aware. For example, neither here nor elsewhere in the image area do thermal-inertia values closely and consistently correspond with the inferred lithofacies areas delineated in Landsat images. On this line, the Lebo Shale Member of the Fort Union has a roughly estimated thermal inertia of 1750 TIU, higher than the representative Wasatch values. Most of this is in the broadest part of the north-south warm zone, however, so the values almost certainly do not represent normal character. The Tullock Member of the Fort Union is estimated at 1300 TIU, almost 10 percent lower than the Fort Union of line A-A'. Such a change is believed to be both real and significant in terms of the geology, but no data are available as to possible lithologic changes of the unit between the two profile areas. The Pierre Shale has a thermal inertia of 1260

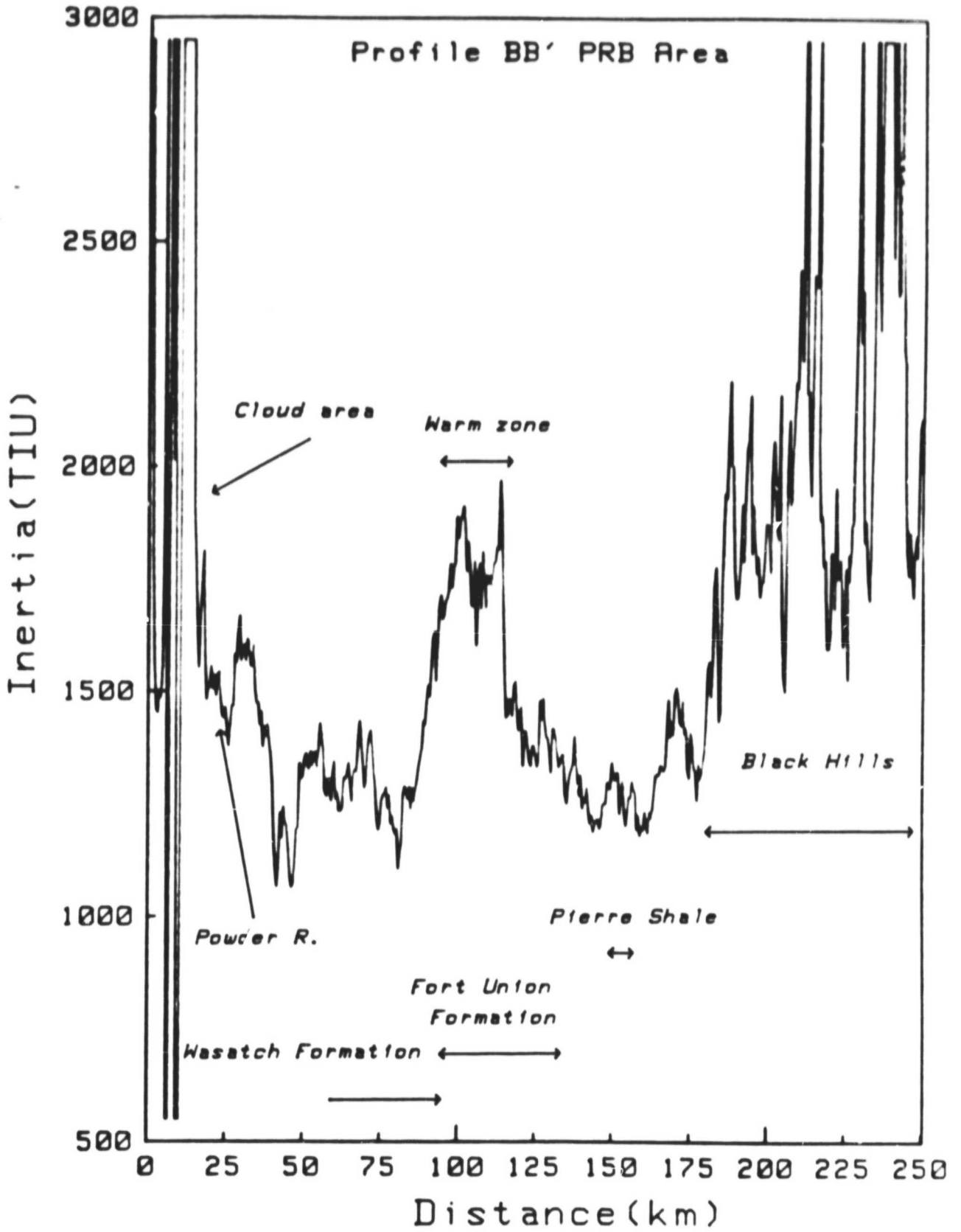


Figure 12.-- Thermal_inertia profile for line B-B'.

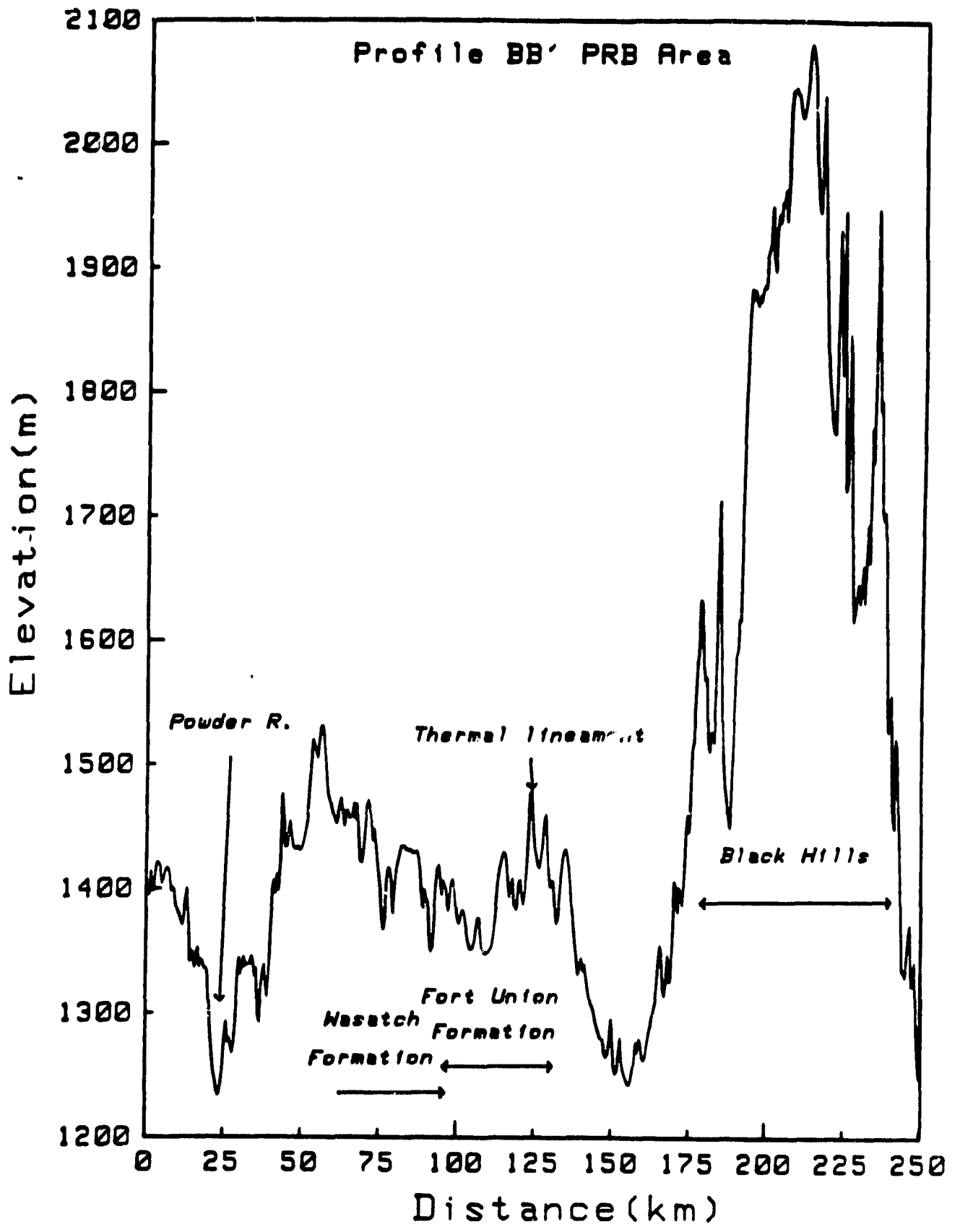


Figure 13.-- Elevation profile for line B-B'.

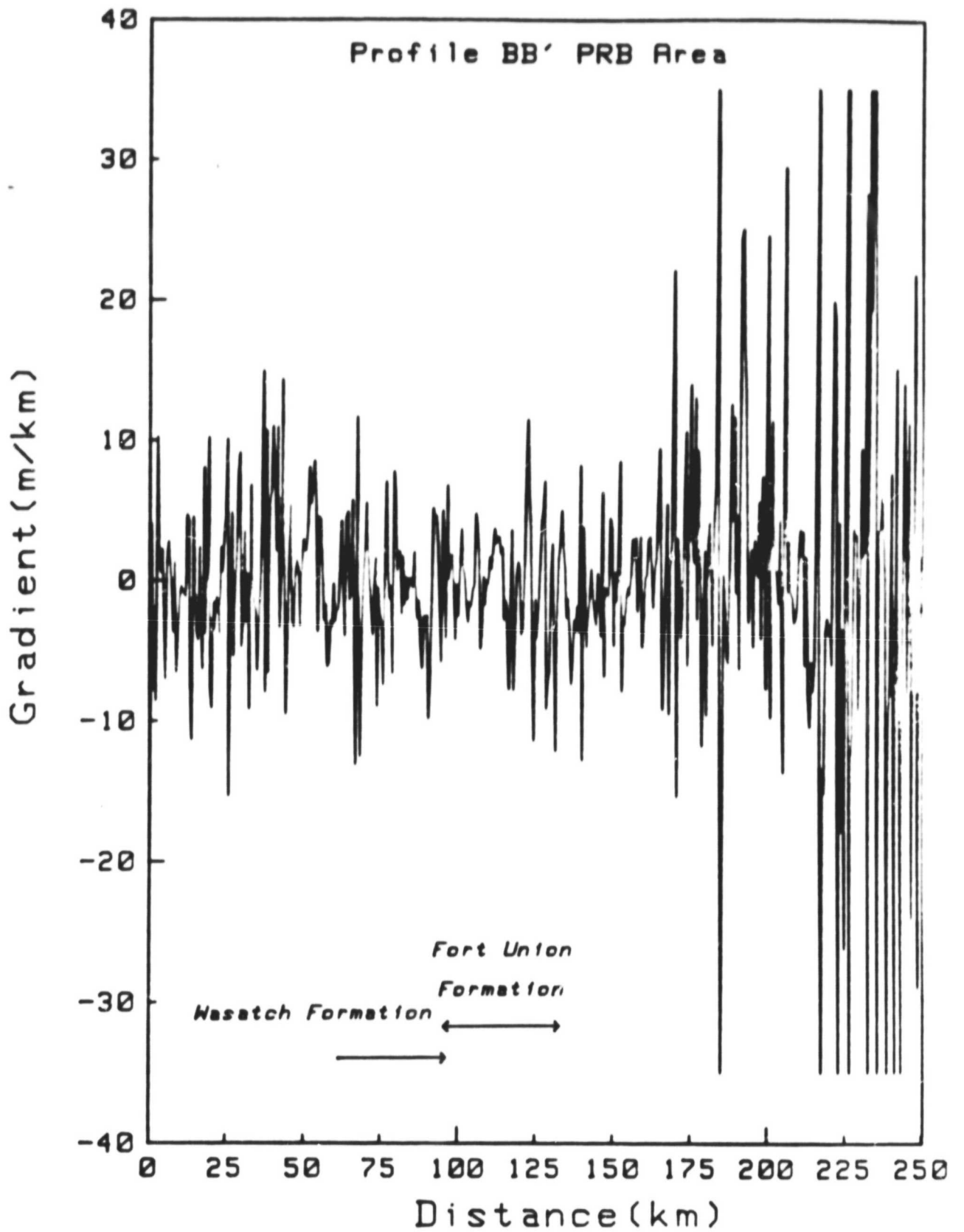


Figure 14.-- Topographic-gradient profile for line B-B'.

TIU, about 5 percent less than observed on line A-A', and again the lowest values of any geologic units on the profile. High and highly variable thermal inertia is seen in the Black Hills portion of the profile as expected in an area of alternating high vegetation density and bare rock exposures.

From this analysis, it appears that thermal data, especially when coupled with topographic information, can aid materially in discriminating geologic formation and member differences, even (as in the Powder River Basin) where units are so variable and exposures so poor that geologists have had real problems or have been unsuccessful in such efforts. It appears that thermal-inertia differences of perhaps as little as 5 percent, and certainly 10-15 percent, can be delineated and used in mapping, probably in terms of both rock units and generalized soils characteristics. So far, patterns seen in thermal-inertia images do not match with vegetation patterns seen in Landsat images and believed to correspond to subtle facies differences. This problem needs further investigation; it may relate to difference in resolution of the two satellites and to differences in depths "seen" by thermal-inertia measurements and vegetation root systems.

2.3.1.2 Geomorphic domains and linear features

An interesting and important aspect of using thermal-inertia images is that erroneous impressions gained from temperature patterns are corrected and a truer picture of surface properties obtained. This is particularly true of night thermal data. For example, the very warm zone around the Black Hills in the night image (fig. 6) disappears in the thermal-inertia image (fig. 7), and a whole new pattern emerges. The contrast of opposite flanks of the Powder

River also disappears, indicating no basic difference in geologic materials across the river. Thus we can use thermal, albedo, and thermal-inertia data in concert to separate physical properties differences (integrated over the top decimeter of the soil or rock profile) from those effects due to such parameters as slope, altitude, and surface reflectance.

For the units underlying most of the Powder River Basin, presently available thermal data and derived products show many unexplained patterns, some of which probably were due to transient (and now untrackable) atmospheric events. Others, however, are believed to reveal real differences in the geologic materials, but current maps in general do not offer a sufficiently detailed base for correlation. Certainly some correlations are found with Landsat-mapped lithofacies, but more day-night pairs covering varying moisture cycles would have been necessary to see through such "noise" as windblown sand, surface-wind cooling patterns, and local moisture variations.

Linear features, often long reaches of streams that appear straight at HCMM resolution, are readily defined in the night images. Many of these coincide with breaks or trends in contoured aeromagnetic data, suggesting that basement tectonic elements have printed through the thick sedimentary sequence to control stream courses. This implies that during sedimentation at earlier times, such features effected some control of sedimentary depositional patterns a conclusion recently elaborated for the Powder River Basin (Slack, 1981).

The most remarkable, previously unrecognized, linear feature appears prominently on the night image of 5 and 27 September (figs. 4 and 15) and also 20 August (fig. 6). Although it is not recognizable as a discrete linear

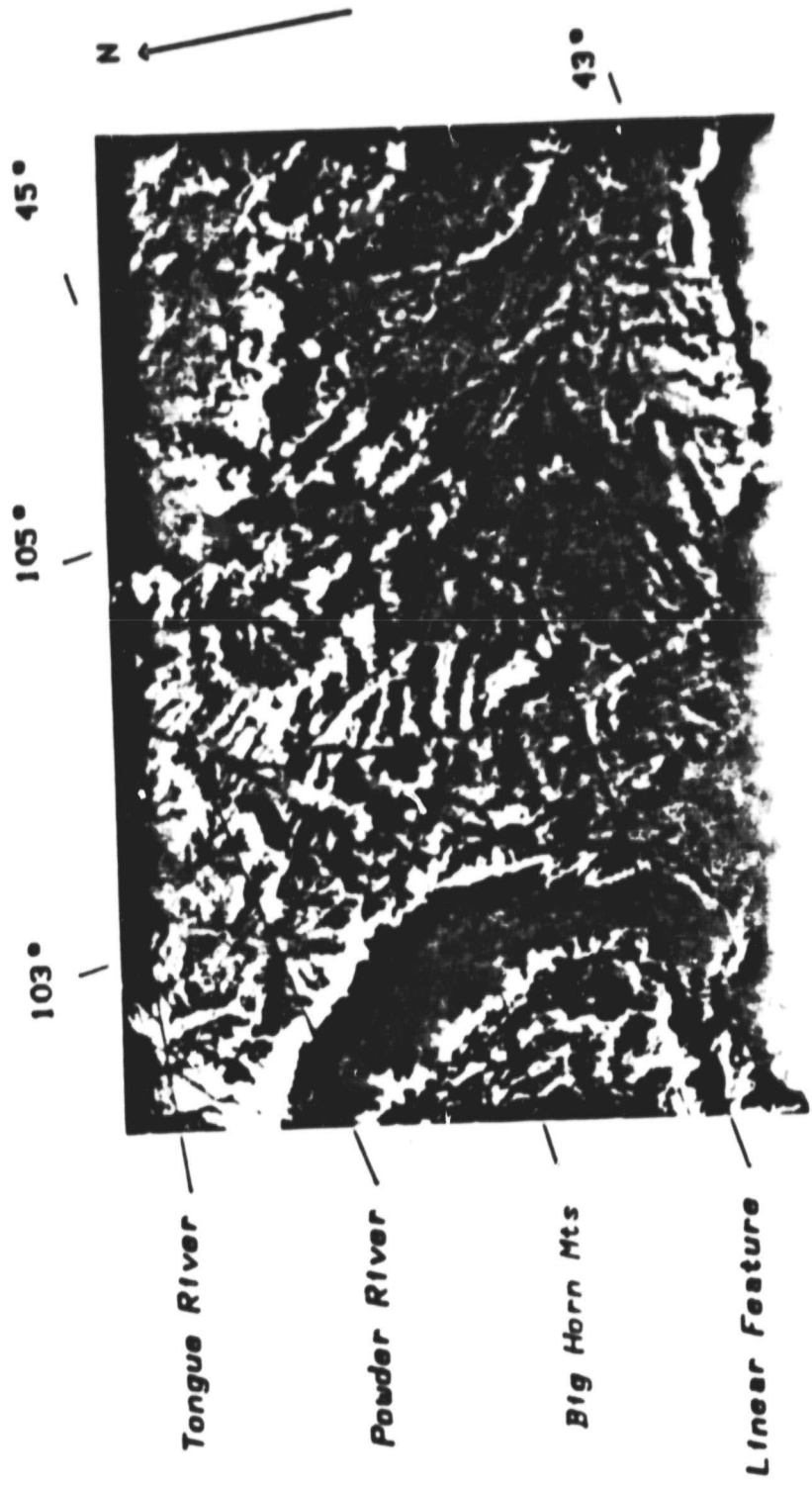


Figure 15.-- Night thermal image. September 27, 1978, of the Powder River Basin, Myo.

feature on Landsat images (fig. 16a), topographic data (fig. 16b) show this lineament as a subtle drainage divide trending about N55°E. On the thermal images the southward-facing side is cooler by 3° or 4° C, and on the 20 August thermal-inertia image (fig. 7), the south side has a 17 percent lower thermal inertia (1215 TIU) than the north side (1460 TIU). Thus, the feature correlates with a subdued drainage divide but it cannot appear due to the slope effect and must represent - at least in part - a physical property difference across the divide. There is no explanation in existing geologic maps (at scales from 1:24,000 to 1:500,000) for this feature or why it separates temperature and topographic domains. The divide is parallel to the prevailing wind direction from the west-south-west as shown in eolian deposits south of the divide. Moreover, the divide also marks a change in direction of wind deposition; deposits to the north are laid down by winds from the north-northwest. It is possible that the relatively common eolian sand cover south of the divide has controlled drainage habit creating the distinctive topographic texture, and the sandy veneer might possibly cause the domain to have lower thermal inertia due to lower moisture retention. It is not likely, however, that the divide lineament itself is wind related. Extended to the northeast, it continues through the linear gap (of the same strike) between the Black Hills and the Bear Lodge Mountains. More important, it directly overlies one of the most significant breaks (fig. 17) in the aeromagnetic-map pattern (U.S. Dept. of Energy, 1979 a, b, and c) of the whole area, it is parallel to and roughly coincident with an inflection in the ground-water temperatures of the Madison Limestone (fig. 18), and its trend passes through several Tertiary intrusives (fig. 19) and possibly even through Lead, South

ORIGINAL PAGE IS
OF POOR QUALITY



Figure 16a.-- Landsat (Band 5) image of the Powder River Basin Area, Wyo. A north-south mosaic line is present roughly 100 Km west of the Black Hills.

ORIGINAL PAGE IS
OF POOR QUALITY

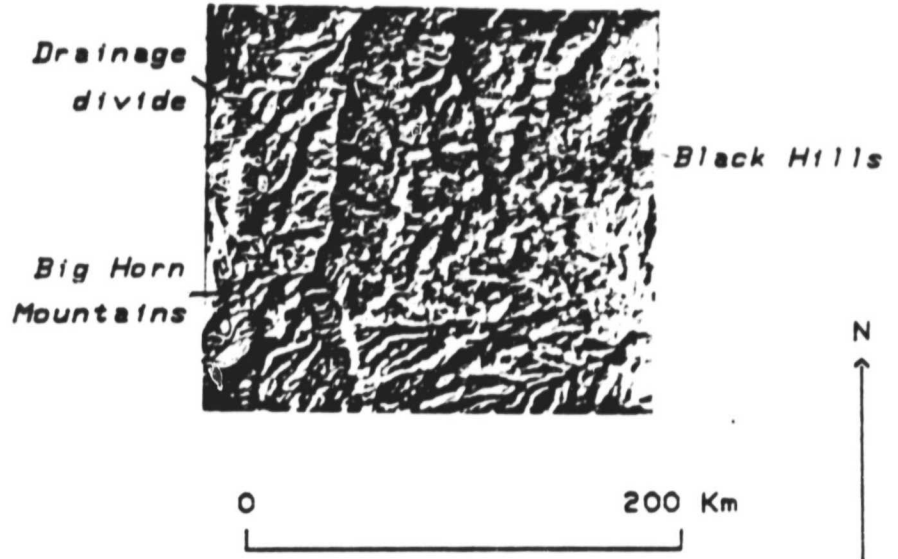


Figure 16b.--Illuminated topography image of the Powder River Basin, Wyo., showing the drainage divide which is coincident with the thermal lineament. The image was computed with a solar declination of -7.8 degrees and a local time of 0930 hrs.

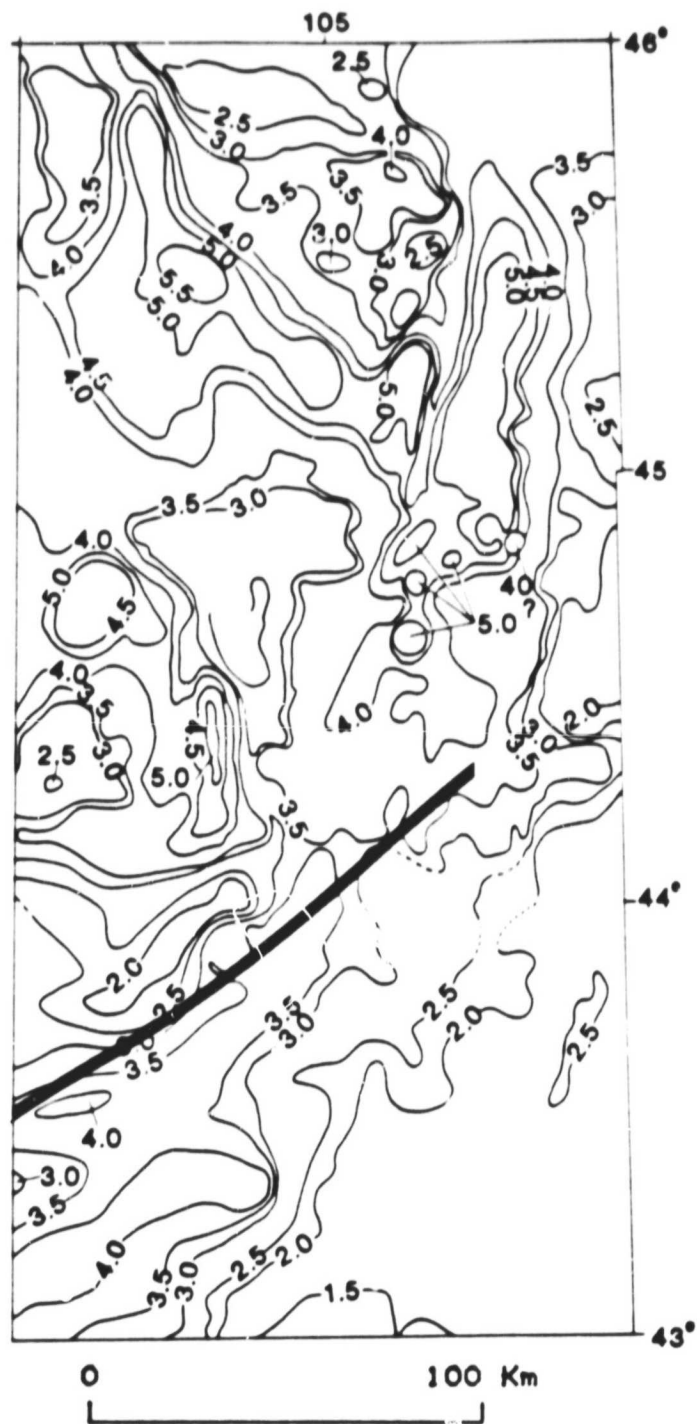


Figure 17.-- Total intensity magnetic field formline map, central Powder River Basin, Wyo. (U.S. Dept of Energy, 1979a-d). The heavy black line shows the position of the thermal lineament.

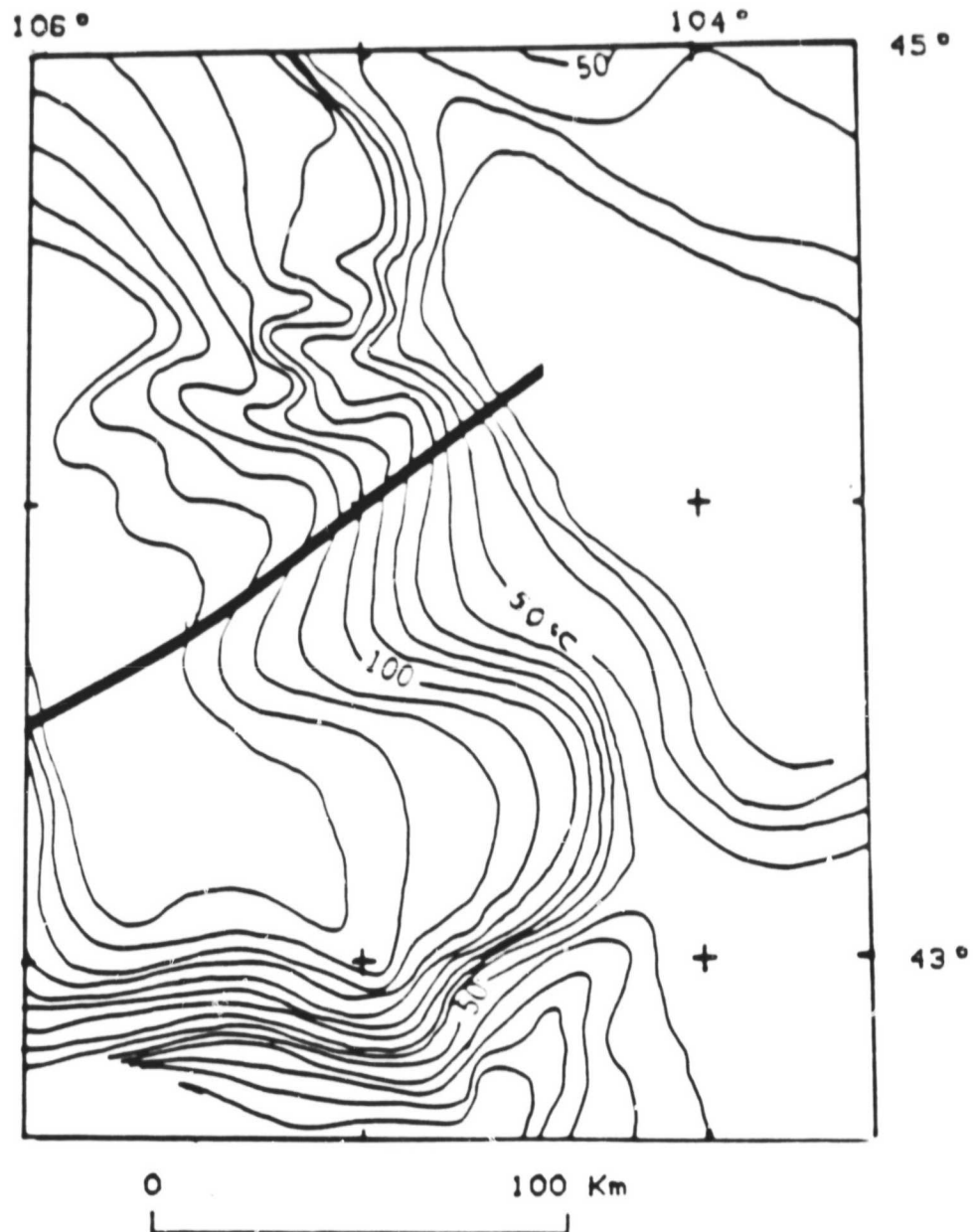


Figure 18.-- Ground water temperatures in the Madison Limestone and equivalent rocks (Head and others, 1978). Heavy black line indicates position of the thermal lineament.

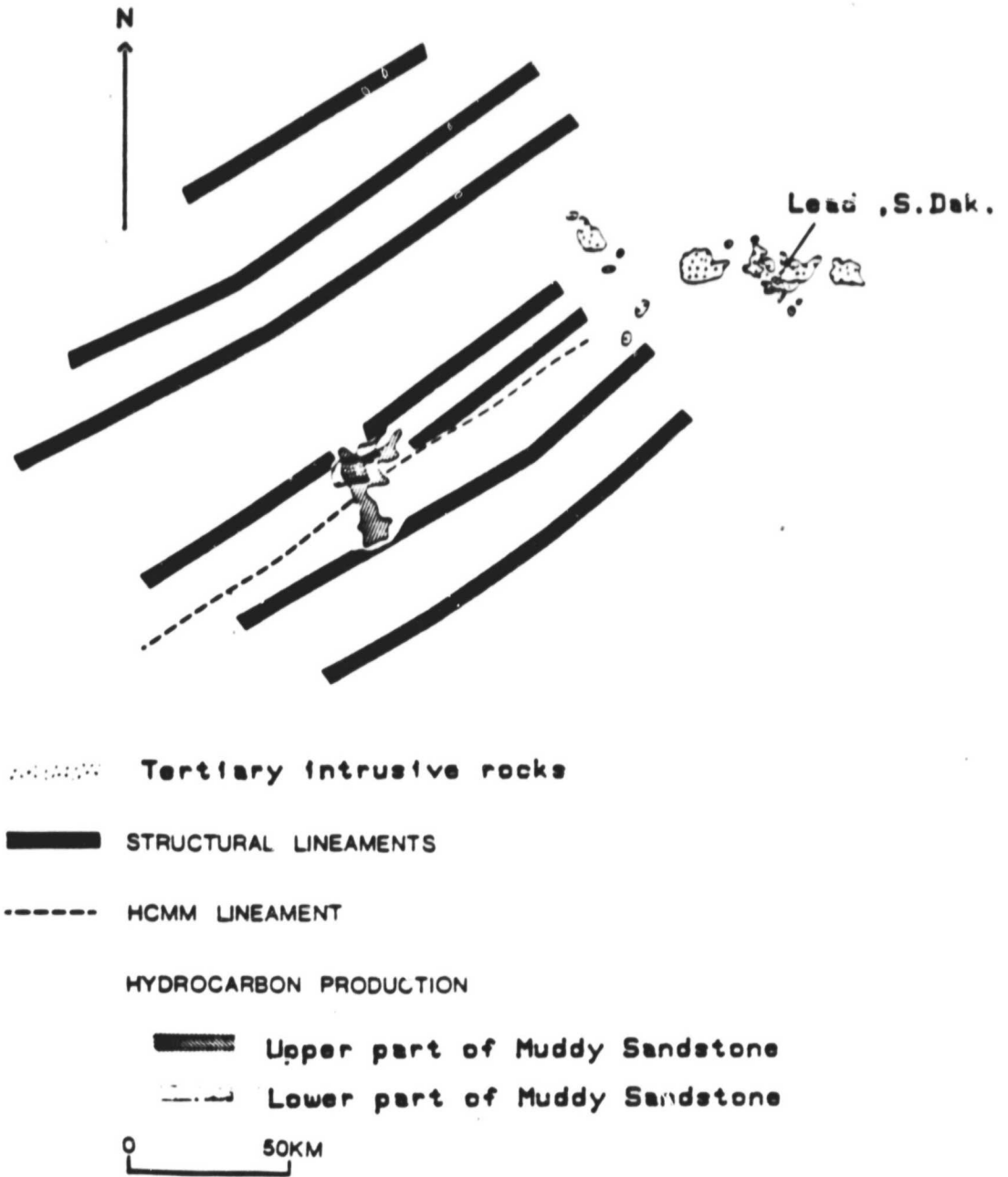


Figure 19.— Location of the thermal lineament with respect to structural lineaments (Slack, 1981) in the Powder River Basin, Wyo.

Dakota location of the Homestake Mine. In addition, stress measurements at Lead (Aggson and Hooker, 1980) imply that the preferred direction for normal faulting would be N50°E, virtually coincident with the orientation of the thermal lineament. Together these pieces of information provide permissive evidence for structural control relating to this feature. A recently published paper (Slack, 1981) presents substantial corroboration for the control. Using subsurface data, Slack proposes that a series of northeast-trending structural lineaments (fig. 19), which he calls the Belle Fourche Arch, have controlled sedimentation in this area and played an important role in determining hydrocarbon accumulation in the southern Powder River Basin. One of his lineaments, Gose Butte, is coincident with part of the thermal feature (fig. 19). Additional supportive evidence for structural control is reflected in the shape of the hydrocarbon producing horizons of the upper and lower parts of the Muddy Sandstone of Cretaceous age (fig. 19).

There is further corroborative satellite evidence for our explanation of the primary cause of the thermal lineament as a thermal-inertia contrast between dissimilar materials. The feature can be seen on two daytime Defense Meteorological Satellite Program (DMSP) thermal satellite images (near noon) and cannot be seen on a nighttime NOAA-5 thermal satellite image (near 9 pm). This latter image is acquired near the time when thermal data should largely be insensitive to thermal-inertia differences because it occurs near the crossing times of the diurnal curves.

We also examined USGS aircraft data across the lineament. Although we had not previously recognized the feature on these data, a very subtle thermal contrast could be observed in the vicinity of the lineament. Largely because

of the slight temperature difference and the regional extent of the feature, it was not recognized on the aircraft data, and this result illustrates convincingly the potential power of regional thermal satellite data over aircraft data for structural-tectonic analysis.

A second, parallel lineament, not a stream divide but separating surface-textural domains, occurs 30 km to the south (figs. 4 and 15) and also overlies an obvious aeromagnetic break. These features appear to mark fundamental structural elements of the southern Powder River Basin and are newly recognized in HCMM data. To the north, parallel lineaments are marked in the images by the Belle Fourche and Little Missouri Rivers.

Information other than on geologic units per se can be gained from these images, most particularly in the demarcation of geomorphic (topographic-temperature) domains and in the discrimination of linear features. Night images are particularly useful in this regard. The 20 August 1978 image (fig. 6) provides very clear definition of major areas of distinctive topography, commonly linked with distinctive temperature patterns. The north and south halves of the basin are distinctly different; the areas east and northeast of the Black Hills differ from each other and from the domains of the basin. Other finer-scale units also are evident. These do not match the mapped geology and, like many geomorphic provinces, are products of a complex development history tied to more factors than the underlying bedrock. We believe that important information can be gained in this aspect of the HCMM images, especially in understanding surface processes during Tertiary and later time. Such information also may lead an understanding of near-surface groundwater hydrology across large, diverse areas. We have examined the domains

from the points of view of mapped geology, ground-water chemistry, mineral and hydrocarbon resources, and tectonic framework, and correspondences are not readily apparent. This is an aspect of the mission data that we did not originally anticipate. However, Schneider and others (1979) showed that the NOAA (National Oceanic and Aeronautics Administration) satellite VHRR (Very High Resolution Radiometer) data with 900-m resolution permitted the defining of geomorphic domains very clearly. This work and our present observations suggest that careful consideration of satellite thermal image data by geomorphologists and hydrologists should be undertaken.

2.3.2 Application to resource studies

2.3.2.1 Oil and gas

It was hypothesized that a few oil and gas fields of the Powder River Basin had enough leakage of gas, probably mostly CO₂, that calcite cementation would have occurred near the surface to make the bedrock more resistant, possibly to form local topographic highs. A few fields do indeed underlie local topographic highs, but this could be fortuitous, and no evidence of leakage and cementation has been cited in the literature. However, a reconnaissance survey of soil-gas helium shows 37 significant helium anomalies within the Wyoming portion of the basin (fig. 20), where most of the oil and gas occurs. The reconnaissance scale of helium sampling does not permit an accurate comparison with individual occurrences of oil and gas except for the largest fields, but it can be said that all but five of the helium anomalies occur over oil and gas fields, and those five are near producing fields. Many



Figure 20.-- Location of helium anomalies, uranium fields, and oil-gas fields in the Powder River Basin, Wyo.

ORIGINAL PAGE IS
OF POOR QUALITY

oil and gas fields do not have overlying helium anomalies, and the implication is considered to be that some fields leak gases upward and many more do not. Perhaps 15-20 percent of oil or gas fields might be considered to have leaked helium, although that number might easily prove twice as large if more detailed sampling were done. The percentage of fields where gases may have produced cementation, especially enough to cause detectable changes in surface-temperature character, clearly would be expected to be small. Thus, it is encouraging to note that visual discrimination suggests thermal-inertia anomalies (20 August image, fig. 7) for 9 out of the 37 areas with anomalous helium values (fig. 20). These areas have consistently and noticeably higher values than the surrounding areas, in keeping with expectations if cementation is locally increased. Most of the areas do not have noticeably different topography than their surroundings. Two of the helium-thermal-inertia areas do not overlie known oil or gas fields but both are surrounded by fields and have several dry holes within the areas. The dry holes may have had only subeconomic shows of oil or gas, in which case leakage to the surface may still have occurred; or perhaps holes simply have not been drilled in the right places. The two areally largest helium anomalies, one over a giant gas field and the other in one over the "barren" areas just described, are marked by fairly distinct oval rings in the thermal-inertia pattern.

Helium anomalies are numerous and areally large in the Montana portion of the basin. They occur in a roughly defined ring which corresponds to the perimeter of a roughly circular area of distinctive topography 75 km wide and approximately bisected by the Powder River. This area is virtually without oil-gas production and few wells are shown on available source maps. But the

helium anomalies correspond to the ring of very warm areas seen in the night 20 August image. We know of no reason to expect such helium anomalies in this region except in association with oil and gas, and the warm areas are mostly areas of outcrop, perhaps where cementation is increased. Information has not yet been found on facies in the subsurface rocks that might contain oil and gas. If the facies are not truly favorable, uneconomic amounts of oil and gas might have been present and leakage could have occurred. If the facies are favorable, the area deserves a closer look for exploration.

An additional point of interest is the possible relationship of HCMM lineaments and oil-gas occurrence. The major thermal lineaments transecting the southern part of the basin (fig. 21) define a block that contains most of the significant helium anomalies. Trends in the helium anomalies as contoured from present data commonly parallel HCMM lineaments. The two largest fields, Fiddler Creek and Clareton, are long and narrow and parallel in trend (and between) the basin-transecting thermal lineaments. The west end of the Clareton field ends in a prominent fork, with the southern one of the main lineaments passing through the fork junction.

2.3.2.2 Uranium

The uranium districts of the Powder River Basin (fig. 20) have local areas of surface alteration as large as 5 by 7 km. These, however, are exposed discontinuously, and differ only slightly in lithologic character and thermal properties relative to the surrounding unaltered ground. If the bedrock were totally exposed, an increase in thermal inertia of perhaps 10 percent might make the altered ground detectable. In any case, the only

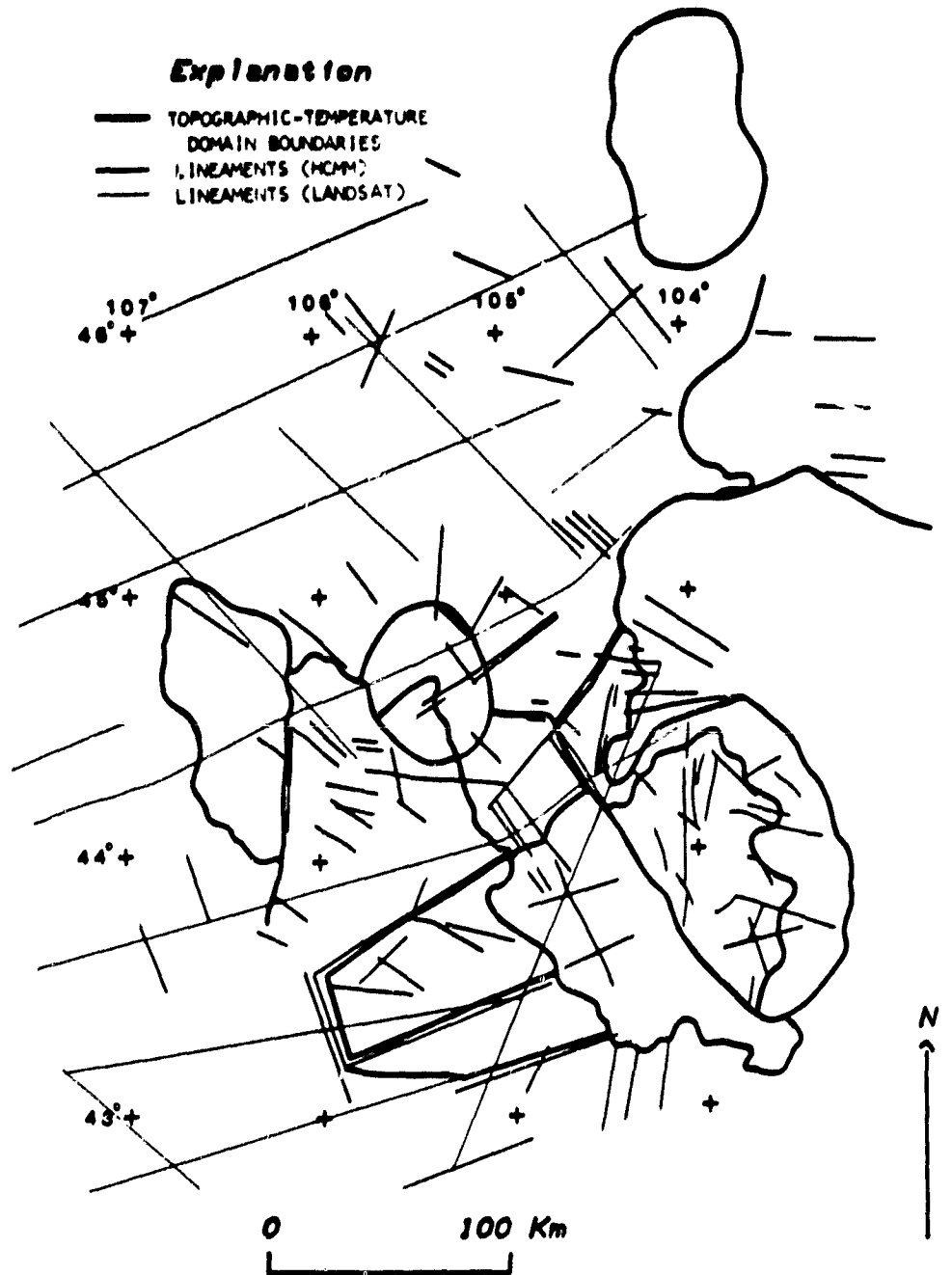


Figure 21.— Major thermal and Landsat (Marris and Raines, 1981) lineaments transecting the southern part of the Powder River Basin, Wyo. and boundaries of the topographic-temperature domains.

thermal-inertia data set does not cover the main uranium areas; the 20 August data end east of the districts or have clouds over the fringe areas where uranium ground occurs. We have examined low-altitude aircraft thermal data for the altered ground, and so far "noise" (soil cover, windblown sand, local topography, and moisture variations) seems to completely overwhelm "signal" related to the discrimination problem.

2.3.2.3 Geothermal flux

Another aspect of our study is to examine the utility of HCMM data for geothermal flux mapping. We found that the underground coal fires now burning north of Sheridan, Wyo., are detectable (barely) on nighttime HCMM thermal images. Comparison with a mosaic of aircraft thermal images of this area (fig. 22) illustrates the scale effects on the appearance of small geothermal anomalies. On the aircraft data the anomalies have a sharp, clearly defined pattern, whereas the satellite data show an indistinct pattern which is not distinguishable from geologic and topographic effects. Also, the satellite appearance of drainage features is distinctly different from the aircraft data. From nighttime aircraft data, the Tongue River appears as a sharp warm anomaly with cooler surroundings. The satellite image, because of its coarser resolution, does not discriminate the narrow water channel, and, thus, the drainage appears entirely as a cool zone.

To examine the expression of geothermal anomalies more fully, HCMM scenes of Yellowstone National Park were analyzed. The region has a classic expression of most of the typical hydrothermal features of a vapor-dominated system. A careful comparison between a nighttime image (fig. 23a) and a detailed

Fires



9/5/78

Sheridan

Fires



Fires



9/27/78

Sheridan

Sheridan

HCMM images

Aircraft image

Figure 22.-- Areas of underground coal fires near Sheridan, Wyo., as seen on HCMM and aircraft thermal data.

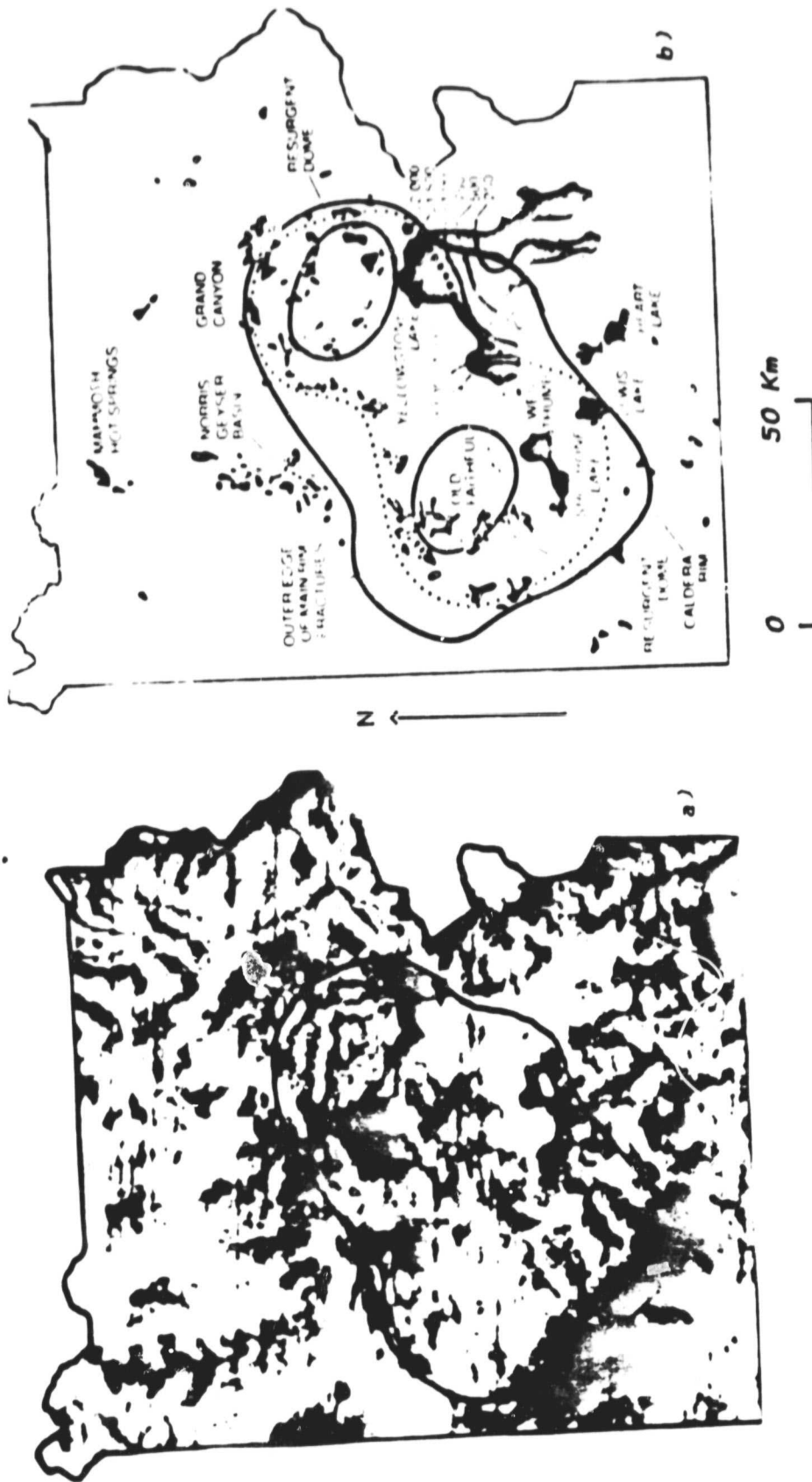


Figure 23a.-- Nighttime thermal image of Yellowstone National Park with caldera outline superimposed.

Figure 23b.-- Location of hydrothermal features (Smith and Christiansen, 1980).

map of the hydrothermal features (Smith and Christiansen, 1980) (fig. 23b) was made using a zoom transfer scope. The hydrothermal features commonly were not expressed as warm anomalies (fig. 24a), and most of the warm anomalies on the images are not hydrothermal-associated features (fig. 24b). These results demonstrate that nighttime satellite images at this scale are unlikely to be useful for detecting similar features elsewhere. Of greater geologic interest was the correlation between the caldera outline, some thermal anomaly lows, and in particular the anomaly bounded by a sharp edge (fig. 23a) which coincides with that part of the gravity field map outlining the southwest side of the caldera (fig. 25b). Although this latter anomaly is a feature with no direct counterpart in Landsat images (fig. 25a), it may provide additional information on the volcanic-tectonic setting. From these brief observations we conclude that the HCMM data can be useful in understanding the regional structural setting of geothermal fields but are not likely to be useful for mapping hydrothermal features.

2.3.2.4 Mapping geologic units in an arid desert environment

The Cabeza Prieta area in Arizona is an arid desert environment with geologic units exposed at a scale suitable for discrimination in HCMM satellite images. The area lies very near the major copper district at Ajo and contains old prospect developments in hydrothermally altered ground. No detailed geologic mapping has been previously done of this area as it contains a proposed Wilderness site. The main objective of our investigation has been to extend the interpretation techniques developed in our Powder River Basin study.

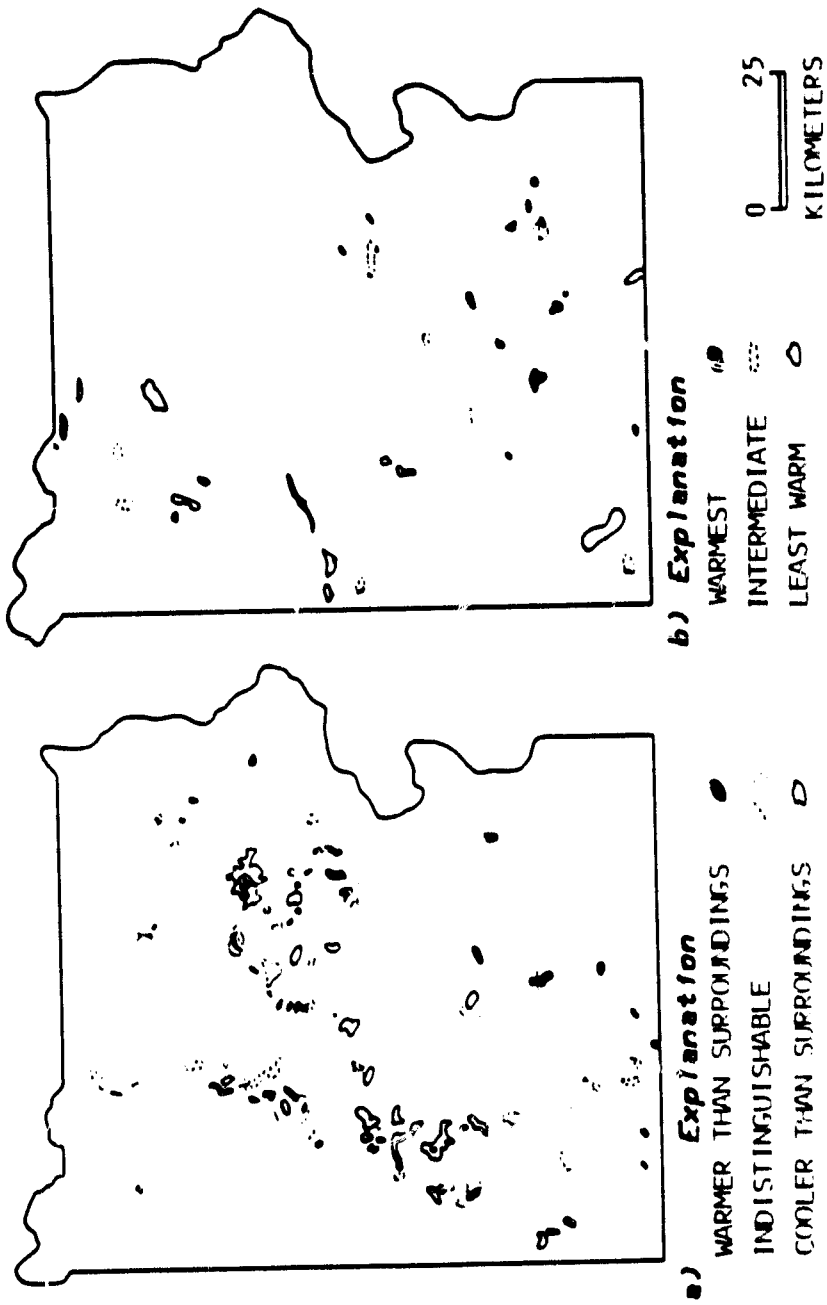
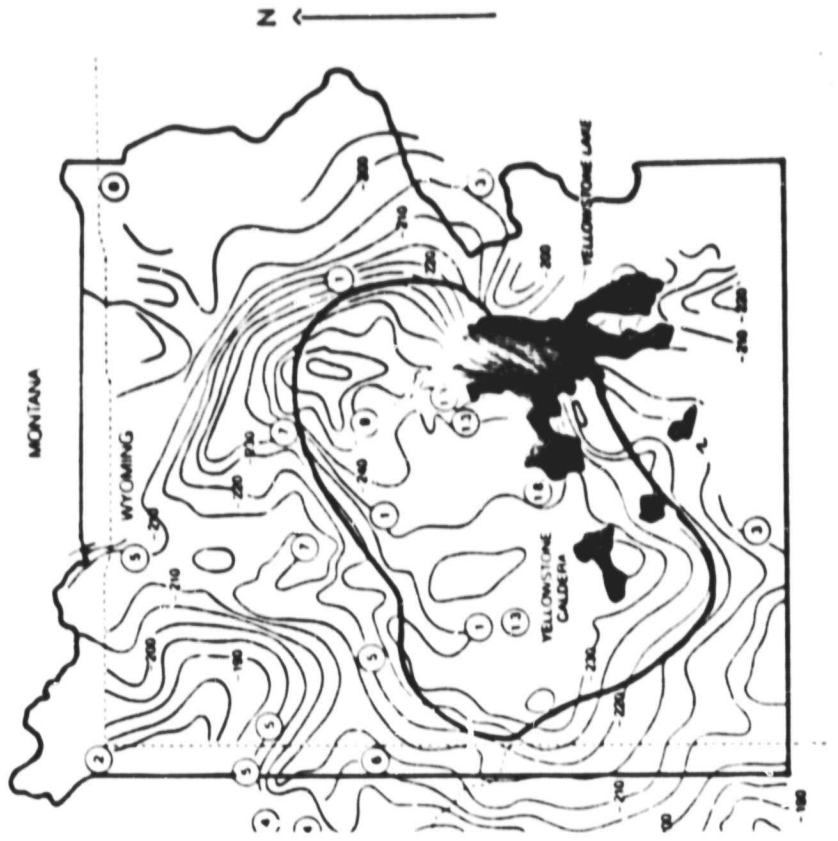


Figure 24a.-- Nighttime temperatures of known hydrothermal features.

Figure 24b.-- Ranking of thermal night anomalies.



a) 0 50 Km b)

Figure 25a.-- Landsat image of Yellowstone National Park with the caldera and park boundaries outlined.

Figure 25b.-- Gravity field contours (Smith and Christensen, 1980).

A thermal-inertia image (fig. 26) was constructed using the April 3 and 4, 1979 scenes (AA0342-09150-3; AA0343-20230-1, 2) with 36-h separation between the day and night acquisition times. The image was then compared to the Ajo geologic map (Kahle and others, compilers, 1978) and an estimate was made of the thermal-inertia values of various geologic materials (table 1). Among the sedimentary deposit materials, a wide range of thermal-inertia values was found. From highest to lowest values these included a wet coal-mine dump near Ajo (1890 TIU), active pediment areas (1360 TIU), stabilized dunes (1065-1300 TIU), and active dunes (830-1065 TIU). The most probable explanation for this ranking is due to the strong effect of moisture content on thermal inertia. Generally, active dunes should have the lowest thermal inertia, as observed, owing to their low density and low capacity to retain moisture.

A somewhat surprising result was that the thermal inertias of the various igneous rock units were measurably different, indicating a finer discrimination capability than previous laboratory data in the literature would suggest (Watson, 1979, 1981a). The literature values of thermal-inertias of igneous rocks show no correlation with either composition or grain size and are indistinguishable from each other. In Cabeza Prieta, however, we found that the felsic intrusives (together with gneiss and schist) had the highest thermal inertias (>2200 TIU), that extrusive rocks of mafic composition had intermediate thermal inertias (approximately 2000 TIU) and that extrusive rocks of less mafic composition had the lowest thermal inertia (<1900 TIU). We believe that the felsic intrusives have the highest thermal inertias because of their high quartz content and high surface density and that the differences among extrusive rocks occur because of density differences associated with the amount of

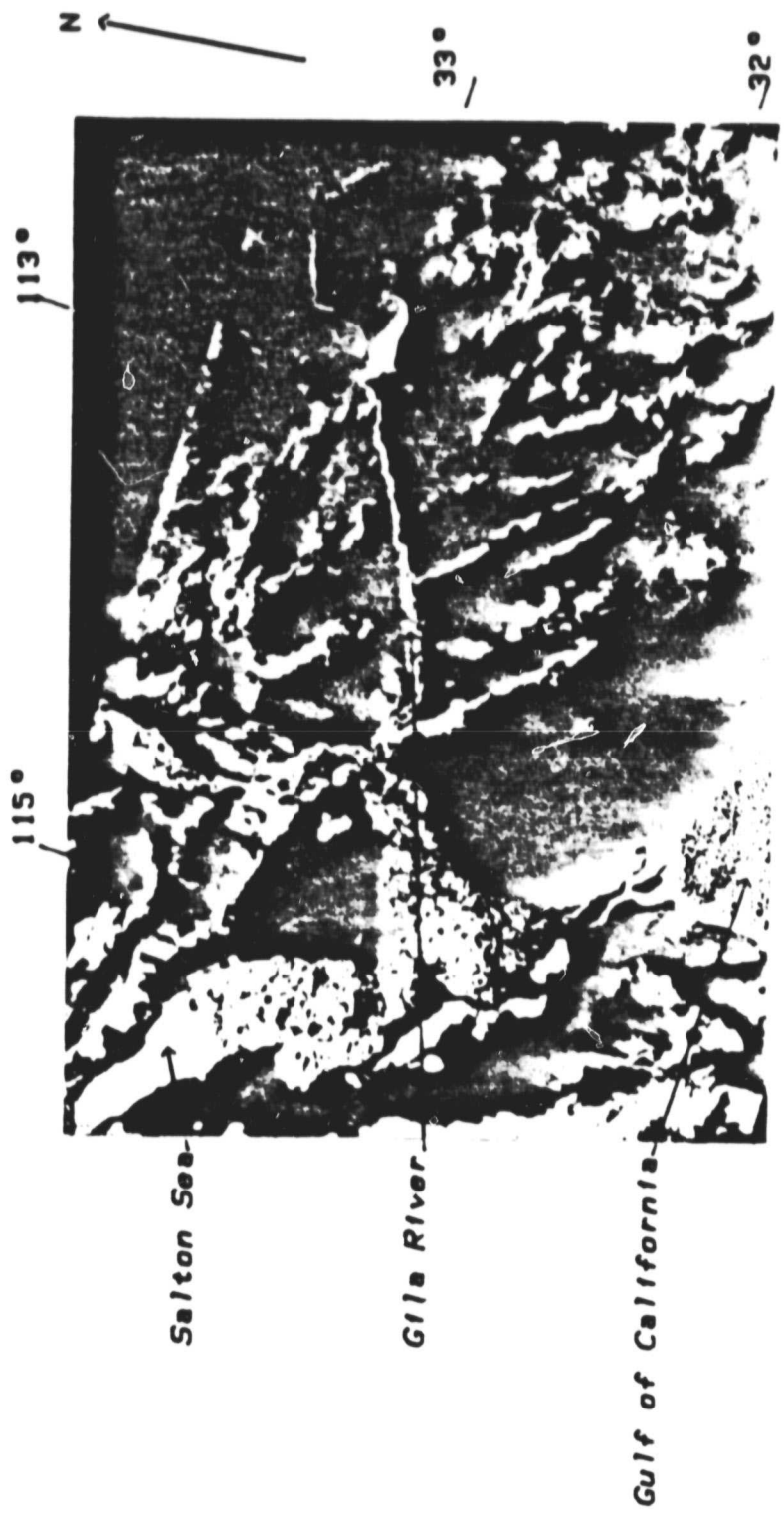


Figure 26.-- Thermal-Inertia Image, April 3/4, 1979 of Cabeza Prieta, Ariz.

ORIGINAL PAGE IS
OF POOR QUALITY

Table 1.--Estimates of thermal inertia of various geologic materials

Geologic Material	Thermal Inertia (TIU)	
	mean	range
Active Dunes	945	(830-1065)
Partially stabilized dunes	1240	
Cluster dunes	1180	(1065-1300)
Active pediment slope	1360	(1300-1475)
Wet mine dump (Ajo)	1890	
Granite, gneiss, schist	2200	(1975-2525)
Mixed intermediate to mafic volcanic rocks	1750	(1550-1950)
Basalt	1950	(1700-2200)

volatiles present during their formation and their mafic content. Although these values are suggestive of the possibility of discriminating among the various units, the large overlap in the range of values (histograms) indicates that classification based solely on thermal inertia differences may not be feasible. The overlap between the units can be attributed to several causes. These units are exposed in the most rugged terrain of the region and thus topographic effects are most pronounced in these parts of the image. The ground that is "sensed" by the technique is a weighted average over the diurnal thermal wavelength (approximately 1 m), with the primary contribution coming from the rock and rock fragments of the upper decimeter. Thus differences in the effects of weathering processes on the various rock types in this environment can produce some degree of thermal-inertia differences.

Because the Powder River Basin was relatively flat terrain the topographic effects were not sufficiently important to be considered. In the Cabeza Prieta area, however, slopes in excess of 20° can be found. To examine the contribution of topography, the thermal inertia measured from remote observations we considered the aspects of elevation and slope separately. The elevation factor due to changes in the solar and sky radiation, has been examined and used to predict the equivalent change in the effective thermal inertia (i.e., that derived from remote rather than in situ measurement) as a function of elevation (Hummer-Miller, 1981b). The effective thermal-inertia gradient under clear-sky conditions should be roughly 100 TIU per kilometer. In Cabeza Prieta, where the maximum relief is 700 m, this maximum correction is only 70 TIU and the factor is additive for increasing elevation (i.e., rocks at higher elevations will appear in the image to have lower thermal inertias).

The slope factor was evaluated by using an algorithm recently developed (Watson, 1981b). The turn has an azimuthal variation proportional to $\cos(\phi - 37.6^\circ)$ where ϕ is the direction of slope measured counterclockwise from north, and thus ridges with an axial orientation of roughly N40°W will display a minimal topographic effect. The most consistent topographic grain in the Cabeza Prieta area is northwest-southeast and thus generally satisfies this constraint. The correction can amount to several hundred TIU's for slopes in excess of ten degrees and orientations orthogonal to N40°W (i.e., N50°E).

The primary intent of this study area was to examine correlations between thermal-inertia values and a variety of common rock types exposed in an arid area. In the process of this analysis we also observed, on the night thermal image, a number of linear features associated with known major faults (San Andreas fault, Garlock fault) and the absence of lineaments in an area near Gila Bend which is noted for the absence of structural features (Gila gap). We also were able to determine a measure of the satellite's spatial frequency response (and thus its ability to detect high-contrast linear features) by the observation that Interstate-10 from Gila Bend to Yuma was observable.

3.0 MODEL DEVELOPMENT

Several advances have been made in the development of techniques to analyze thermal-infrared data. An algorithm to determine the sensible-heat flux from simple field measurements (wind speed, air and ground temperatures) has been developed. It provides a direct solution, in parametric form, that can be displayed graphically or tabularly. This method has an advantage over the previous iterative solution in that the computation is both very fast and

it also provides a clearer understanding of the drag coefficient, with its variation and response to different conditions. At low wind speeds the drag coefficient cannot be treated as a constant. Both the computational speed and analysis of the drag coefficient can be important for remote-sensing applications involving thermal scanner data (Watson, 1980).

A substantial advance was the development of a method, based solely on remote-sensing data, to estimate those meteorological effects which must be known for thermal-inertia mapping. It assumes that the atmospheric fluxes are spatially invariant and that the solar, sky, and sensible heat fluxes can be approximated by a simple mathematical form. Coefficients are determined from a least-squares method by fitting observational data to our thermal model. A comparison between field measurements and the model-derived flux shows that good agreement can be achieved. An analysis of the limitations of the method was also made (Watson and Hummer-Miller, 1981a).

This new method of estimating atmospheric parameters was the basis for a revised thermal-inertia algorithm (Watson, 1981a). The new form is:

$$P_{ij} = (\bar{P} \cdot \Delta \bar{V} + C(\lambda, \delta) (\bar{A} - A_{ij})) / \Delta V_{ij}$$

where A_{ij} and ΔV_{ij} are the corresponding albedo and temperature difference of the ith pixel and jth line. \bar{A} and \bar{V} are the mean values for the area in question, and \bar{P} is a select value for the mean thermal inertia (generally 1500 TIU). $C(\lambda, \delta)$ is a function of the site latitude, λ , and the solar declination, δ . The advantage of this algorithm lies in the fact that we are dealing with albedo and thermal differences rather than absolute values. Thus, the computed thermal inertia is less sensitive to offsets caused by calibration

errors or atmospheric backscattering and transmission effects.

Other modeling studies centered around developing an algorithm for elevation correction of temperature and thermal-inertia images (Hummer-Miller, 1981b). They are based on application of the linearized Fourier series method (Watson, 1975; Watson, 1979) to simple forms of the solar flux (Hummer-Miller, 1981a) derived from a representative set of field observations. It was found that flux variations with elevation can cause changes in the mean diurnal temperature gradient from -4° to -14° C per km (evaluated at 2000 m). Changes in the temperature-difference gradient of 1° - 2° per km are also produced and these are equivalent to an effective thermal-inertia gradient of 100 TIU per km.

In addition, a simple topographic slope correction method has been developed using the linearized thermal model and assuming slopes less than about 20° . The correction can be used to analyze individual thermal images or composite products such as temperature difference or thermal inertia. Simple curves were determined for latitudes of 30° and 50° (Watson, 1981b). The form is easily adapted for analysis of HCMM images using the DMA (Defense Mapping Agency) digital terrain data (Watson, 1981b).

A major concern in this investigation has been the accurate registration of day and night images. We have developed an image-registration algorithm which appears to be substantially better than the current registration products provided by NASA (Watson and others, 1981). The initial test of this algorithm used the 20 August 1978 data of the Powder River Basin. A small number, less than ten, of very clearly delineated features, generally the water-dam interfaces of reservoirs, were selected as control. Subsequently,

an affine transformation was determined by best fitting these points. Our first test indicates a residual error of < 2 pixels. The NASA product for the same scene displays errors of many pixels resulting in "double drainage" effects and an offset of several kilometers.

During the initial stages of our experimentation with control points, we expected that the drainage pattern in the Powder River Basin was substantial enough to provide extensive control for registration. We discovered, however, that drainages are often unreliable identification features and the resulting control points were too inaccurate to provide the transformation coordinates. We also experimented with cross-correlation techniques in the Cabeza Prieta area but were unsuccessful owing to the strong topographic grain. The affine transformation which we employed has the additional advantage that it can be adapted to very fast computer processing schemes (Braccini and Marino, 1980).

4.0 DIGITAL IMAGE PROCESSING

This section presents an outline of the image processing techniques used in this study. Figure 27 is a simplified flow diagram of the basic processing steps; the computer programs referenced in this diagram are included in Appendix A. The initial processing involves obtaining the HCMM computer-compatible tapes (CCT) and altering the data format to be consistent with our computer software. Sometimes the area of interest spans two scenes and, consequently, must be appended into a single file. To produce enhanced images of these products, the appropriate area of the image is statistically sampled to form a histogram and to derive the mean, median, mode, variance, standard

IMAGE PROCESSING

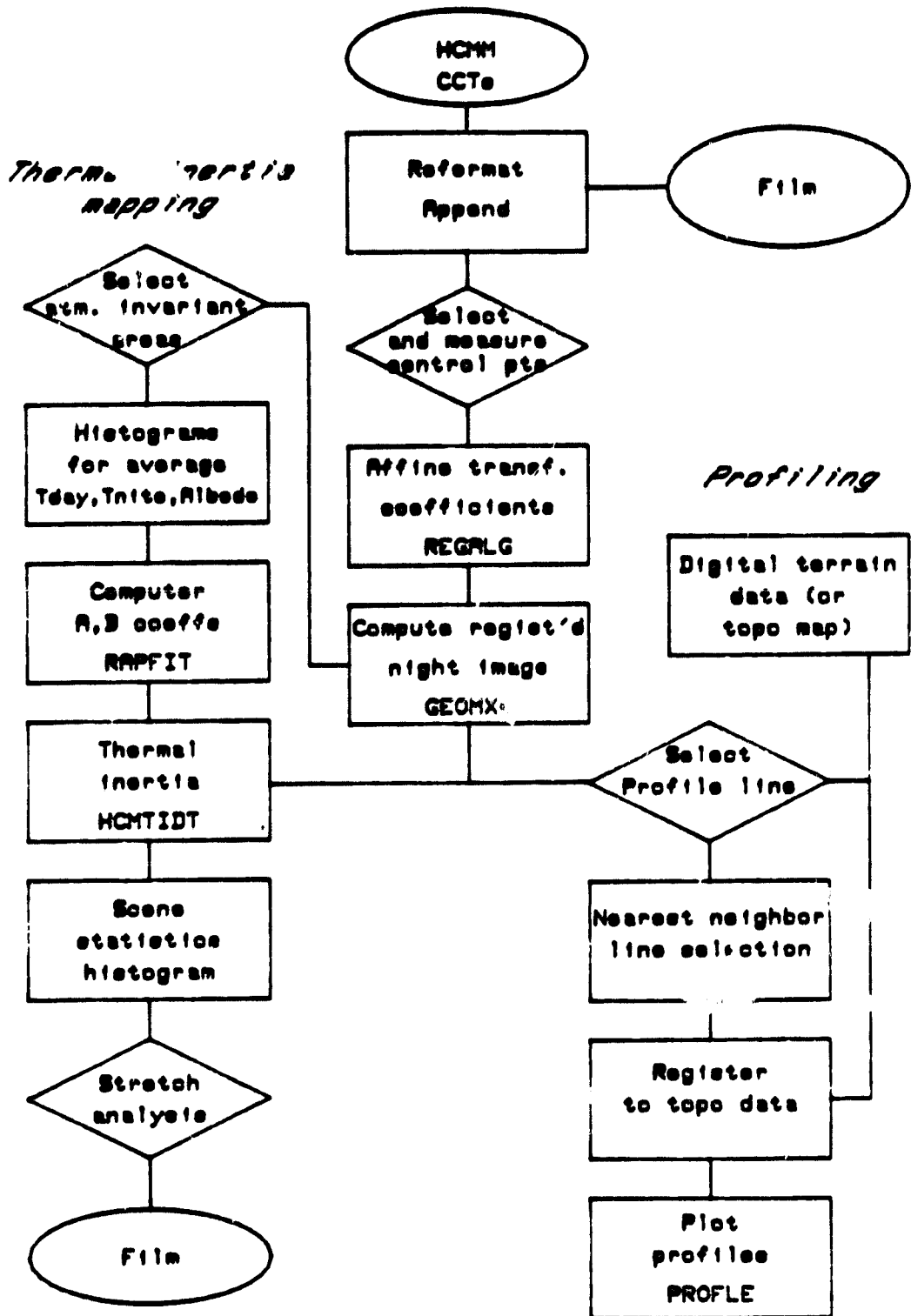


Figure 27.-- Flow chart of the image processing procedure.

deviation, and cumulative frequencies. With these statistics a decision is made as to how the scene contrast should be enhanced using an appropriate transformation of the scene brightness. From our experience a 1 or at most 2 percent linear stretch of the data produces a good starting point. Thus the 1 or 2 percent and 98 or 99 percent points are transformed linearly to the extremes of a 256-step gray scale (0 and 255) and the center density value (D_n) of the distribution is transformed linearly to the center of the gray scale ($127 D_n$). Other useful products include linear stretches on paper where a single print character is assigned for each D_n value and color-coding on film.

The next processing operation is performed to register the night-thermal file to the day files. This operation, including a discussion of the general considerations, are detailed in Watson and others (1981). Control features are selected from the positive transparency images produced from the CCT and locations are measured to one pixel accuracy. These values are then used to determine the affine coefficients for a best-fit transformation (REGALG). This transformation provides a rotation correction for the inclined satellite orbital tracks, an origin shift, and scale changes both along and across the scan line. The actual registration of the night file is then performed using the affine transformation coefficients in the GEOMX4 computer program. This program assigns radiometric values to the newly registered image employing a nearest-neighbor method.

At this stage the data are in the appropriate format for thermal-inertia and temperature-difference mapping. The algorithms which we use (Watson, 1981a) employ average scene values of albedo, day temperature, and night

temperature. The portion of the scene from which these values are determined is based on the assumption of atmospheric invariance and thus, as a minimum constraint must be cloud-free on both images. The program RAPFIT is then used to compute the appropriate coefficients for this algorithm, and the program HCMTIDT is employed to construct both temperature-difference and thermal inertia files. The resulting files are then processed using these techniques described in the beginning paragraph of 4.0.

Another analysis technique used in this study is to construct profiles across the image data. The end points of particular profiles are chosen and digital values along the line are obtained for all products: day reflectance, day thermal, registered night thermal, and thermal inertia using a nearest-neighbor algorithm. The corresponding elevation profile is obtained by digitizing the appropriate portion of a 1:250,000 topographic map and adjusting it to match the satellite data. This task is made easier if the profiles cross distinct features such as reservoirs and rivers. After the elevation data are registered to the satellite data, the program PROFLE is used to plot the profiles and cross plot pairs of data values. The profiles can be plotted at various scales and thus directly overlaid on any base material for comparison. The cross-plotting option is valuable for examining correlations (for example, we observed that the day thermal versus elevation data fit the adiabatic lapse rate).

5.0 REFERENCES

- Aggson, J. R., and Hooker, V. E., 1980, In-situ rock stress determination: techniques and applications, in *Underground Mining Handbook*: Society of Mining Engineers of AIME, New York. in press.
- Braccini, C., and Marino, G., 1980, Fast Geometrical Manipulations of Digital Images: *Computer Graphics and Image Processing*, v. 13, no. 4, p. 127-141.
- Head, W. J., Kilty, K. T., Knotteh, R. K., 1978, Maps showing formation temperatures and configurations of the tops of the Minnelusa Formation and the Madison Limestone, Powder River Basin, Wyoming, Montana, and adjacent areas: U.S. Geological Survey Open-File, 78-905, 10 p.
- Hummer-Miller, 1981a, Diurnal variation of four flux parameters fit to field observations: Submitted to *Journal of Geophysical Research*.
- Hummer-Miller, 1981b, Estimation of surface temperature variations due to changes in sky and solar flux with elevation: *Geophysical Research Letters* (in press).
- Kahle, Katherine, Conway, D., and Haxel, G., compilers, 1978, *Compilation geologic map of the Ajo 1° by 2° quadrangle, Arizona*: Washington D. C., U.S. Geological Survey, 2 sheets, 1:250,000.
- Love, J. D., Weitz, J. L., and Hose, R. K., compilers, 1955, *Geologic map of Wyoming*: Washington, D. C., U.S. Geological Survey, 1 sheet, 1:500,000.
- Marrs, R. W., and Raines, G. L., 1981, *Tectonics of the Powder River Basin, Wyoming and Montana interpreted from Landsat imagery (abs)*: *Sedimentary Tectonics: Principles and Applications*, Laramie, Wyoming, May 3-5, 1981, *Summaries*, p. 19.

- Miller, S. H., Watson, K., and Kipfinger, R., 1980, Ground support data from July 10 to July 29, 1978, for HCMM thermal satellite data of the Powder River Basin, Wyoming: U.S. Geological Survey Open-File, 80-469, 43 p.
- Raines, G. L., Offield, T. W., and Santos, E. S., 1978, Remote-sensing and subsurface definition of facies and structure related to uranium deposits, Powder River Basin, Wyoming: Economic Geology, v. 73, p. 1706-1723.
- Schneider, S. R., McGinnis, Jr., D. F., and Pritchard, J. A., 1979, Use of satellite infrared data for geomorphology studies: Remote Sensing of Environment, v. 8, p. 313-330.
- Slack, P. B., 1981, Paleotectonics and hydrocarbon accumulation, Powder River Basin, Wyoming: American Association of Petroleum Geologists, p. 730-743.
- Smith, R. B., and Christiansen, R. L., 1980, Yellowstone Park as a window on the earth's interior: Scientific American, v. 242, p. 104-117.
- U.S. Department of Energy, 1979a, Aerial gamma ray and magnetic survey, Powder River II Project, Torrington Quadrangle, Wyoming and Nebraska: Report GJBX-158.
- _____ 1979b, Aerial gamma ray and magnetic survey, Powder River II Project, Gillette Quadrangle, Wyoming: Report GJBX-82.
- _____ 1979c, Aerial gamma ray and magnetic survey, Powder River II Project, Newcastle Quadrangle, Wyoming: Report GJBX-82.
- _____ 1979d, Aerial gamma ray and magnetic survey, Powder River II Project, Ekalaka Quadrangle, Montana: Report GJBX-82.
- Watson, K., 1975, Geologic applications of thermal infrared images: Proceedings IEEE, v. 63, p. 128-137.

- Watson, K., 1979, Thermal phenomena and energy exchange in the environment, in Mathematical and Physical Principles of Remote Sensing Centre National D'Etudes Spatiales, Toulouse, France, p. 104-174.
- _____ 1980, Direct computation of the sensible heat flux: Geophysical Research Letters, v. 7, no. 8, p. 616-618.
- _____ 1981a, Regional thermal-inertia mapping from an experimental satellite: Geophysics (in press).
- _____ 1981b, Topographic slope correction for analysis of thermal-infrared images: NTIS (in press).
- Watson, K., and Hummer-Miller, S., 1981a, A simple algorithm to estimate the effective regional atmospheric parameters for thermal-inertia mapping: Remote Sensing of the Environment (in press).
- Watson, K., Hummer-Miller, S., and Sawatzky, D. L., 1981b, Registration of Heat Capacity Mapping Mission day and night images: Photogrammetric Engineering (in press).

5.1 APPENDIXES

Listings of the following computer programs described in section 4.0 follow:

REGALG

RAPFIT

GEOMX4

HCMTIDT

PROFLE

```

30  I REGALG To compute best fit affine transformation for HCMM regist.
20  I Program language is extended Basic.
30  I Program written by K.watson
40  OPTION BASE 1
50  STANDARD
60  INTEGER I,Printer
70  DIM Xold(100),Yold(100),Xnew(100),Ynew(100),Name$(50),S(3),R(3),Xt(100),Yt(100),GS(60),Counter
(100),Pxl(4),Lxl(4)
80  PRINTER IS 16
90  LINPUT "Do you wish to read an input file Y or enter values manually N",Anz$
100 IF Anz$="Y" THEN GOTO 130
110 LINPUT "Do you wish to store an input file Y or N",Any$
120 IF Any$="N" THEN GOTO 350
130 LINPUT "Enter Filename for Day(new) points",File1$
140 IF Any$="Y" THEN CREATE File1$,10
150 LINPUT "Enter Filename for Nite(old) points",File2$
160 IF Any$="Y" THEN CREATE File2$,10
170 IF Any$="Y" THEN GOTO 350
180 ASSIGN #1 TO File1$
190 READ #1;N
200 Nnum=N
210 REDIM Counter(N)
220 READ #1;GS ! Implies a title which is ignored
230 FOR I=1 TO N
240 READ #1;Ynew(I),Xnew(I)
250 Counter(I)=I
260 NEXT I
270 ASSIGN #1 TO File1$
280 ASSIGN #1 TO File2$
290 READ #1;Jmax
300 READ #1;GS ! Ignored title
310 FOR I=1 TO N
320 READ #1;Yold(I),Xold(I)
330 NEXT I
340 GOTO 530
350 INPUT "Enter number of control point quadruples",N
360 REDIM Xold(N),Yold(N),Xnew(N),Ynew(N),Xt(N),Yt(N),Counter(N)
370 Printer=16
380 PRINTER IS Printer ! For debugging
390 LINPUT "Enter a descriptive name <50 char for this registration",Name$
400 INPUT "Enter the maximum lines and pixels from old image",Lmax,Pmax
410 PRINT PAGE
420 PRINT LIN(10),SPA(5),"To enter control points use the format:"
430 PRINT " Day(new) Night(old)"
440 PRINT " scan no,pixel no , scan no,pixel no"
450 FOR I=1 TO N
460 ! NOTE:Scan=Line
470 PRINT LIN(9),SPA(20),"Control point: ";VAL$(I)
480 INPUT "Scan_new,Pixel_new,Scan_old,Pixel_old",Ynew(I),Xnew(I),Yold(I),Xold(I)
490 Counter(I)=I
500 PRINT PAGE
510 NEXT I
520 Enter: PRINTER IS 16
530 PRINT PAGE
540 PRINT LIN(10),SPA(15)," DATA CHECK"
550 PRINT "Control no NEW OLD"
560 PRINT " Line Pixel Line Pixel"
570 FOR I=1 TO N
580 PRINT USING 590;Counter(I),Ynew(I),Xnew(I),Yold(I),Xold(I)

```

```

590 IMAGE DDD, 6X,DDDDDD,4X,DDDDDD, 6X,DDDDDD,6X,DDDDDD
600 NEXT I
610 LINPUT "Are values correct -Y or N ?",Ans$
620 IF Ans$(1,1)="Y" THEN GOTO Cont
630- INPUT "Do you wish to delete values YES or NO ?",Aq$
640 IF Aq$(1,1)<>"Y" THEN GOTO 840
650 INPUT "How many controls to delete ?",Number
660 DIM Check(50)
670 REDIM Check(Number)
680 PRINT "Enter control numbers in any order"
690 MAT INPUT Check
700 MAT SORT Check(*) DES
710 FOR Z=1 TO Number
720 N=N-1
730 MAT SEARCH Counter(*),LOC(Check(2));Istart
740 FOR I=Istart TO N
750 Xold(I)=Xold(I+1)
760 Yold(I)=Yold(I+1)
770 Xnew(I)=Xnew(I+1)
780 Ynew(I)=Ynew(I+1)
790 Counter(I)=Counter(I+1)
800 NEXT I
810 NEXT Z
820 REDIM Xold(N),Xnew(N),Yold(N),Ynew(N)
830 GOTO 530
840 INPUT "Enter control number for incorrect values",K
850 PRINT LIN(20),SPA(5),"Ynew,Xnew,Yold,Xold=";Ynew(K),Xnew(K),Yold(K),Xold(K)
860 INPUT "Enter correct values for all 4 parameters",Ynew(K),Xnew(K),Yold(K),Xold(K)
870 GOTO 530
880 Cont: LINPUT "Do you wish to list control points on printer.",List$
890 IF List$(1,1)<>"Y" THEN GOTO 980
900 PRINTER IS 0
910 PRINT "Control no          NEW          OLD"
920 PRINT "          Line          Pixel          Line          Pixel"
930 FOR I=1 TO N
940 PRINT USING 590;Counter(I),Ynew(I),Xnew(I),Yold(I),Xold(I)
950 IMAGE DDD,7X,DDDDD,2X,DDDDD, 9X,DDDDD,2X,DDDDD
960 NEXT I
970 PRINT LIN(5)
980 CALL Bilinear(Xnew(*),Ynew(*),Xold(*),R(*),N)
990 CALL Bilinear(Xnew(*),Ynew(*),Yold(*),S(*),N)
1000      ! Where: Xold=R(1)*Xnew+R(2)*Ynew+R(3)
1010      !         Yold=S(1)*Xnew+S(2)*Ynew+S(3)
1020      ! Thus to transform a night image the new DN values are computed:
1030      ! DNnew(Pixel,Line)=DNold(P,L)
1040      ! where P=R(1)*Pixel+R(2)*Line+R(3)
1050      ! and L=S(1)*Pixel+S(2)*Line+S(3)
1060 PRINTER IS 0
1070 Del12=R(1)*S(2)-S(1)*R(2)
1080 Del13=R(3)*S(1)-S(3)*R(1)
1090 Del23=R(2)*S(3)-R(3)*S(2)
1100 Px1(1)=S(2)-R(2)
1110 Px1(2)=S(2)*Pmax-R(2)
1120 Px1(3)=S(2)*Pmax-R(2)*Lmax
1130 Px1(4)=S(2)-R(2)*Lmax
1140 Lx1(1)=R(1)-S(1)
1150 Lx1(2)=R(1)-S(1)*Pmax
1160 Lx1(3)=R(1)*Lmax-S(1)*Pmax
1170 Lx1(4)=R(1)*Lmax-S(1)
1180 MAT Lx1=Lx1+(Del13)

```

```

1190 MAT Lx1=Lx1/(Del12)
1200 MAT Px1=Px1/(Del23)
1210 MAT Px1=Px1/(Del12)
1220 MAT SEARCH Px1(*),MAX;Pxmax
1230 MAT SEARCH Px1(*),MIN;Pxmin
1240 MAT SEARCH Lx1(*),MAX;Lxmax
1250 MAT SEARCH Lx1(*),MIN;Lxmin
1260 Dpix=Pxmax-Pxmin+1
1270 Dlin=Lxmax-Lxmin+1
1280 Alpha=R(1)*(Pxmin-1)+R(2)*(Lxmin-1)+R(3)
1290 Beta=S(1)*(Pxmin-1)+S(2)*(Lxmin-1)+S(3)
1300 C2=Alpha*S(2)-Beta*R(2)
1310 C3=Alpha*S(1)-Beta*R(1)
1320 Pix_old_mean=SUM(Xold)/N
1330 Pix_new_mean=SUM(Xnew)/N
1340 Lin_new_mean=SUM(Ynew)/N
1350 Lin_old_mean=SUM(Yold)/N
1360 Del=Del12
1370 Pix_off=S(2)/Del*Pix_old_mean-R(2)/Del*Lin_old_mean-C2/Del-Pix_new_mean
1380 Lin_off=-(S(1)/Del)*Pix_old_mean+R(1)/Del*Lin_old_mean+C3/Del-Lin_new_mean
1390 Cos_theta=(R(1)+S(2))/2
1400 Sin_theta=(S(1)-R(2))/2
1410 DEG
1420 Theta=ATN(Sin_theta/Cos_theta)
1430 Mag_x=SQR(R(1)^2+S(1)^2)
1440 Mag_y=SQR(R(2)^2+S(2)^2)
1450 PRINT "SOLUTION FOR:"
1460 PRINT Name$
1470 PRINT
1480 PRINT "Original image is ";Pmax;" pixels by ";Lmax;" lines."
1490 PRINT
1500 PRINT
1510 STANDARD
1520 PRINT "R=";R(1);R(2);Alpha
1530 PRINT
1540 PRINT "S=";S(1);S(2);Beta
1550 PRINT
1560 PRINT "BK mod:R(3)= ";R(3);" S(3)= ";S(3)
1570 PRINT
1580 PRINT "where: DNnew(Pixel,Line)=DNold(P,L)"
1590 PRINT
1600 PRINT "      P=R(1)*Pixel+R(2)*Line+R(3)"
1610 PRINT "      L=S(1)*Pixel+S(2)*Line+S(3)"
1620 PRINT
1630 PRINT " New image size: ";Dpix;" pixels by ";Dlin;" lines."
1640 PRINT
1650 PRINT " Mean rotation angle :";Theta
1660 PRINT " Magnification :-X ";Mag_x;" -Y ";Mag_y
1670 PRINT
1680 PRINT " Offset:      Pixels ";Pix_off
1690 PRINT "              Lines  ";Lin_off
1700 PRINTER IS Printer
1710 Plotting: CALL Plot("Initial controls:",Xold(*),Yold(*),Xnew(*),Ynew(*),N,Name$,Counter(*))
1720 Residual=0
1730 PRINTER IS 0
1740 Max_residual=0
1750 PRINT
1760 PRINT " Control no.          Xt          Xt          Residual"
1770 Del=Del12
1780 C2= Del23

```

```

1790 C3=Del13
1800 FOR I=1 TO N
1810 Xt(1)=(Xold(1)*S(2)-Yold(1)*R(2)-C2)/Del
1820 Yt(1)=-((Xold(1)*S(1)-Yold(1)*R(1)-C3)/Del
1830 Max_red=(Xt(1)-Xnew(1))^2+(Yt(1)-Ynew(1))^2
1840 PRINT Counter(I),Xt(1),Yt(1),SUR(Max_red)
1850 Residual=Max_red+Residual
1860 Max_residual=MAX(Max_red,Max_residual)
1870 IF Max_residual=Max_red THEN I_max_res=Counter(I)
1880 NEXT I
1890 Max_res=SQR(Max_residual)
1900 Residual=SQR(Residual/(N-1))
1910 FIXED 2
1920 PRINTER IS 0
1930 PRINT
1940 PRINT
1950 FIXED 2
1960 PRINT " Mean residual vector length =" ; Residual ; " pixels"
1970 PRINT " Max residual vector length =" ; Max_res ; " pixels" ; " at point " ; I_max_res
1980 PRINT
1990 CALL Plot("Transformed controls:",Xt(*),Yt(*),Xnew(*),Ynew(*),N,Name$,Counter(*))
2000 GOTO Enter
2010 END
2020 SUB Bilinear(X(*),Y(*),Z(*),M(*),N)
2030 I Z=M(1)*X+M(2)*Y+M(3) LEAST SQUARES ESTIMATE FOR M
2040 OPTION BASE 1
2050 DIM S(100,3),Transpose(3,100),Inverse(100,100),Dum(100,100),Z(100,1),M(3,1)
2060 REDIM S(N,3),Transpose(3,N),Inverse(N,N),Dum(N,N),Z(N,1)
2070 FOR I=1 TO N
2080 S(1,1)=X(I)
2090 S(1,2)=Y(I)
2100 S(1,3)=1
2110 Z(1,1)=Z(I)
2120 NEXT I
2130 MAT Transpose=TRN(S)
2140 MAT Dum=Transpose*S
2150 MAT Inverse=INV(Dum)
2160 MAT Dum=Inverse*Transpose
2170 MAT M1=Dum*Z
2180 FOR J=1 TO 3
2190 M(J)=M1(J,1)
2200 NEXT J
2210 SUBEND
2220 SUB Plot(Plot_title$,Xnew(*),Ynew(*),Xold(*),Yold(*),N,Name$,Counter(*))
2230 OPTION BASE 1
2240 INTEGER I
2250 STANDARD
2260 PLOTTER IS 13,"GRAPHICS"
2270 GRAPHICS
2280 LOCATE 5,150,5,95
2290 MOVE 10,97
2300 LABEL Plot_title$ " " ; Name$
2310 MAT SEARCH Xnew,MAX;Xmax
2320 MAT SEARCH Xold,MAX;Xmax1
2330 Xmax=MAX(Xmax,Xmax1)
2340 MAT SEARCH Yold,MAX;Ymax1
2350 MAT SEARCH Ynew,MAX;Ymax
2360 Ymax=MAX(Ymax,Ymax1)
2370 MAT SEARCH Ynew,MIN;Ymin
2380 MAT SEARCH Yold,MIN;Ymin1

```

```

2390 Ymin=MIN(Ymin,Ymin1)
2400 MAT SEARCH Xold,MIN;Xmin1
2410 MAT SEARCH Xnew,MIN;Xmin
2420 Xmin=MIN(Xmin,Xmin1)
2430 SHOW Xmin-25,Xmax+25,Ymax+25,Ymin-25
2440 LINE TYPE 1
2450 FRAME
2460 LORG 2
2470 CSIZE 2.5
2480 FOR I=1 TO N
2490 MOVE Xold(I),Yold(I)
2500 DRAW Xnew(I),Ynew(I)
2510 Xx=Xnew(I)-Xold(I)
2520 Yy=Ynew(I)-Yold(I)
2530 IF Yy=0 THEN GOTO 2550
2540 LDIR Xx,Yy
2550 MOVE Xnew(I),Ynew(I)
2560 IF Xx>=0 THEN LABEL ">"&VAL$(Counter(I))
2570 IF Xx<=0 THEN GOTO 2620
2580 LORG 8
2590 LDIR -Xx,-Yy
2600 LABEL VAL$(Counter(I))&"<"
2610 LORG 2
2620 NEXT I
2630 SETGU
2640 LDIR 0
2650 CSIZE 3.3
2660 MOVE 69,3
2670 LORG 5
2680 LABEL "CONT to continue;DUMP GRAPHICS for hard copy"
2690 PAUSE
2700 EXIT GRAPHICS
2710 SUBEND
2720 END

```



```

10  I  RAPFIT To perform the regional atmospheric fitting.
20  I  Program language is extended Basic.
30  I  Program written by K.Watson
40  I  Mapping algorithm development.
50  I  ENTER: SITE LATITUDE AND SOLAR DECLINATION.
60  I  PROGRAM COMPUTES Tday AND Tnite FOR THE HCM4 TIMES ,
70  I  VARYING THE Tsky AND Sky_factor.
80  I  INPUT OBSERVATIONAL DATA
90  I  Tdayo,Tniteo;Albedo
100 I  COMPUTE THE Standard Deviation for temp data - Shade print output.
110 Picons=SQR(PI*3600*24)
120 OPTION BASE 1
130 DIM Flux1(24),Temp(24),Phi(24),Flux(24),Strings(10)(80)
140 DIM P1(24,24),P5(24,24),Cosz(24),Dev(20,20)
150 INTEGER I,K,L,Delik
160 DEG
170 I  RECALL THE Phi's.
180 ASSIGN #1 TO "Phi_m"
190 READ #1;M
200 IF M=24 THEN GOTO 230
210 PRINT "ERROR : ;";M;" P  VALUES - SHOULD BE 24"
220 STOP
230 READ #1;Phi(*)
240 ASSIGN #1 TO "Phi_m"
250 INPUT "Enter the site latitude(Degrees) ",Latitude
260 INPUT "Enter the solar declination(Degrees) ",Solar_dec
270 OUTPUT 9;"R"
280 ENTER 9;T5
290 W=F1/12
300 W1=F1/(12*3600)
310 So=1360
320 Sigma=5.67E-8
330 I  FIXED PARAMETERS.
340 Emissivity=1
350 Slope=0
360 Azimuth=0
370 Flux_diffuse=0
380 INPUT "Enter the mean day Temp (DEG K) from scene data",Tdayo
390 INPUT "Enter the mean nite Temp (DEG K) from scene data",Tniteo
400 C1=CCS(Latitude)*COS(Solar_dec)
410 S1=SIN(Latitude)*SIN(Solar_dec)
420 Cosz(1)=C1+S1
430 FOR K=2 TO 24
440 Cosz(K)=C1*COS((K-1)*15)+S1
450 IF Cosz(K)<0 THEN Cosz(K)=0
460 NEXT K
470 C21=SIN(Slope)*SIN(Azimuth)*COS(Solar_dec)
480 C22=COS(Latitude)*COS(Slope)-SIN(Slope)*COS(Azimuth)*SIN(Latitude)
490 C2=C22*COS(Solar_dec)
500 C23=SIN(Latitude)*COS(Slope)+COS(Latitude)*COS(Azimuth)*SIN(Slope)
510 C23=C23*SIN(Solar_dec)
520 INPUT "Enter mean 'A' %",Albedo
530 Inertia=1500
540 Deviation2=10000
550 Cons2=Inertia/Picons
560 I  LOOP PARAMETERS. FIRST LOOP
570 PRINTER IS 0
580 PRINT " Tsky","Sky factor", " Deviation"
590 Return: PRINTER IS I6

```

```

600 INPUT "Tsky_max",Tsky_max
610 INPUT "Tsky_min",Tsky_min
620 INPUT "Dtsky",Dtsky
630 INPUT "Sky_factor_max",Sky_factor_max
640 INPUT "Sky_factor_min",Sky_factor_min
650 INPUT "Dsky_factor",Dsky_factor
660 Dev_min=1E9
670 Ken: FOR Tsky=Tsky_min TO Tsky_max STEP Dtsky
680 PRINT "Tsky=";Tsky
690 Flux_sky=Sigma*Tsky^4
700 FOR Sky_factor=Sky_factor_min TO Sky_factor_max STEP Dsky_factor
710 OUTPUT #1;"R"
720 ENTER #;Month,Day,Hour,Minute,Second
730 PRINT TAB(20);"Sky_factor=";Sky_factor,Hour;" ";Minute
740 Flux_direct=So*(1-Sky_factor)
750 FOR I=1 TO 24
760 X=(1-I)*.15
770 Cosz1=Cosz(1)
780 IF Cosz1<0 THEN Cosz1=0
790 Flux1(I)=(1-Albedo)*(Flux_diffuse+Cosz1*Flux_direct)+Emissivity*Flux_sky
800 NEXT I
810 Sum=0
820 FOR I=1 TO 24
830 Sum=Flux1(I)+Sum
840 NEXT I
850 Sum=Sum/M
860 Vo=(Sum/(Emissivity*Sigma))^-.25
870 Alpha=3*Emissivity*Sigma*Vo^3
880 Cons=Cons2/Alpha
890 Cons1=Alpha^4/3
900 FOR I=1 TO 24
910 Flux(I)=Flux1(I)+Alpha*Vo
920 NEXT I
930 FOR I=1 TO 24
940 FOR K=1 TO 24
950 L=I-K+1
960 IF L<1 THEN L=L+24
970 Delik=0
980 IF I=K THEN Delik=1
990 P5(I,K)=Cons2*Phi(L)+Cons1*Delik
1000 NEXT K
1010 NEXT I
1020 MAT P1=INV(P5)
1030 I FORM Temp
1040 MAT Temp=P1*Flux
1050 I REMEMBER Temp(K) is at time K-1 hours. (measured from noon)
1060 Tday=(Temp(2)+Temp(3))*0.5
1070 Tnite=(Temp(14)+Temp(15))*0.5
1080 I1=(Tsky-Tsky_min)/Dtsky+1
1090 J1=(Sky_factor-Sky_factor_min)/Dsky_factor+1
1100 Dev(I1,J1)=SUR((Tday-Tday0)^2+(Tnite-Tnite0)^2)
1110 Dev_min=MIN(Dev_min,Dev(I1,J1))
1120 IF Dev(I1,J1)=Dev_min THEN Tsky_opt=Tsky
1130 IF Dev(I1,J1)=Dev_min THEN Sky_factor_opt=Sky_factor
1140 PRINTER IS 0
1150 PRINT Tsky,Sky_factor,Dev(I1,J1);I1;J1
1160 PRINTER IS 16
1170 NEXT Sky_factor
1180 NEXT Tsky
1190 BEEP

```

```

1200 PRINT "Optimum (at: Tsky =";Tsky_opt,"sky_factor =";Sky_factor_opt
1210 GOTO Return
1220 INPUT "Enter THE I (Tsky) AND J (Sky_factor) VALUES",I,J
1230 Tskyo=310+(10-I)*10
1240 Sky_factoro=(J0-1)*.05
1250 I LOOP PARAMETERS. SECOND LOOP
1260 FOR Tsky=Tskyo-2 TO Tskyo+2 STEP 1
1270 PRINT "Tsky=";Tsky
1280 Flux_sky=Signo*Tsky^4
1290 FOR Sky_factor=Sky_factoro-.02 TO Sky_factor+.02 STEP .01
1300 OUTPUT 5;"R"
1310 E=TLR 9;Month,Day,Hour,Minute,Second
1320 PRINT TAB(20);"Sky_factor=";Sky_factor,Hour;" ";Minute
1330 Flux_direct=Sc°.6*(1-Sky_factor)
1340 FOR I=1 TO 24
1350 X=(1-I)*15
1360 Ccsz1=Cosz(1)
1370 IF Cosz1<0 THEN Ccsz1=0
1380 Flux1(I)=(1-Albedo)*(Flux_diffuse+Cosz1*Flux_direct)+Emissivity*Flux_sky
1390 NEXT I
1400 Sum=0
1410 FOR I=1 TO 24
1420 Sum=Flux1(I)+Sum
1430 NEXT I
1440 Sum=Sum/M
1450 Vc=(Sum/(Emissivity*Sigma))^*.25
1460 Alpha=3*Emissivity*Sigma*Vo^3
1470 Cons=Cons2/Alpha
1480 Cons1=Alpha^4/3
1490 FOR I=1 TO 24
1500 Flux(I)=Flux1(I)+Alpha*Vo
1510 NEXT I
1520 FOR I=1 TO 24
1530 FOR K=1 TO 24
1540 L=I-K+1
1550 IF L<1 THEN L=L+24
1560 Delir=0
1570 IF I=K THEN Delir=1
1580 P5(I,K)=Cons2*Phi(L)+Cons1*Delir
1590 NEXT K
1600 NEXT I
1610 MAT P1=INV(P5)
1620 I FORM Temp
1630 MAT Temp=P1*Flux
1640 I REMEMBER Temp(K) is at time K-1 hours. (measured from noon)
1650 Tday=(Temp(2)+Temp(3))*0.5
1660 Tnite=(Temp(14)+Temp(15))*0.5
1670 I1=(Tsky-250)/5+1
1680 J1=Sky_factor/.05+1
1690 Dev(I1,J1)=SUK((Tday-Tskyo)^2+(Tnite-Tniteo)^2)
1700 PRINT Tsky,Sky_factor,Dev(I1,J1)
1710 NEXT Sky_factor
1720 NEXT Tsky
1730 Min_dev=1E15
1740 FOR I=1 TO 5
1750 FOR J=1 TO 6
1760 Min_dev=MIN(Min_dev,Dev(I,J))
1770 IF Dev(I,J)=Min_dev THEN Io=I
1780 NEXT J

```

```
1790 NEXT I
1800 Tsky=Tskyo+(10-3)*I
1810 Sky_factor=Sky_factoro+(J0-3)*.01
1820 STOP
1830 END
```

```

PROGRAM GEOMX4
C.....
C.....
C..... REMOTE SENSING ARRAY PROCESSING PROCEDURES
C..... U. S. GEOLOGICAL SURVEY, DENVER, COLORADO
C..... BRANCH OF PETROPHYSICS AND REMOTE SENSING
C..... DON L. SAWATZKY
C.....
C
C      GEOMX4 GENERATES A RECTIFIED IMAGE FILE FROM A DISTORTED IMAGE
C FILE AND FROM COEFFICIENTS FOR RECTIFICATION, R AND S, DETERMINED FOR AN
C AFFINE TRANSFORMATION OF THE DISTORTED FILE.
C INPUT FILE STRUCTURE CONSISTS OF A HEADER RECORD CONTAINING TWO
C INTEGERS FOR LINE LENGTH, LENREC, IN PIXELS AND NUMBER OF LINES,
C NORECS. NORECS NUMBER OF DATA RECORDS FOLLOW, EACH RECORD CONTAINING LENREC
C BYTES OF 8-BIT DATA. OUTPUT FILE HEADER RECORD CONTAINS TWO INTEGERS OF LINE
C LENGTH, NPIXOUT, AND NUMBER OF RECORDS, LMAX. INPUT PARAMETERS, IPIXIN AND NPIX
C XIN, ALLOW TAKING A SUBSET OF THE INPUT FILE. OUTPUT PARAMETERS LMAX, MNPIX
C , AND MXPIX ARE SELECTED ON THE LINE LENGTH OF THE INPUT FILE AND DEGREE
C OF ROTATION REQUIRED FOR RECTIFICATION. SECTIONS OF THE OUTPUT FILE OF LENGTH
C LMAX AND CONTAINING PIXELS MNPIX TO MXPIX ARE GENERATED BY ONE OR MORE ITER
C ATIONS OF THIS PROGRAM. SECTIONS ARE CONCATENATED IN SUBSEQUENT PROCESSING.
C SECTIONING THE OUTPUT FILE IS DONE IN RESPONSE TO THE MESSAGE: "INBUF ARRAY
C TOO SMALL."
C
C.....DECLARATIONS
      REAL R(3),S(3)
      LOGICAL*1 INBUF(200000),OUTBUF(3000)
      INTEGER FCBIN(35),FCBOUT(35)
C.....
C.....SET PARAMETERS
      WRITE(6,99)
99  FORMAT(1X,'ENTER PIXEL/LINE COEFFICIENTS ':)
      READ(5,96) R,S
      WRITE(6,98)
98  FORMAT(1X,'ENTER INPUT FIRST PIXEL, NO. PIXELS')
      READ(5,96) IPIXIN,NPIXIN
      WRITE(6,97)
97  FORMAT(1X,'ENTER MAX. OUTPUT LINES,MIN/MAX PIXEL ':)
      READ(5,96) LMAX,MNPIX,MPPIX
96  FORMAT(G16.0)
C.....
C.....OPEN DATA FILE TO TRANSFORM
      READ(8) LENREC,NORECS
C.....SETUP WORK ARRAY
      NRECS=MIN(200000/LENREC,NORECS)
      MXLINE=NRECS
      MNLINE=1
      J1=LENREC*MOD(1,NRECS)+1
      J2=J1+LENREC-1
      DO 90 I=1,NRECS
90  READ(8) (INBUF(J),J=J1,J2)
C.....
C.....OPEN OUTPUT DATA FILE
      NPIXOUT=MXPIX-MNPIX+1
      IF(NPIXOUT.LE.3000.AND.NPIXIN.LE.3000)GO TO 110
100 STOP ' ?DATA FILES EXCEED BUFFER WIDTH.'
110 WRITE(9) NPIXOUT,LMAX
C.....READ/WRITE LOOP
      DO 210 LINE=1,LMAX
      DO 200 IPX=MNPIX,MXPIX

```

```

INPX=R(1)*(IPX) + R(2)*(LINE) + R(3)
IF(INPX.LT.1.OR.INPX.GT.NPXIN) THEN
OUTBUF(IPX-MNPX+1)=.FALSE.
ELSE
INLINE=S(1)*(IPX) + S(2)*(LINE) + S(3)
IF(INLINE.LT.1.OR.INLINE.GT.NRECS) THEN
OUTBUF(IPX-MNPX+1)=.FALSE.
ELSE
C.....CHECK LIST FOR SCANLINE IN WORK ARRAY
IF(INLINE.GE.MNLINE.AND.INLINE.LE.MXLINE) GOTD120
C.....ELSE READ SCANLINE INTO LIST AND WORK ARRAY
IF(INLINE.LT.MNLINE) STOP 'INBUF ARRAY TOO SMALL!!'
DO 115 I=MXLINE+1,INLINE
IREC=MOD(I,NRECS)*LENREC
115 READ(3,REC=INLINE) (INBUF(J),J=IREC+1,IREC+NPXIN)
MXLINE=INLINE
MNLINE=MXLINE-NRECS+1
120 OUTBUF(IPX-MNPX+1)=INBUF(LENREC*MOD(INLINE,NRECS)+INPX)
ENDIF
ENDIF
200 CONTINUE
210 WRITE(9) (OUTBUF(J),J=1,NPXOUT)
C.....
C.....FINIS
300 STOP
END

```

```

PROGRAM MCMTID
C THIS PROGRAM COMPUTES A RELATIVE THERMAL INERTIA AND TEMP DIFF
C IMAGE FILES FROM HCMM DATA.
C
C DIMENSION I1(35), I2(35), I3(35), I4(35), IB1(2000), IB2(2000),
C & IB3(2000)
C DIMENSION TEMP(256), ALB(256), IS(35)
C DIMENSION I6(35), IDUM(2000), IDT(2000)
C DATA 11/3*0.1, 1, 30*0/, 12/3*0.1, 1, 30*0/, 13/3*0.1, 1, 30*0/
C DATA 14/16, 0, 0, 1, 1, 30*0/, 15/8, 0, 0, 1, 1, 30*0/, 16/8, 0, 0, 1, 1, 30*0/
C INTEGER*2 IT(2000)
C
C OPEN NOON THERMAL FILE
C
C WRITE(6, FMT='('' OPEN DAY THERMAL FILE''')
C CALL DISKIO (0, 12, IB1, 11)
C
C OPEN NIGHT THERMAL FILE
C
C WRITE(6, FMT='('' OPEN NIGHT THERMAL FILE''')
C CALL DISKIO (0, 13, IB2, 12)
C
C OPEN NOON ALBEDO FILE"
C
C WRITE(6, FMT='('' OPEN NOON ALBEDO FILE''')
C CALL DISKIO (0, 14, IB3, 13)
C
C OPEN THERMAL INERTIA OUTPUT FILE
C
C WRITE(6, FMT='('' OPEN THERMAL INERTIA OUTPUT FILE''')
C W=I1(2)
C X=I2(2)
C Y=I3(2)
C W1=I1(3)
C X1=I2(3)
C Y1=I3(3)
C MAXP=AMINI(W, X, Y)
C MAXL=AMINI(W1, X1, Y1)
C I4(2)=MAXP
C I4(3)=MAXL
C CALL DISKIO (0, 15, 0, 14)
C
C OPEN TEMP DIFF OUTPUT FILE
C
C WRITE(6, FMT='('' OPEN TEMP DIFF OUTPUT FILE''')
C I5(2)=MAXP
C I5(3)=MAXL
C CALL DISKIO (0, 16, 0, 15)
C
C OPEN DUMMY FILE
C
C WRITE(6, FMT='('' OPEN DUMMY FILE''')
C I6(2)=MAXP
C I6(3)=MAXL
C CALL DISKIO (0, 17, 0, 16)
C
C INPUT AVERAGE PARMS
C
C WRITE (6, FMT='('' ENTER AVERAGE VALUES A, TD, TN''')
C ACCEPT * ,AAVE, ATD, ATN
C TYPE * ,AAVE, ATD, ATN
C WRITE (6, FMT='('' ENTER LATITUDE AND SOLAR DEC IN DEG''')

```

```

ACCEPT * ,XLAM,DELTA
TYPE * ,XLAM,DELTA
XLAM=FLAM*0.017453
DELTA=DELTA*0.017453
DEG=1./COS(XLAM-DELTA)
OO=1353*(1.-.2*SQRT(DEG))
C=-OO*.82*.184*(COS(XLAM)+0.44*DELTA* SIN(XLAM))
B=(ATD-ATN)*1500-C*AAVE
TYPE * ,OO
TYPE * ,C
TYPE * ,B
WRITE (6,FMT='(11 P REL = (B+C*ALB)/DT)')

C
C COMPUTE TEMP AND ALB CALIBRATION FILES
C
DO 2 I=1,256
2 ALB(K)=(K-1)*0.00392157
C1=14421.537
C2=1251.1591
C3=-118.21376
DO 11 LK=1,256
11 TEMP(LK)=C2/(ALOG(C1/(LK-1-C3)+1))

C
C MAIN READ/WRITE LOOP
C
DO 3 I=1,MAXL
CALL DISKIO (9,12,IB1,11)
CALL UNPACK(1B1,11(2))
CALL DISKIO (9,13,IB2,12)
CALL UNPACK(1B2,12(2))
CALL DISKIO (9,14,IB3,13)
CALL UNPACK(1B3,13(2))

C
DO 4 K=1,MAXP
NUM1=1B1(K)+1
NUM2=1B2(K)+1
NUM3=1B3(K)+1
TD=TEMP(NUM1)
TN=TEMP(NUM2)
AA=ALB(NUM3)
IDUM(K)=255
S=TD-TN
X=(AA-AAVE)*100
Y=ATD-TD
IF (X.GE.2.AND.Y.GE.15) GO TO 21
IF (TN.LE.265) GO TO 21
Z=-S
IF (S.LE.0.AND.Z.LE.10) GO TO 22
IF (S.LE.0) GO TO 21
IT(K)=(B+C*AA)/S
IDT(K)=S
IF (IT(K).EQ.3550) IT(K)=3560
IF (IT(K).EQ.1000) IT(K)=990
GO TO 4
21 IT(K)=1000
IDT(K)=255
IDUM(K)=0
GO TO 4
22 IT(K)=3550
IDT(K)=0
IDUM(K)=255
4 CONTINUE
CALL DISKIO (10,15,IT,14)

```



```
CALL PACK(IDT,15(2))
CALL DISKIO (10,16,1DT,15)
CALL PACK(IDUM,16(2))
CALL DISKIO (10,17,1DUM,16)
CONTINUE
3
C
C CLOSE FILES
C
CALL DISKIO (6,12,0,11)
CALL DISKIO (6,13,0,12)
CALL DISKIO (6,14,0,13)
CALL DISKIO (6,15,0,14)
CALL DISKIO (6,16,0,15)
CALL DISKIO (6,17,0,16)
STOP
END
```

```

10   I PHOFLE      Profiling routines. 3/2/81
20   I Program language is extended Basic.
30   I Program written by K. Watson
40   OPTION BASE 1
50   DIM Tuay(1500), Thite(1500), Elev(1500), X(1500), Y(1500), Dum(1500), Derv(1500), Inert(1500), Dt(1500), Topo(1500), Mean(1500)
- 60   DIM M(2000), Z(2000), X2(2000), Topx(2000), S$(80), A$(5)(41)
70   INTEGER Dn(4000)
80   PRINTER IS 16
90   Elev_corr=0      I Initialize elevation correction indicator
100  Enable=0        I Initialize for profile plotting
110  INPUT "Enter profile ie. A,B", Profile$(1,1)
120  Profiles=Profile$&Profile$&" "
130  INPUT "Enter area name ie. PRB", Area$
140  File_sp$=Area$&Profile$(1,1)
150  Function_keys: 1
160      ON KEY #0 GOTO Topo_gen
170      ON KEY #1 GOTO Image_gen
180      ON KEY #2 GOTO Proi_plot
190      ON KEY #3 GOTO Feature
200      ON KEY #4 GOTO File_edit
210      ON KEY #5 GOTO Cross_cor
220      ON KEY #6 GOTO Cross_plot_sngl
230      ON KEY #7 GOTO Cross_plot_mult
240      ON KEY #8 GOTO Topo_Resample
250      ON KEY #9 GOTO Elev_correct
260      ON KEY #10 GOTO Report_plot
270      IF Elev_corr=1 THEN Profile$=Profile$&" elev corr"
280  MASS STORAGE IS ":C"
290  EXIT GRAPHICS
300  PRINT PAGE
310  PRINT " KEY #0 Generate topo binary file from PERKIN output"
320  PRINT " KEY #1 Generate image binary file"
330  PRINT " KEY #2 Plot a profile"
340  PRINT " KEY #3 Select a feature for matching profiles"
350  PRINT " KEY #4 File edit"
360  PRINT " KEY #5 Cross correlate two images"
370  PRINT " KEY #6 Cross plot two data files(report)"
380  PRINT " KEY #7 Cross plot multiple data files"
390  PRINT " KEY #8 Resample the topo data to match images"
400  PRINT " KEY #9 Determine elevation correction to temp data"
410  PRINT " KEY #10 Profile plotting(report)"
420  PRINT " MASS STORAGE SET TO :C"
430  DISP "Select option"
440      GOTO 430
450      !
460      ! *****
470      !
480  Topo_gen: 1 To generate topo binary file from digitized records.
490  OVERLAP
500  BUFFER #1
510  PRINT PAGE
520  INPUT "Enter number of input files from DIGIND",M
530  File$="Topp#B"      I *****
540  DISP "Generating \opo file."
550  I=0
560  FOR N=1 TO M
570  ON END #1 GOTO 640
580  ASSIGN #1 TO File$

```

```

590 READ #1;K
600 REDIM R(K)
610 READ #1;Curves
620 READ #1;Xlower,Xupper
630 READ #1;R(°)
640 ASSIGN #1 TO °
650 FOR L=1 TO K
660 Z(L+1+2)=R(L)*12*.0254 I Convert from ft to m.
670 NEXT L
680 I=1+K
690 NEXT N
700 REWIND ":T15"
710 REDIM Z(I+2)
720 Z(1)=1
730 Z(2)=.15875 I km . Assumes 1/40 ° spacing on 1:250,000 map
740 Fileout$="Topc"&Profile$(1,2)
750 FCREATE Fileout$,52
760 FPRINT Fileout$,Z(*)
770 DISP "Finished"
780 WAIT 500
790 SERIAL
800 GOTO Function_keys
810 I
820 I *****
830 I
840 Image gen: I To generate image binary files.
850 OVERLAP
860 BUFFER #1
870 PRINT #1
880 I Regular Perkin image files
890 I
900 LINPUT "Enter file type ie Tday,Tnite,Refl",Filex$
910 DISP "Generating image file."
920 X$=Profile$(1,1)&"":T15"
930 IF Filex$="Tday" THEN FS$="TD"&X$
940 IF Filex$="Tnite" THEN FS$="TN"&X$
950 IF Filex$="Refl" THEN FS$="RD"&X$
960 INPUT "Enter starting pixel and line",Ps,Ls
970 INPUT "Enter ending pixel and line",Pn,Ln
980 INPUT "Enter number of data blocks ",No_blocks
990 Cl=(Ls-Ln)/(Ps-Pn)
1000 J=1 I Profile element counter
1010 I=1 I Block no
1020 FOR I=1 TO No Blocks I INSERT FAST ALGORITHM HERE.
1030 CAT TO AS(*)FS&VALS(I)
1040 IF LEN(AS(1))<>0 THEN GOTO 1090
1050 REWIND ":T15"
1060 PRINT "FS&VALS(I) not on tape.Insert correct tape and CONT"
1070 PAUSE
1080 GOTO 1030
1090 ASSIGN #1 TO FS&VALS(I) I
1100 READ #1;S$
1110 N=POS(S$,"Lines")
1120 Lines=VAL(S$(N+5,N+7))
1130 M=POS(S$,"Pixels")
1140 Pixels=VAL(S$(M+6,M+8))
1150 PRINT "Lines,Pixels=";Lines,Pixels
1160 REDIM Dn(Pixels*Lines)
1170 READ #1;Dn(*)
1180 FOR K=1 TO Pixels

```

```

1190 Yy=C1*(K-1)+1
1200 Lj=INT(Yy)
1210 IF Yy-Lj>.5 THEN Lj=Lj+1
1220 Z(J)=Dn((Lj-1)*Pixels+K)
1230 I PRINT J,Z(J)          I Use for editing.
1240 J=J+1 I Increment profile counter
1250 NEXT K
1260 ASSIGN @1 TO *
1270 NEXT I
1280 REWIND ":T15"
1290 J=J-1 I Reset pixel counter
1300 REDIM Z(J)
1310 K1=14421.587 I Temp calib Dn to Temp
1320 K2=1251.1591
1330 K3=-118.21376
1340 Dist=SQRT((Pn-Ps)^2+(Ln-Ls)^2)*.47717/J I km approx units
1350 REDIM Z(J),X(J)
1360 IF (Filex$="Tday") OR (Filex$="Tnite") THEN GOTO Temp_cal
1370 IF Filex$="Refl" THEN GOTO Refl_cal
1380 Temp_cal: FOR I=1 TO J
1390 Z(I)=K2/LOG(K1/(Z(1)-K3)+1)
1400 IF Z(I)<260 THEN Z(I)=260
1410 NEXT I
1420 GOTO Bin_store
1430 Refl_cal: FOR I=1 TO J
1440 Z(I)=Z(1)/255*100 I % refl
1450 NEXT I
1460 GOSUB Bin_store
1470 GOTO Function_keys
1480 Bin_store: I
1490 DISP "Binary store"
1500 Dum(1)=J I No values
1510 Dum(2)=Dist I DX increment in km.
1520 FOR I=3 TO J+2
1530 Dum(I)=Z(I-2) I Normal statement.
1540 NEXT I
1550 REDIM Dum(J+2)
1560 Filename$=Filex$[1,4]&Profile$[1,2]
1570 FCREATE Filename$,52
1580 FPRINT Filename$,Dum(*)
1590 PRINT PAGE
1600 DISP "Finished"
1610 SERIAL
1620 RETURN
1630 I
1640 I *****
1650 I
1650 Prof_plot: I On CRT or at 1:1,000,000 on 9872S.
1670 INPUT "Select plotter option: 0 CRT , 1 9872S",Plotter
1680 PRINT PAGE
1690 GOSUB File_read
1700 GOSUB File_plot
1710 IF Plotter=0 THEN EXIT GRAPHICS
1720 IF V=1 THEN GOTO 1690
1730 GOTO Function_keys
1740 File_read: INPUT "Enter file type ie Tday,Tnite,Refl,Elev,Derv,Dt,Inert,Mean",File$
1750 REDIM X(1500),Y(1500),Z(1500)
1760 Filename$=File$[1,4]&Profile$[1,2]
1770 IF (File$="Tday") OR (File$="Tnite") THEN GOTO 2080
1780 IF (File$="Refl") OR (File$="Elev") THEN GOTO 2080

```

```

1790 IF File$="Derv" THEN GOTO 2080
1800 IF File$="Mean" THEN GOTO 1820
1810 IF (File$="Dt") OR (File$="Inert") THEN GOTO Dt_form
1820 Dt_form: FREAD "Toay"&Profile$(1,2),X(*)
1830 J=X(1)
1840 Dist=X(2)
1850 FREAD "Tnit"&Profile$(1,2),Y(*)
1860 REDIM X(J+2),Y(J+2),Z(J+2)
1870 IF (File$="Dt") OR (File$="Inert") THEN MAT Z=X-Y
1880 IF File$="Mean" THEN MAT Z=X+Y
1890 IF File$="Mean" THEN MAT Z=Z*.5
1900 IF (File$="Dt") OR (File$="Mean") THEN GOTO 2110
1910 Inert_form: FREAD "Refl"&Profile$(1,2),X(*)
1920 IF ATea$="PKB" THEN GOTO 1950
1930 PRINT "Need to reset alpha,beta coeff at Inert_form"
1940 PAUSE
1950 Alpha=52265.8      ! Powder River Basin Parameters.
1960 Beta=-61744
1970 MAT X=X*(.01)      ! Convert to fractions
1980 FOR L=2 TO J+2
1990 IF Z(L)>0 THEN GOTO 2020
2000 Z(L)=2550
2010 GOTO 2060
2020 Z(L)=(Alpha+Beta*X(L))/Z(L)
2030 IF Z(L)<500 THEN Z(L)=450
2040 IF Z(L)>3000 THEN Z(L)=3000
2050 Dum(2)=Dist ! Dx increment in km.
2060 NEXT L
2070 GOTO 2110
2080 FREAD Filename$,Z(*)
2090 J=Z(1)
2100 Dist=Z(2)
2110 FOR I=1 TO J
2120 Z(I)=Z(I+2)
2130 X(I)=(I-1)*Dist
2140 NEXT I
2150 REDIM X(J),Z(J)
2160 RETURN
2170 !
2180 !
2190 !
2200 File_plot: SERIAL ! IF V=1 THEN REPEAT
2210 IF Enable=1 THEN GOTO File_cont
2220 IF Plotter=0 THEN PLOTTER IS 13,"GRAPHICS"
2230 IF Plotter=0 THEN GRAPHICS
2240 IF Plotter=0 THEN GOTO File_cont
2250 IF V=0 THEN PLOTTER IS 7,5,"9872A" ! First time
2260 File_cont: BEEP
2270 Dz=5
2280 IF (File$(1,1)="E") OR (File$(1,2)="To") THEN Dz=100
2290 IF File$(1,2)="De" THEN Dz=10
2300 IF File$(1,2)="In" THEN Dz=500
2310 Y$=File$
2320 IF (Y$(1,1)="T") OR (Y$(1,1)="D") THEN Y$=Y$*(K)
2330 IF Y$(1,1)="M" THEN Y$="Mean temp(K)"
2340 IF Y$(1,1)="E" THEN Y$=Y$*(m)
2350 IF Y$(1,1)="R" THEN Y$=Y$*(h)
2360 IF Y$(1,2)="De" THEN Y$="Gradient(m/km)"
2370 IF Y$(1,2)="Dt" THEN Y$="Temp diff(K)"
2380 IF Y$(1,1)="I" THEN Y$="Inertia(TIU)"

```

```

2390 X$="Distance (km)"
2400 MAT SEARCH Z(*),MAX;Zmax
2410 MAT SEARCH Z(*),MIN;Zmin
2420 Zmin=INT(Zmin/Dz)*Dz
2430 Zmax=(INT(Zmax/Dz)+1)*Dz
2440 Dzs=(Zmax-Zmin)*.125/8.5
2450 Dxs=X(J)*.125/8.5
2460 FOR I=1 TO J
2470 X(I)=(I-1)*Dist
2480 NEXT I
2490 IF Plotter=0 THEN GOTO 2670
2500 DEG
2510 LIMIT 0,400,0,285
2520 LORG 5
2530 CSIZE 2.75
2540 X1=(1.5*25.4-12.5)*100/285
2550 X2=X1+X(J)*100/285      I Proper scale
2560 Y1=(1.5*25.4+14)*100/285
2570 Y2=Y1+150*100/285
2580 MOVE (X1+X2)*.5,Y1-.5*25.4*100/285
2590 LABEL X$
2600 LDIR 90
2610 MOVE X1-.9*25.4*100/285,(Y1+Y2)*.5
2620 LABEL Y$
2630 LDIR 0
2640 LOCATE X1,X2,Y1,Y2
2650 FRAME
2660 LORG 5
2670 SCALE 0,X(J),Zmin,Zmax
2680 OUTPUT 705;"VS2;"
2690 MOVE 0,Zmax
2700 DRAW X(J),Zmax
2710 DRAW X(J),Zmin
2720 AXES 10,Dz,0,Zmin,10,2
2730 FOR I=1 TO J
2740 IF I=1 THEN MOVE X(1),Z(1)
2750 DRAW X(I),Z(I)
2760 NEXT I
2770 OUTPUT 705;"VN;"
2780 CSIZE 2
2790 LORG 8
2800 FOR Ys=Zmin TO Zmax STEP Dz
2810 MOVE -Dxs,Ys
2820 LABEL VAL$(Ys)
2830 NEXT Ys
2840 LORG 6
2850 FOR W=0 TO X(J) STEP 20
2860 MOVE W,Zmin-Dzs
2870 LABEL VAL$(W)
2880 NEXT W
2890 LORG 5
2900 MOVE X(J)*.5,Zmax-Dzs*2
2910 LABEL "Profile "&Profile$(1,2)&" "&" "&Area$&" Area"
2920 IF Plotter=0 THEN LABEL "CONT to continue"
2930 IF Plotter=0 THEN PAUSE
2940 PEN 0
2950 IF Plotter=0 THEN EXIT GRAPHICS
2960 IF Plotter=0 THEN GOTO 2990
2970 IF X(J)*25.4>7 THEN OUTPUT 705;"AF;"
2980 IF X(J)*25.4<=7 THEN OUTPUT 705;"AH;"

```

```

2990 INPUT "Enter 0 to END and 1 to plot another profile",V
3000 IF V=1 THEN RETURN
3010 IF Plotter=0 THEN GOTO End1
3020 IF X(J)*25.4>7 THEN OUTPUT 705;"AF;"
3030 IF X(J)*25.4<=7 THEN OUTPUT 705;"AH;"
-3040 End1: GOTO Function_keys
3050 I
3060 I *****
3070 I
3080 Feature: GOSUB File_read
3090 Feat: INPUT "Enter Feature and approx pixel value",K5,Jp
3100 J1=Jp-12
3110 IF J1<1 THEN J1=1
3120 J2=Jp+12
3130 IF J2>J THEN J2=J
3140 Sp=0
3150 INPUT "Use CONT to list and 1 to plot",Sp
3160 IF Sp=0 THEN GOTO List
3170 READ: X2(J2-J1+1),Dum(J2-J1+1)
3180 L=0
3190 FOR K=J1 TO J2
3200 L=L+1
3210 X2(L)=K
3220 Dum(L)=Z(K)
3230 NEXT K
3240 Lmax=L
3250 MAT SEARCH Dum(*),MAX;Rmax
3260 MAT SEARCH Dum(*),MIN;Rmin
3270 Dr=Rmax-Rmin
3280 Feature_plot: PLOTTER IS 12,"GRAPHICS"
3290 GRAPHICS
3300 LOCATE 10,100,20,90
3310 SCALE J1,J2,Rmin,Rmax
3320 GRID 1,(Rmax-Rmin)*.1,J1,Rmin
3330 FOR L=1 TO Lmax
3340 IF L=1 THEN MOVE X2(L),Dum(L)
3350 DRAW X2(L),Dum(L)
3360 NEXT L
3370 LORG 6
3380 FOR L=1 TO Lmax STEP 2
3390 MOVE X2(L),Rmin-(Rmax-Rmin)*.05
3400 LABEL VAL$(X2(L))
3410 NEXT L
3420 LORG 4
3430 MOVE (J1+J2)*.5,Rmin-.04*Dr
3440 LABEL Files
3450 MOVE Jp,Rmax+Dr*.02
3460 LABEL K$
3470 LORG 1
3480 MOVE X2(1),Rmax+Dr*.02
3490 LABEL "CONT to continue"
3500 PAUSE
3510 PEN 0
3520 EXIT GRAPHICS
3530 GOTO 3630
3540 List: PRINT SPA(10),"Feature ";K$
3550 Min=1E99
3560 FOR I=J1 TO J2
3570 Min=MIN(Z(I),Min)
3580 NEXT I

```

```

3590 FOR I=J1 TO J2
3600 IF Z(I)<>MIN THEN PRINT I,Z(I)
3610 IF Z(I)=MIN THEN PRINT I,Z(I)," ***** "
3620 NEXT I
3630 INPUT "Enter 0 to examine other features ; 1 to terminate",T
3640 IF T=0 THEN GOTO Feature
3650 IF T=1 THEN GOTO Function_keys
3660 I
3670 I *****
3680 I
3690 Cross_cor: I PROFLL To cross correlate profiling data for images.
3700 I Method: Shift means to 0 and variances to 1
3710 I Form cross correl sum for varying delays.
3720 I Take data in 100 pixel sets( See Kmax)
3730 PRINT PAGE
3740 INPUT "Enter function1 ie Tday,Tnite,Ref1 ....",X$
3750 INPUT "Enter function2 ie Tday,Tnite,Ref1 ....",Y$
3760 DISP "Cross corellation."
3770 FREAD Y$(1,4)&Profile$(1,2),R(*)
3780 IF (X2(1)=R(1)) AND (X2(2)=R(2)) THEN GOTO 3830
3790 PRINT "Files are not same type - recneck"
3800 PRINT "Length=";X(1),X(2),"Dist=";R(1),R(2)
3810 INPUT "Do you wish to continue anyway ?",Anz$
3820 IF Anz$(1,1)="N" THEN STOP
3830 J=X2(1)
3840 I=J-X2(2)
3850 I Max: Kmax=J DIV 100
3860 J=100
3870 PRINTEK IS 0
3880 PRINT
3890 PRINT " List of correlation for ";X$;" and ";Y$;" Profile";Profile$
3900 PRINT
3910 FOR K=1 TO KMax
3920 I1=(K-1)*100+1
3930 I2=I1+J-1
3940 PRINT "From pixel "&VAL$(I1)&" to "&VAL$(I2)
3950 FOR I=I1 TO I2
3960 X(I-I1+1)=X2(I+2)
3970 Y(I-I1+1)=R(I+2)
3980 NEXT I
3990 REDIM X(J),Y(J),Dum(J),Z(J)
4000 Meanx=SUM(X)/J I Transform to Mean=0 Dev=1
4010 Meany=SUM(Y)/J
4020 MAT X=(-Meanx)+X
4030 MAT Y=(-Meany)+Y
4040 MAT Dum=X.X
4050 Var=SUM(Dum)/J
4060 MAT X=(1/SQR(Var))*X
4070 MAT Dum=Y.Y
4080 Var=SUM(Dum)/J
4090 MAT Y=(1/SQR(Var))*Y
4100 PRINT
4110 PRINT " Delay ";X$;" ";Y$
4120 FOR Delay=-5 TO 5
4130 Sum1=0
4140 FOR I=6 TO J-5
4150 D=I+Delay
4160 Sum1=ABS(X(1)*Y(D))+Sum1
4170 Next: NEXT I
4180 PRINT " ";Delay,Sum1

```



```

4190 NLXT Delay
4200 NLXT K
4210 PRINTER IS 16
4220 GOTO Function_keys
4230 |
4240 | .....
4250 |
4260 Cross_plot_sngl: |
4270 Plot_count=1
4280 DISP "Cross plotting - single."
4290 INPUT "Select plotter option: 0 CRT , 1 9872S",Plotter
4300 IF Plotter=0 THEN PLOTTER IS 13,"GRAPHICS"
4310 IF Plotter=1 THEN PLOTTER IS 7,5,"9872A"
4320 IF Plotter=) THEN LIMIT 0,400,0,285
4330 Cross_cont: INPUT "Enter filename for Xaxis ie Tday,Tnite...",X$
4340 INPUT "Enter filename for Yaxis ie Tuay,Tnite...",Y$
4350 Fx$=X$(1,2)
4360 Fy$=Y$(1,2)
4370 IF Fx$(1,2)="To" THEN FREAD "Tday"&Profile$(1,2),X(*)
4380 IF Fy$(1,2)="To" THEN FREAD "Tday"&Profile$(1,2),Y(*)
4390 IF Fx$(1,2)="Tn" THEN FREAD "Tnit"&Profile$(1,2),X(*)
4400 IF Fy$(1,2)="Tn" THEN FREAD "Tnit"&Profile$(1,2),Y(*)
4410 IF Fx$(1,2)="Re" THEN FREAD "Re1"&Profile$(1,2),X(*)
4420 IF Fy$(1,2)="Re" THEN FREAD "Re1"&Profile$(1,2),Y(*)
4430 IF Fx$(1,2)="E1" THEN FREAD "Elev"&Profile$(1,2),X(*)
4440 IF Fy$(1,2)="E1" THEN FREAD "Elev"&Profile$(1,2),Y(*)
4450 IF Fx$(1,2)="De" THEN FREAD "Derv"&Profile$(1,2),X(*)
4460 IF Fy$(1,2)="De" THEN FREAD "Derv"&Profile$(1,2),Y(*)
4470 IF (Fx$(1,2)="In" OR (Fy$(1,2)="In") THEN GOTO Inert_read
4480 IF (Fx$(1,2)="Dt" OR (Fy$(1,4)="Dt") THEN GOTO Dt_read
4490 IF (Fx$(1,2)="Me" OR (Fy$(1,4)="Me") THEN GOTO Dt_read
4500 GOTO Plotting_setup
4510 Inert_read: |
4520 Alpha=52265.8 | Powder River Basin Parameters.
4530 Beta=-61744
4540 FREAD "Toay"&Profile$(1,2),X2(*)
4550 FREAD "Tnit"&Profile$(1,2),Z(*)
4560 FREAD "Re1"&Profile$(1,2),Dum(*)
4570 AEDIM Dum=(RO*(2))
4580 MAT Dum=Dum*(.01) | Convert Re1 to a fraction
4590 MAT X2=X2-Z
4600 MAT X2=X2*(Beta)
4610 MAT X2=X2+(Alpha)
4620 MAT X2=X2/Dum
4630 FOR I=1 TO RO*(X2)
4640 IF X2(I)<1000 THEN X2(I)=1000
4650 IF X2(I)>3000 THEN X2(I)=3000
4660 IF Fx$="In" THEN MAT X=X2
4670 IF Fy$="In" THEN MAT Y=X2
4680 GOTO 4480
4690 Dt_read: FREAD "Toay"&Profile$(1,2),X2(*)
4700 FREAD "Tnit"&Profile$(1,2),Z(*)
4710 IF (Fx$="Dt" OR (Fy$="Dt") THEN MAT X2=X2-Z
4720 IF (Fx$="Me" OR (Fy$="Me") THEN MAT X2=X2+Z
4730 IF (Fx$="Me" OR (Fy$="Me") THEN MAT X2=X2+Z
4740 IF (Fx$="Dt" OR (Fy$="Me") THEN MAT X=
4750 IF (Fy$="Dt" OR (Fy$="Me") THEN MAT Y=
4760 GOTO 4500
4770 Plotting_setup: IF (Fx$<>"In" OR (Fy$<>"In") THEN J=X(1)
4780 IF (Fx$<>"In" OR (Fy$<>"Dt") THEN X=X(2)

```

```

4790 IF (FAS="In") OR (FAS="Dt") THEN J=2(1)
4800 IF FAS="Me" THEN J=2(1)
4810 IF (FAS="In") OR (FAS="Dt") THEN Dist=2(2)
4820 IF FAS="Me" THEN Dist=2(2)
4830 FOR I=1 TO J
4840 X(I)=X(1+2)
4850 Y(I)=Y(1+2)
4860 NEXT I
4870 REDIM X(J),Y(J),X2(J),Z(J)
4880 DX=10
4890 DY=10
4900 IF X(I,1)="L" THEN DX=100
4910 IF Y(I,1)="E" THEN DY=100
4920 IF X(I,1)="I" THEN DX=500
4930 IF Y(I,1)="I" THEN DY=500
4940 IF (X(I,2)="Tn") OR (X(I,2)="Dt") THEN DX=5
4950 IF X(I,2)="Me" THEN DX=5
4960 IF (Y(I,2)="Tn") OR (Y(I,2)="Dt") THEN DY=5
4970 IF Y(I,2)="Me" THEN DY=5
4980 IF X(I,1)="R" THEN DX=5
4990 IF Y(I,1)="R" THEN DY=5
5000 IF Plotter=0 THEN LOCATE 20,100,10,90
5010 GOSUB Point_plot
5020 CSIZE 2
5030 LORG 5
5040 MOVE (Xmax+Xmin)*.5,Ymax
5050 LABEL "Profile "&Profile$
5060 IF Plotter=0 THEN GOTO 5210
5070 INPUT "Enter 0 to END and 1 to continue plots",S2
5080 IF S2=0 THEN GOTO 5160
5090 IF Plot_count=4 THEN GOTO Reset_plot
5100 Plot_count=Plot_count+1 ! Increment plot counter
5110 GOTO Cross_cont
5120 Reset_plot: OUTPUT 705;"AH;"! Next page
5130 OUTPUT 705;"AH;"
5140 Cross_plot=1
5150 GOTO Cross_cont
5160 OUTPUT 705;"AH;"
5170 OUTPUT 705;"AH;"
5180 DISP "FINISHED."
5190 PEN 0
5200 GOTO Function_keys
5210 LORG 2
5220 MOVE Xmin,Ymax+Yr
5230 LABEL "CONT to continue;DUMP GRAPHICS to copy"
5240 PAUSE
5250 PEN 0
5260 EXIT GRAPHICS
5270 INPUT "Enter 0 to continue and 1 to DIGITIZE plotted points",28
5280 IF 28=0 THEN GOTO Function_keys
5290 GRAPHICS
5300 POINTER (Xmin+Xmax)*.5,(Ymin+Ymax)*.5,2
5310 DIGITIZE Xc,Yd ! Position cursor
5320 MAT Z=X-Xd
5330 MAT Z=Z.Z
5340 MAT X2=Y-Yd
5350 MAT X2=X2.X2
5360 MAT Z=Z+X2
5370 MAT SEARCH Z(*),MIN;Zmin
5380 MAT SEARCH Z(*),LOC(Z(K)=Zmin);K

```

C - 2 96

ORIGINAL PAGE IS
OF POOR QUALITY

```
5390 MOVE (Xmin+Xmax)*.5,Ymax+Yr
5400 LABEL "Pixel 1";VAL$(K);" .Use CONT to continue"
5410 PAUSE
5420 GOTO 5260
5430 1
5440 1 .....
5450 1
5460 Cross_plot_mult: 1          Cross plots of Tday,Tnite,Topo etc.  2/20/81
5470 PRINT PAGE
5480 INPUT "Select plotter option: 0 CRT , 1 9872S",Plotter
5490 DISP "Cross plotting - multiple."
5500 GOSUB Mult_file_read
5510 GOTO Cont_mult
5520 Mult_file_read: 1
5530 P$=PROB1I$(1,2)
5540 IF Area$="PRD" THEN GOTO 5570
5550 PRINT "need to revise P mapping parms at Pcoef"
5560 PAUSE
5570 Pcoef: Alpha=52285.6      1 Powder River Basin Parameters.
5580 Beta=-61744
5590 FREAD "Tday"&P$,Toay(*)
5600 FREAD "Elev"&P$,Topo(*)
5610 FREAD "Tnit"&P$,Tnite(*)
5620 FREAD "Derv"&P$,Derv(*)
5630 FREAD "Refl"&P$,Refl(*)
5640 Dist=Topo(2)
5650 J=Topo(1)
5660 FOR L=1 TO J
5670 X(L)=(L-1)*Dist
5680 Tday(L)=Toay(L+2)
5690 Tnite(L)=Tnite(L+2)
5700 Topo(L)=Topo(L+2)
5710 Derv(L)=Derv(L+2)
5720 Dt(L)=Toay(L)-Tnite(L)
5730 Mean(L)=(Toay(L)+Tnite(L))/2
5740 Refl(L)=Refl(L+2)*.01      1 Convert to fractions
5750 Inert(L)=(Alpha+Beta*Refl(L))/Dt(L)
5760 IF Inert(L)>2500 THEN Inert(L)=2950
5770 IF Inert(L)<1000 THEN Inert(L)=550
5780 IF Refl(L)>.2 THEN Refl=.245
5790 IF Derv(L)>30 THEN Derv(L)=35
5800 IF Derv(L)<-30 THEN Derv(L)=-35
5810 NEXT L
5820 REDIM Tday(J),Tnite(J),Topo(J),X(J),Y(J),Derv(J),Dt(J),Inert(J),Refl(J),Mean(J)
5830 RETURN
5840 Cont_mult: 1
5850 IF Plotter=0 THEN PLOTTER IS 13,"GRAPHICS"
5860 IF Plotter=1 THEN PLOTTER IS 7,5,"9872A"
5870 GRAPHICS
5880 FOR K=1 TO 20
5890 IF K MOD 4=1 THEN LOCATE 10,50,60,90
5900 IF K MOD 4=2 THEN LOCATE 10,50,10,40
5910 IF K MOD 4=3 THEN LOCATE 70,110,60,90
5920 IF K MOD 4=0 THEN LOCATE 70,110,10,40
5930 ON K GOSUB P1,P2,P3,P4,P5,P6,P7,P8,P9,P10,P11,P12,P13,P14,P15,P16,P17,P18,P19,P20
5940 IF (K MOD 4=0) AND (Plotter=0) THEN PLOTTER IS 13,"GRAPHICS"
5950 IF (K MOD 4=0) AND (Plotter=1) THEN OUTPUT 705;"EC;" 1 Enable cutter
5960 IF (K MOD 4=0) AND (Plotter=1) THEN OUTPUT 705;"AF;" 1 Adv and cut
5970 NEXT K
5980 IF Plotter=1 THEN OUTPUT 705;"AH;" 1 Adv and cut
```

```

5990 PLEN 0
6000 EXIT GRAPHICS
6010 DISP "FINISHED."
6020 GOTO Function keys
- 6030 P1: MAT X=Topo      ! Tday vs Elev
6040 MAT Y=Tday
6050 X$="Topo"
6060 Y$="Tday"
6070 Dx=100
6080 Dy=5
6090 GOTO Cont
6100 P2: MAT X=Derv      ! Tday vs Derv
6110 MAT Y=Tday
6120 X$="Derv"
6130 Y$="Tday"
6140 Dx=10
6150 Dy=5
6160 GOTO Cont
6170 P3: MAT X=Refl     ! Tday vs Refl
6180 MAT Y=Tuay
6190 X$="Refl"
6200 Y$="Toay"
6210 Dx=.05
6220 Dy=5
6230 GOTO Cont
6240 P6: MAT X=Derv     ! Tnite vs Derv
6250 MAT Y=Tnite
6260 X$="Derv"
6270 Y$="Tnite"
6280 Dx=10
6290 Dy=5
6300 GOTO Cont
6310 P5: MAT X=Topo     ! Tnite vs Topo
6320 MAT Y=Tnite
6330 X$="Topo"
6340 Y$="Tnite"
6350 Dx=100
6360 Dy=5
6370 GOTO Cont
6380 P7: MAT X=Refl     ! Tnite vs Refl
6390 MAT Y=Tnite
6400 X$="Refl"
6410 Y$="Tnite"
6420 Dx=.05
6430 Dy=5
6440 GOTO Cont
6450 P9: MAT X=Topo     ! Refl vs Topo
6460 MAT Y=Refl
6470 X$="Topo"
6480 Y$="Refl"
6490 Dx=100
6500 Dy=.05
6510 GOTO Cont
6520 P11: MAT X=Inert   ! Refl vs Inert
6530 MAT Y=Refl
6540 X$="Inert"
6550 Y$="Refl"
6560 Dx=500
6570 Dy=.05
6580 GOTO Cont

```

ORIGINAL PAGE IS
OF POOR QUALITY

```
6590 P10: MAT X=Derv | Reil vs Derv
6600 MAT Y=Reil
6610 X$="Derv"
6620 Y$="Reil"
6630 Dx=10
6640 Dy=.05
6650 GOTO Cont
6660 P15: MAT X=Dt | Inert vs Dt
6670 MAT Y=Inert
6680 X$="Dt"
6690 Y$="Inert"
6700 Dx=5
6710 Dy=500
6720 GOTO Cont
6730 P13: MAT X=Topo! Inert vs Topo
6740 MAT Y=Inert
6750 X$="Topo"
6760 Y$="Inertia"
6770 Dx=100
6780 Dy=500
6790 GOTO Cont
6800 P14: MAT X=Derv! Inert vs Derv
6810 MAT Y=Inert
6820 X$="Derv"
6830 Y$="Inertia"
6840 Dx=10
6850 Dy=500
6860 GOTO Cont
6870 P17: MAT X=Topo! Dt vs Elev
6880 MAT Y=Dt
6890 X$="Elev"
6900 Y$="Dt"
6910 Dx=500
6920 Dy=5
6930 GOTO Cont
6940 P16: MAT X=Derv! Dt vs Derv
6950 MAT Y=Dt
6960 X$="Derv"
6970 Y$="Dt"
6980 Dx=10
6990 Dy=5
7000 GOTO Cont
7010 P19: MAT X=Tnite! Tday vs Tnite
7020 MAT Y=Tday
7030 X$="Tnite"
7040 Y$="Tday"
7050 Dx=5
7060 Dy=10
7070 GOTO Cont
7080 P4: | LABEL
7090 P8: |
7100 P12: |
7110 P16: |
7120 P20: GOTO Plot_label
7130 Cont: |
7140 Point_plot: |
7150 MAT SEARCH X(*),MAX;Xmax
7160 MAT SEARCH Y(*),MAX;Ymax
7170 MAT SEARCH X(*),MIN;Xmin
7180 MAT SEARCH Y(*),MIN;Ymin
```

ORIGINAL PAGE IS
POOR QUALITY.

```
7190 Xmin=INT(Xmin/Dx)*Dx
7200 Xmax=(INT(Xmax/Dx)+1)*Dx
7210 Ymin=INT(Ymin/Dy)*Dy
7220 Ymax=(INT(Ymax/Dy)+1)*Dy
7230 Xr=(Xmax-Xmin)*.05
7240 Yr=(Ymax-Ymin)*.05
7250 IF Plotter=U THEN GOTO 7540
7260 LORG 5
7270 C=12E 2
7280 IF Plot_count=1 THEN GOTO Plt_1
7290 IF Plot_count=2 THEN GOTO Plt_2
7300 IF Plot_count=3 THEN GOTO Plt_3
7310 Plt_1: Xset=8.5*25.4
7320 X1=Xset+69.85
7330 X2=X1+3.75*25.4
7340 Y1=158.75
7350 Y2=254
7360 GOTO 7520
7370 Plt_2: X1=69.65
7380 X2=165.1
7390 Y1=38.1
7400 Y2=133.35
7410 GOTO 7520
7420 Plt_3: X1=69.65
7430 X2=165.1
7440 Y1=158.75
7450 Y2=254
7460 GOTO 7520
7470 Plt_3: Xset=8.5*25.4
7480 X1=Xset+69.85
7490 X2=Xset+165.1
7500 Y1=38.1
7510 Y2=133.35
7520 Zz=100/(11*25.4)
7530 LOCATE X1*Zz,X2*Zz,Y1*Zz,Y2*Zz
7540 SCALE Xmin,Xmax,Ymin,Ymax
7550 AXES Dx,Dy,Xmin,Ymin
7560 LORG 6
7570 MOVE (Xmin+Xmax)/2,Ymin-Yr*.5
7580 FOR R=1 TO 2
7590 IF R=1 THEN Z$=X$
7600 IF R=2 THEN Z$=Y$
7610 IF Z$(1,1)="M" THEN Z$="Mean temp(K)"
7620 IF Z$(1,1)="T" THEN Z$="256"(K)"
7630 IF Z$(1,2)="Dt" THEN Z$="Temp diff(K)"
7640 IF Z$(1,2)="De" THEN Z$="Gradient(m/km)"
7650 IF Z$(1,2)="E1" THEN Z$="Elevation(m)"
7660 IF Z$(1,2)="In" THEN Z$="Inertia(TIU)"
7670 IF Z$(1,2)="Re" THEN Z$="Refl(%)"
7680 IF R=1 THEN X$=Z$
7690 IF R=2 THEN Y$=Z$
7700 NEXT R
7710 LABEL X$
7720 DEG
7730 LDIR 90
7740 LORG 4
7750 MOVE Xmin-Xr*3.5,(Ymin+Ymax)/2
7760 LABEL Y$
7770 IDIR 0
7780 FOR I=1 TO J
```

```

7790 MOVE X(I),Y(I)
7800 LABEL ". ."
7810 NLAT 1
7820 CSIZE 2.2
7830 LORG 6
7840 FOR X=Xmin TO Xmax STEP Dx
7850 MOVE X,Ymin-Yr*.5
7860 LABEL VALS(X)
7870 NEXT X
7880 LORG 8
7890 FOR Ya=Ymin TO Ymax STEP Dy
7900 MOVE Xmin-Xr*.5,Ya
7910 LABEL VALS(Ya)
7920 NEXT Ya
7930 CSIZE 3.3
7940 RETURN
7950 Plot_label: 1
7960 SCALE 0,1,0,1
7970 LORG 1
7980 MOVE .2,.75
7990 IF Area$="PRB" THEN LABEL "Powder River Basin Area"
8000 IF Area$="CP" THEN LABEL "Cabeza Prieta Area"
8010 MOVE .5,.5
8020 IF Area$="PRB" THEN LABEL "Aug 20,1978"
8030 IF Area$="CP" THEN LABEL "Apr 3-4,1979"
8040 MOVE .5,.25
8050 LABEL "Profile"&Profile$
8060 IF Plotter=0 THEN DUMP GRAPHICS
8070 RETURN
8080 !
8090 ! *****
8100 !
8110 Topo_resample: 1 To spline-smooth topo data and restore as Elev binary.
8120 ! and Derv binary.
8130 ! Special correction to Dist and for topo interp.
8140 PRINT PAGE
8150 DISP "Topo resample."
8160 FREAD "Tday"&Profile$(1,2),Tday(*)
8170 FREAD "Topo"&Profile$(1,2),Topx(*)
8180 J=Tday(1)
8190 Dist=Tday(2)
8200 K=Topx(1)
8210 Distz=Topx(2)
8220 FOR I=1 TO J
8230 X(I)=(I-1)*Dist ! Image file
8240 NEXT I
8250 FOR I=1 TO K
8260 Topx(I)=Topx(I+2)
8270 X2(I)=(I-1)*Distz
8280 NEXT I
8290 ! To interpolate topo data
8300 DIM Xb(4,3),Xbtrn(3,4),Dumx(3,3),Inv(3,3),F(4,1),Rum(3,1),G(3,1)
8310 MAT Xb=(1)
8320 Xb(1,1)=((0=Xb(1,2))=Xb(1,3))
8330 Xb(3,1)=4
8340 Xb(3,2)=2
8350 Xb(4,1)=9
8360 Xb(4,2)=3
8370 MAT Xbtrn=TRN(Xb)
8380 MAT Dumx=Xbtrn*Xb

```

ORIGINAL PAGE IS
OF POOR QUALITY

```
6390 MAT Inv=INV(Dumx)
6400 Del=Dist/(2*Distz)      I =D/2
6410 L=J
6420 Imax=INT(Distz*K/Dist)
6430 IF J>Imax THEN J=Imax      I Truncate all files to Jmax
6440 FOR I=2 TO J-1
6450 IF (X(I)>X2(L)) AND (X(I)<=X2(L+1)) THEN GOTO Interp
6460 L=L+1
6470 GOTO 6450
6480 Interp: F(1,J)=Topx(L-1)
6490 F(2,J)=Topx(L)
6500 F(3,J)=Topx(L+1)
6510 F(4,J)=Topx(L+2)
6520 MAT Run=Xdtrn*F
6530 MAT G=Inv*Run
6540 Zb=(I-1)*2*Del-(L-2)
6550 Dum(1)=G(1,J)/3*(Del^2+3*Zb^2)+G(2,J)*Zb+G(3,J)
6560 Derv(1)=2*G(1,J)*Zb+G(2,J)
6570 NextJ: NEXT I
6580 Dum(1)=Topx(1)      I End points
6590 Dum(J)=Topx(J)
6600 Derv(1)=(Topx(2)-Topx(1))/Distz
6610 Derv(J)=(Topx(J)-Topx(J-1))/Distz
6620 REDIM Dum(J),Derv(J),2(J)
6630 MAT Z=Dum
6640 REDIM Topo(J+2),Derv(J+2)      I Store output as binary files.
6650 FOR I=J TO 1 STEP -1
6660 Topo(I+2)=Dum(I)
6670 Derv(I+2)=Derv(I)
6680 NEXT I
6690 Topo(1)=J
6700 Derv(1)=J
6710 Topo(2)=Dist
6720 Derv(2)=Dist
6730 REDIM Topo(J+2),Derv(J+2)
6740 DISP "Storing binary files."
6750 FCREATE "Elev"&Profile$(1,2),52
6760 FCREATE "Derv"&Profile$(1,2),52
6770 FPRINT "Elev"&Profile$(1,2),Topo(*)
6780 FPRINT "Derv"&Profile$(1,2),Derv(*)
6790 DISP "FINISHED"
6800 GOTO Function_keys
6810 !
6820 ! *****
6830 !
6840 File_edit: I To edit binary files.
6850 PRINT PAGE
6860 INPUT "Enter File to be edited ie, Tday,Tnite,Ref1,Topo...",Filein$
6870 Filename$=Filein$(1,4)&Profile$(1,2)
6880 REDIM Dum(1500)
6890 FREAD Filename$,Dum(*)
6900 J=Dum(1)
6910 Dist=Dum(2)
6920 PRINT Filename$," J=";J," Dist=";Dist
6930 PRINT LIN(1)
6940 PRINT "Dum(3)=";Dum(3),"Dum("&VAL$(J+2)&")=";Dum(J+2)
6950 Edit_feature: PRINT "PAUSE AT Edit_feature"
6960 PAUSE
6970 Dum(1)=494      I ***** SPECIAL MOD FOR PRB BB *****
6980 Dum(2)=.508
```



```

8990 FOR I=3 TO 496: Sp cludge for BB'
9000 Dum(I)=Dum(I+2)
9010 NEXT I
9020 REDIM Dum(496)
9030 BLEEP
9040 PAUSE
9050 INPUT "Do you wish to re-store this file?",AS
9060 IF AS(1,1)<>"Y" THEN GOTU Edit_feature
9070 PURGE Filename$
9080 FCREATE Filename$,52
9090 FPRINT Filename$,Dum(*)
9100 GOTU function_keys
9110 I
9120 I .....
9130 I
9140 Elev correct: DISP " Elevation correction."
9150 FREAD "Tday"&Profile$(1,2),Tday(*)
9160 FREAD "Tnit"&Profile$(1,2),Tnite(*)
9170 FREAD "Elev"&Profile$(1,2),Topo(*)
9180 J=Topo(1)
9190 Dist=Topo(2)
9200 L=0
9210 INPUT "Enter starting and ending distances for elev correl",D1,D2
9220 I1=D1/Dist+1
9230 I2=D2/Dist+1
9240 FOR I=I1+2 TO I2+2
9250 L=L+1
9260 X(L)=Tday(I)
9270 Y(L)=Topo(I)
9280 Z(L)=Tnite(I)
9290 X2(L)=(Tday(I)+Tnite(I))/2
9300 NEXT I
9310 REDIM X(L),Y(L),Z(L),X2(L)
9320 CALL Linear(Y(*),X(*),L,Alpha_day,Beta_day,Dev_day)
9330 CALL Linear(Y(*),Z(*),L,Alpha_nite,Beta_nite,Dev_nite)
9340 CALL Linear(Y(*),X2(*),L,Alpha_mean,Beta_mean,Dev_mean)
9350 PRINTER IS 0
9360 FIXED 4
9370 FPRINT "Tday= "&VAL$(Alpha_day)&" * Elev + "&VAL$(Beta_day)&" +/- "&VAL$(Dev_day)
9380 FPRINT "Tnite= "&VAL$(Alpha_nite)&" * Elev + "&VAL$(Beta_nite)&" +/- "&VAL$(Dev_nite)
9390 PRINT "Tmean= "&VAL$(Alpha_mean)&" * Elev + "&VAL$(Beta_mean)&" +/- "&VAL$(Dev_mean)
9400 PRINT
9410 STANDARD
9420 PRINTER IS 16
9430 PRINT LIN(5)
9440 PRINT "Use CONT to rename Tday and Tnit as Tdt and Tnt ."
9450 PRINT "and store elevation correction values in Tday and Tnit."
9460 PAUSE
9470 RENAME "Tday"&Profile$(1,2) TO "Tdy"&Profile$(1,2)
9480 RENAME "Tnit"&Profile$(1,2) TO "Tnt"&Profile$(1,2)
9490 FCREATE "Tday"&Profile$(1,2),52
9500 FCREATE "Tnit"&Profile$(1,2),52
9510 Elev_corr=1 I Set elevation correction indicator
9520 Alpha=Alpha mean
9530 FOR I=1 TO J
9540 Tday(I+2)=Tday(I+2)-Alpha*(Topo(I+2)-1400)
9550 Tnite(I+2)=Tnite(I+2)-Alpha*(Topo(I+2)-1400)
9560 NEXT I
9570 FPRINT "Tday"&Profile$(1,2),Tday(*)
9580 FPRINT "Tnit"&Profile$(1,2),Tnite(*)

```

```

9590 PRINTER IS 0
9600 PRINT
9610 PRINT "To restore data files;"
9620 PRINT "PURGE Tday.. ;RENAME Tdy.. TO Tday.. "
9630 PRINT "PURGE Tnt.. ;RENAME Tnt.. TO Tnt.. "
9640 PRINT
9650 PRINTER IS 16
9660 DISP "FINISHED."
9670 GOTO Function_keys
9680 |
9690 | .....
9700 |
9710 Report plot: |
9720 DISP "Report plotting."
9730 SERIAL
9740 PLOTTER IS 7,5,"9672A"
9750 GOSUB Mult file read
9760 MAT Reil=Reil*(100) | Convert back to %
9770 Dx=25
9780 X$="Distance(km)"
9790 MAT SEARCH X(*),MAX;Xmax
9800 Xmin=0
9810 Dx=(Xmax-Xmin)*.125/6
9820 DEG
9830 FOR I=1 TO 4: Four sheets
9840 IF I=1 THEN GOTO Plots1
9850 IF I=2 THEN GOTO Plots2
9860 IF I=3 THEN GOTO Plots3
9870 IF I=4 THEN GOTO Plots4
9880 Plots1: MAT Y=Tday
9890 Y$="Temp(K)"
9900 Dy=5
9910 Sp$=" - Day."
9920 MAT Dum=Tnte
9930 D$="Temp(K)"
9940 Day=5
9950 Sp2$=" - Night."
9960 GOTO 10230
9970 Plots2: MAT Y=Topo
9980 Y$="Elevation(m)"
9990 Dy=100
10000 Sp$=""
10010 MAT Dum=Derv
10020 D$="Gradient(m/km)"
10030 Sp2$=""
10040 Day=10
10050 GOTO 10230
10060 Plots3: MAT Y=Dt
10070 Y$="Temp(K)"
10080 Dy=5
10090 Sp$=" - Temp air."
10100 MAT Dum=Mean
10110 D$=Y$
10120 Sp2$=" - Temp mean."
10130 Day=Dy
10140 GOTO 10230
10150 Plots4: MAT Y=Reil
10160 Y$="Reil(%)"
10170 Dy=5
10180 Sp$=""

```

```

10190 PAI Dur=InertL
10200 Dy=500
10210 Dp="Inertia(TIU)"
10220 Sp2$=""
10230 FOR P=1 TO 2
10240 LIMIT U,400,0,2d5
10250 LOG 5
10260 CSIZE 2.75
10270 IF P=1 THEN X1=(2*25.4-12.5)*100/2d5
10280 IF P=2 THEN X1=X1+.5*25.4*100/2d5
10290 X2=X1+5.5*25.4*100/2d5
10300 Y1=(2*25.4+14)*100/2d5
10310 Y2=Y1+.5*25.4*100/2d5
10320 MOVE X1+.5*25.4*100/2d5,Y1-.5*25.4*100/2d5
10330 LABEL X1
10340 LDIF Y1
10350 MOVE X1-.9*25.4*100/2d5,Y1+4.25*25.4*100/2d5
10360 IF P=2 THEN Y1=D5
10370 LABEL Y1
10380 LDIF X1
10390 LOCATE X1,X2,Y1,Y2
10400 FRAME
10410 LOG 5
10420 IF P=2 THEN MAT Y=Dur
10430 IF P=2 THEN Dy=Dy
10440 IF P=2 THEN Sp2$=Sp2$
10450 IAT SEARCH Y(*),MAX;Ymax
10460 IAT SEARCH Y(*),MIN;Ymin
10470 Ymin=INT(Ymin/Dy)*Dy
10480 Ymax=(INT(Ymax/Dy)+1)*Dy
10490 Dyp=(Ymax-Ymin)*.125/8.5
10500 SCALE Xmin,Xmax,Ymin,Ymax
10510 AXES Dx,Dy,Xmin,Ymin,4,2
10520 OUTPUT 705;"VS2;"
10530 MOVE Xmin,Ymax
10540 DRAW Xmax,Ymax
10550 DRAW Xmax,Ymin
10560 FOR Ic=1 TO J          ! Draw curve
10570 IF Ic=1 THEN MOVE X(Ic),Y(Ic);
10580 DRAW X(Ic),Y(Ic)
10590 NEXT Ic
10600 OUTPUT 705;"VN;"
10610 CSIZE 2          ! Label axes
10620 LOG 8
10630 FOR Ys=Ymin TO Ymax STEP Dy
10640 MOVE Xmin-Dxs,Ys
10650 LABEL VALS(Ys)
10660 NEXT Ys
10670 LOG 6
10680 FOR Xs=Xmin TO Xmax STEP Dx
10690 MOVE Xs,Ymin-Dys
10700 LABEL VALS(Xs)
10710 NEXT Xs
10720 LOG 5
10730 MOVE (Xmin+Xmax)*.5,Ymax-Dys*2
10740 LABEL "Profile "&Profile$(1,2)&" "&Sp2$&" "&Area$&" Area"
10750 PEN 0
10760 NEXT P
10770 OUTPUT 705;"AH;"
10780 OUTPUT 705;"AH;"

```

```

10700 NEXT I
10800 OUTPUT 705;"AN:"
10810 GOTO function_keys
10820 I
10830 I .....
10840 I
10850 SUM Linear(X(*),Y(*),L,Alpha,Beta,Dev)
10860 I Fit Y = Alpha*X + Beta +/- Dev
10870 OPTION BASE 1
10880 DIM A1(500,1),Y1(500,1),Xtrns(1,500),D(1,1),R(1,1),F(1,1)
10890 REDIM A1(L,1),Y1(L,1),Xtrns(1,L)
10900 FOR I=1 TO L
10910 A1(I,1)=A(I)
10920 Y1(I,1)=Y(I)
10930 Xtrns(I,1)=X(I)
10940 Xmean=SUM(X1)/L
10950 Ymean=SUM(Y1)/L
10960 MAT A1=A1-(Xmean)
10970 MAT Y1=Y1-(Ymean)
10980 MAT Xtrns=Xtrns*(X1)
10990 MAT D=ATRS(X1)
11000 MAT R=INV(D)
11010 MAT F=Xtrns*Y1
11020 MAT F=R*D
11030 Alpha=F(1,1)
11040 Beta=Ymean-Alpha*Xmean
11050 MAT A1=A1+(Xmean)
11060 MAT Y1=Y1+(Ymean)
11070 MAT A1=A1*(Alpha)
11080 MAT A1=A1+(Beta)
11090 MAT A1=A1-Y1
11100 MAT A1=A1*X1
11110 Dev=SQR(SUM(A1)/(L-1))
11120 SUBEND
11130 SUB Fast_Find(X(*),Dx,L,Xupper,Xlower,Xmin,Xmax)
11140 I Output is Amin, Amax
11150 OPTION BASE 1
11160 REDIM X(L)
11170 Xmin=SUM(X)/L DIV Dx*Dx
11180 MAT SEARCH X(*),LOC(>=Xupper);Nupper
11190 Xmax=Xmin+Dx
11200 Max_search:MAT SEARCH X(*),LOC(>Xmax);N
11210 IF N-Nupper<L*.04 THEN min
11220 Xmax=Xmax+Dx
11230 GOTO Max_search
11240 Min:MAT SEARCH X(*),LOC(<=Xlower);Nlower
11250 Xmin=Xmin-Dx
11260 Min_search:MAT SEARCH X(*),LOC(<Xmin);N
11270 IF N-Nlower<L*.04 THEN Finish
11280 Xmin=Xmin-Dx
11290 GOTO Min_search
11300 Finish:SUBEND
11310 END

```

5.2 REFERENCE MATERIAL